UNCLASSIFIED

AD NUMBER

AD470827

NEW LIMITATION CHANGE

TO

Approved for public release, distribution unlimited

FROM

Distribution authorized to U.S. Gov't. agencies and their contractors; Critical Technology; Sep 1965. Other requests shall be referred to the Air Force Materials Laboratory, Attn: Metals and Ceramics Division, Wright-Patterson AFB, OH 45433.

AUTHORITY

AFSC/IST [WPAFB], per ltr 21 Mar 1989

THIS PAGE IS UNCLASSIFIED

AFML-TR-65-2
PART II, VOL. I

AD470827

TERNARY PHASE EQUILIBRIA IN TRANSITION METAL-BORON-CARBON-SILICON SYSTEMS

PART II. TERNARY SYSTEMS
VOL. I. Ta-Hf-C SYSTEM

E. RUDY

AEROJET-GENERAL CORPORATION

TECHNICAL REPORT No. AFML-TR-65-2, PART II, VOL. I

SEPTEMBER 1965

AIR FORCE MATERIALS LABORATORY
RESEARCH AND TECHNOLOGY DIVISION
AIR FORCE SYSTEMS COMMAND
WRIGHT-PATTERSON AIR FORCE BASE, OHIO

NOTICES

When Government drawings, specifications, or other data are used for any purpose other than in connection with a definitely related Government procurement operation, the United States Government thereby incurs no responsibility nor any obligation whatsoever; and the fact that the Government may have formulated, furnished, or in any way supplied the said drawings, specifications, or other data, is not to be regarded by implication or otherwise as in any manner licensing the holder or any other person or corporation, or conveying any rights or permission to manufacture, use, or sell any patented invention that may in any way be related thereto.

Qualified users may obtain copies of this report from the Defense Documentation Center.

The distribution of this report is limited because it contains technology identifiable with items on the Mutual Defense Assistance Control List excluded from export under U. S. Export Control Act of 1949, as implemented by AFR 400-10.

Copies of this report should not be returned to the Research and Technology Division unless return is required by security considerations, contractual obligations, or notice on a specific document.

400 - November 1965 - 18-323-773

AFML-TR-65-2
PART II, VOL. I

TERNARY PHASE EQUILIBRIA IN TRANSITION METAL-BORON-CARBON-SILICON SYSTEMS

PART II. TERNARY SYSTEMS
VOL. I. Ta-Hf-C SYSTEM

E. RUDY

FOREWORD

The work described in this report was performed at the Materials Research Laboratory, Aerojet-General Corporation, Sacramento, California, under USAF Contract No. AF 33(615)-1249. The contract was initiated under Project No. 7350, Task No. 735001. The work was administered under the direction of the Air Force Materials Laboratory, Research and Technology Division, with Captain R. A. Peterson acting as Project Engineer, and Dr. E. Rudy, Aerojet-General Corporation, as Principal Investigator. Professor Dr. Hans Nowotny, University of Vienna, served as consultant to the project.

The project, which includes the experimental and theoretical investigation of selected ternary systems in the system classes Me_1-Me_2-C, Me-B-C, Me_1-Me_2-B, Me-Si-B, and Me-Si-C, was initiated on 1 January 1964.

The author wishes to acknowledge the help received from Dr. C. E. Brukl, who performed the majority of the lattice parameter calculations, and from D. P. Harmon, J. Hoffman, R. Cobb, and St. Windisch, who were of assistance during the course of the experimental work.

Chemical analysis of the alloys was carried out under the supervision of Mr. W.E. Trahan, Quality Control Division of Aerojet-General Corporation. The author also wishes to thank Mr. R. Cristoni, who prepared the illustrations, and Mrs. J. Weidner, who typed the report.

The excellent book by F. N. Rhines, Phase Diagrams in Metallurgy[1], was extensively consulted in questions regarding nomenclature and interpretation of the equilibria.

The manuscript of this report was released by the author May 1965 for publication as an RTD Technical Report.

Other reports issued under USAF Contract AF 33(615)-1249 have included:

Part I. Related Binaries

Volume I, Mo-C System

Volume II, Ti-C and Zr-C System

Part III. Special Experimental Techniques

Volume I, High Temperature Differential Thermal Analysis

Part IV. Thermochemical Calculations

Volume I, Thermodynamic Properties of Group IV, V, and VI Binary Transition Metal Carbides.

This technical report has been reviewed and is approved.

W. G. RAMKE,
Chief, Ceramics and Graphite Branch,
Materials and Ceramics Division,
Air Force Materials Laboratory

ABSTRACT

The ternary alloy system tantalum-hafnium-carbon was investigated by means of X-ray, DTA, melting point, and metallographic techniques on chemically analyzed alloys, and a complete phase diagram for temperatures above 1000°C was established.

The system is characterized by a very high melting solid solution of the refractory monocarbides in both binary systems, and a limited exchange of hafnium in the low- and high-temperature modification of Ta_2C. Four Class II four-phase reaction planes as well as three limiting tie lines occur in the concentration area metal-monocarbide solution.

The results of this investigation are discussed and compared with previous, partial investigations of this system. Fields of application are outlined.

TABLE OF CONTENTS

ILLUSTRATIONS

Illustrations (continued)

Illustrations (continued)

Illustrations (continued)

TABLES

I. INTRODUCTION AND SUMMARY

A. INTRODUCTION

The binary alloy system tantalum-hafnium has received considerable attention during the past few years as a promising material system for the development of oxidation resistant alloys. Many of the intended applications are under carbonaceous conditions or the alloys are in direct contact with carburizing agents. A knowledge of the ternary system with carbon is therefore of con derable interest. The phase diagram shows the nature and compositions of the reaction products to be expected to form from a given metal alloy at a given temperature, and serves, therefore, as a useful guide in the selection of the optimum alloy compositions for the specific application problem. Finally, due to the nature of the equilibria occurring in this system, tantalum-hafnium-carbon alloys are probably one of the most promising material combinations for the development of the thermalshock-resistant carbide-metal composite structures.

An effort was therefore made to clarify the high temperature phase relationships in this system. Special attention was directed towards the accurate establishment of the maximum solidus temperatures of the very high melting monocarbide solution, and the clarification of the phase-relationships in the concentration area between the metal and the monocarbide solid solution. Wherever possible, preference was given to the more concise and informative graphical data presentation, in lieu of a compilation in tabular form.

B. SUMMARY

The alloy system tantalum-hafnium-carbon was investigated using hot-pressed, electron beam-melted, vacuum-sintered (2 to 5 x 10^{-6} Torr),and quenched alloy material. The investigations were carried out with X-ray, DTA, metallographic, and melting point techniques. The majority of the alloys was chemically analysed for their content of free and combined carbon. A number of alloys were analyzed for the metal components, and also were examined upon contamination by oxygen.

1. Binary Systems

The binary systems hafnium-carbon and tantalum-carbon were described in previous reports[2, 3]. The binary system tantalum-hafnium (Figure 1) was only superficially examined in this investigation and the following results were established.

a. Tantalum and hafnium form a continuous series of solid solutions at temperatures above ~ 1900°C. The melting curves show an invariant (minimum) point at 2130 ± 20°C and a hafnium concentration of approximately 80 atomic percent.

b. Below approximately 1900°C a miscibility gap between the body centered modifications of both metals is formed. The critical point is located at ~50 atomic % hafnium.

c. The body centered cubic (β) high temperature modification of hafnium (transformation point ~1800°C) is stabilized to lower temperatures by solid solution formation with tantalum. The interaction between the boundary curve of the miscibility gap of the body-centered cubic solution and the solvus curve (bcc solution) of the equilibrium

(Ta, Hf) (bcc) — α-Hf-ss produces a eutectoid reaction. The eutectoid point is located at ~83 atomic % hafnium and 1100 ± 30°C.

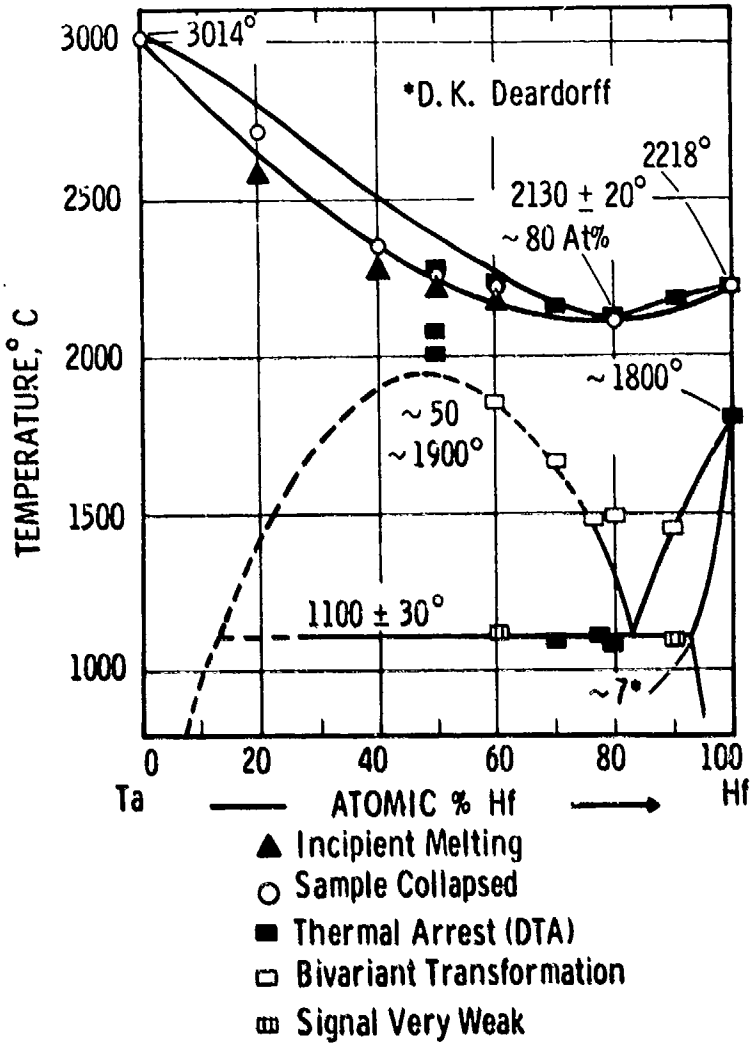

Figure 1. Tentative Phase Diagram Tantalum-Hafnium

In its basic details, these data are in confirmation of the results obtained by D.K. Deardorff[4] and the more recent investigations by H. Kato and M.I. Copeland[5].

2. Constitution Diagram Tantalum-Hafnium-Carbon(Fig. 2)

a. The Face-Centered Cubic (B1) Monocarbide Phase (δ)

Tantalum monocarbide (a = 4.456 Å) and hafnium monocarbide (a = 4.640 Å) form a continuous series of solid solutions. The lattice parameters show a nearly linear variation between the parameters of the binary compounds at the respective carbon concentrations. The melting point maximum reported for this solid solution at approximately 80 mole % TaC[6] does not exist (Figure 3)

b. Carbon-Rich Equilibria

No new intermediate compounds are formed and the only reaction occurring in this concentration area is the formation of the eutectic. The temperatures and compositions of the eutectic vary smoothly from 3445°C and 61 At% C for the binary TaC-C eutectic, to 3180° and 65 At% C in the binary hafnium-carbon system.

c. Metal-Rich Equilibria

Four Class II four-phase reaction temperature planes occur in the concentration region between the metal and monocarbide solution:

(1) Class II Four-Phase Equilibrium at 2550°C.

The four-phase reaction proceeding at 2550°C is represented by the reaction equation

$$\text{Liquid} + \beta\text{-Ta C-ss}(\gamma') \xrightarrow[T \leq 2550^\circ]{T \geq 2550^\circ} (\text{Ta, Hf})\,(\beta) + (\text{Ta, Hf})\text{C}_{1-x}\,(\delta)$$

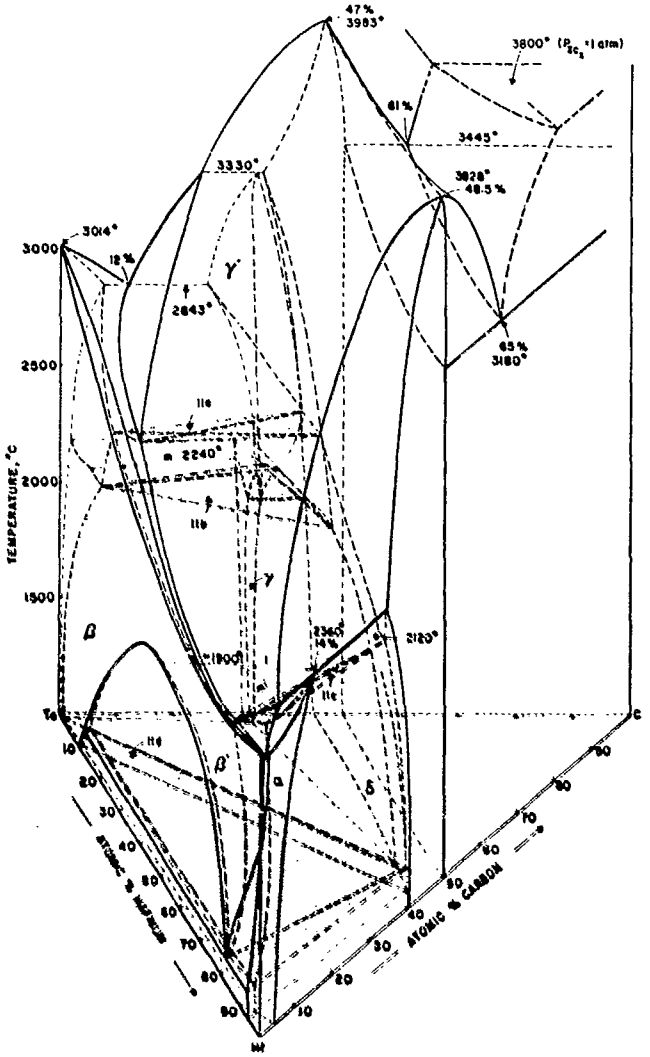

Figure 2. Constitution Diagram Tantalum-Hafnium-Carbon

Table 1. Four Phase Reaction Plane $L + \gamma' \leftrightarrow \beta + \delta$ at 2550°C: Equilibrium Concentrations of the Phases

Phase	Concentrations, At% Ta	Hf	C
Liquid	69	27	4
(Ta, Hf) (β)	75	23	~ 2
$(Ta, Hf)_2C(\gamma')$	46	19	35
$(Ta, Hf)C_{1-x}(\delta)$	37	26	37

(2) Class II Four-Phase Equilibrium at 2230° (II_b in Figure 2)

The four-phase reaction proceeding at this temperature can be presented as:

$$\beta\text{-}Ta_2C\text{-ss}\ (\gamma') + Ta, Hf\ (\beta) \underset{T \leq 2230°}{\overset{T \geq 2230°}{\rightleftharpoons}} \alpha\text{-}Ta_2C\text{-ss}\ (\gamma) + (Ta, Hf)C_{1-x}\ (\delta)$$

Table 2. Four-Phase Reaction Plane $\gamma' + \beta \leftrightarrow \gamma + \delta$ at 2230°: Equilibrium Concentrations of the Phases

Phase	Concentrations, At% Ta	Hf	C
$\beta\text{-}Ta_2C\text{-ss}\ (\gamma')$	~ 53	13	34
Ta, Hf (β)	81	17	~ 2
$\alpha\text{-}Ta_2C\text{-ss}\ (\gamma)$	~ 57	11	32
$(Ta, Hf)C_{1-x}\ (\delta)$	32	31	37

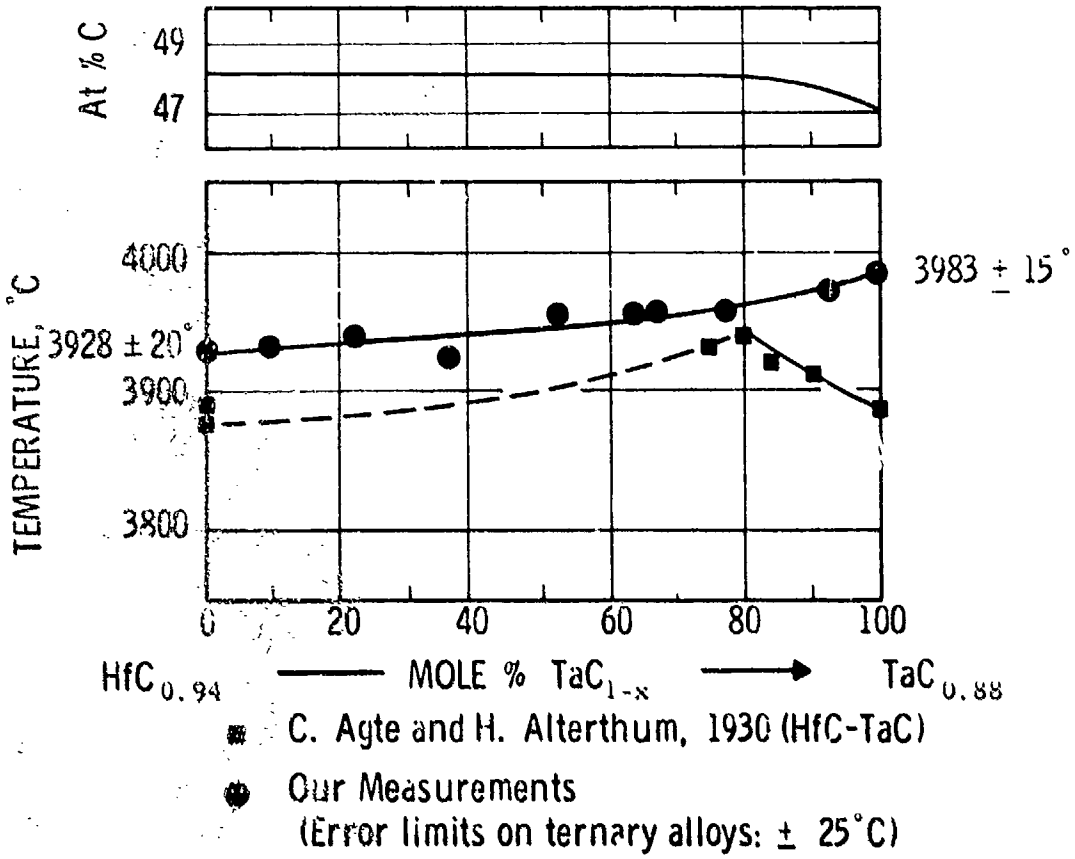

Figure 3. Maximum Solidus Temperatures of the Crystal Solution $(Ta, Hf)C_{1-x}$
Top: Concentration Line of Maximum Melting (± 0.3 At%)

(3) **Class II Four-Phase Equilibrium at 2130°C (II_c in Figure 2)**

The four-phase reaction proceeding at this temperature can be presented as:

$$\alpha\text{-Hf-ss } (\alpha) + \text{Liquid} \xrightleftharpoons[T \leq 2130^\circ]{T \geq 2130^\circ} (Hf, Ta)\ (\beta) + (Hf, Ta)C_{1-x}\ (\delta)$$

Table 3. Four-Phase Reaction Plane $\alpha + L \leftrightharpoons \beta + (\delta)$ at 2130°C: Equilibrium Concentrations of the Phases

Phase	Concentrations, At% Ta	Hf	C
α-Hf-ss (α)	9	84	7
Liquid	16	82	~2
Hf-Ta (β)	15	84	~1
$(Hf, Ta)C_{1-x}(\delta)$	6	58	36

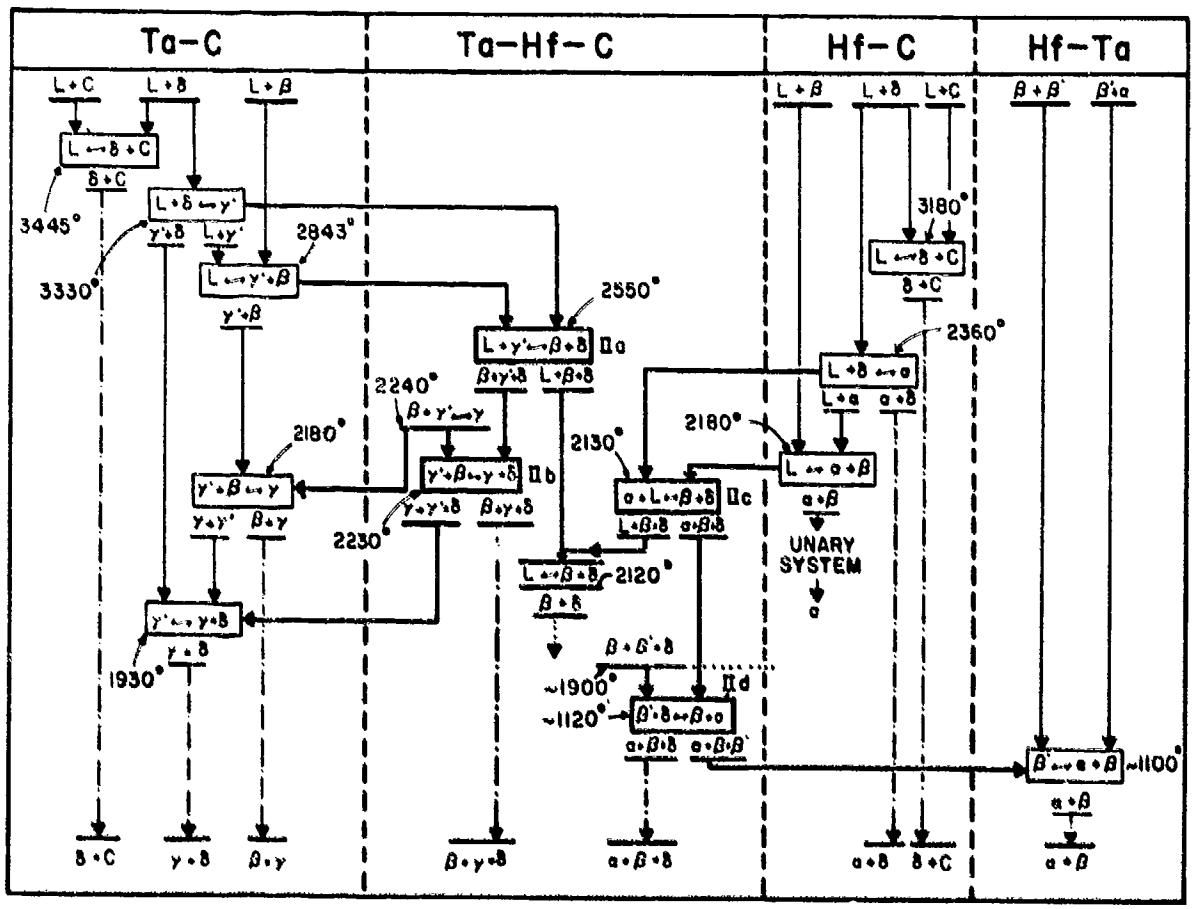

Figure 4. Schell-Schultz Diagram for the System Tantalum-Hafnium-Carbon

(4) Class II Four-Phase Equilibrium at ~1120°C. (II_d in Figure 2)

The four-phase reaction proceeding at this temperature can be presented as:

$$(Ta, Hf)\ (\beta) + (Ta, Hf)C_{1-x}\ (\delta) \underset{T \leq 1120°}{\overset{T \geq 1120°}{\rightleftharpoons}} (Ta, Hf)\ (\beta) + \text{a-Hf-ss}\ (\alpha)$$

Table 4. Four-Phase Reaction Plane $\beta' + \delta \hookleftarrow \beta + \alpha$ at ~1120°C: Equilibrium Concentrations of the Phases

Phase	Concentration, At% Ta	Hf	C
(Ta, Hf) (β')	16	83	~1
$(Ta, Hf)C_{1-x}$ (δ)	~3	56	41
(Ta, Hf) (β)	81	18	~1
α-Hf-ss (α)	~5	93	2

(5) Limiting Tie Lines

In addition to the four-phase action planes, three limiting tie lines occur in the system.

(a) The maximum tie line (dotted line in Figure 2) marks the ternary decomposition of the α-Ta_2C phase in a quasi-binary peritectoid reaction:

$$\alpha\text{-}Ta_2C\text{-ss}\ (\gamma) \underset{T \leq 2240°}{\overset{T \geq 2240°}{\rightleftharpoons}} \beta\text{-}Ta_2C\text{-ss}\ (\gamma') + Ta, Hf\ (\beta)$$

Two three-phase equilibria result from this reaction towards lower temperatures.

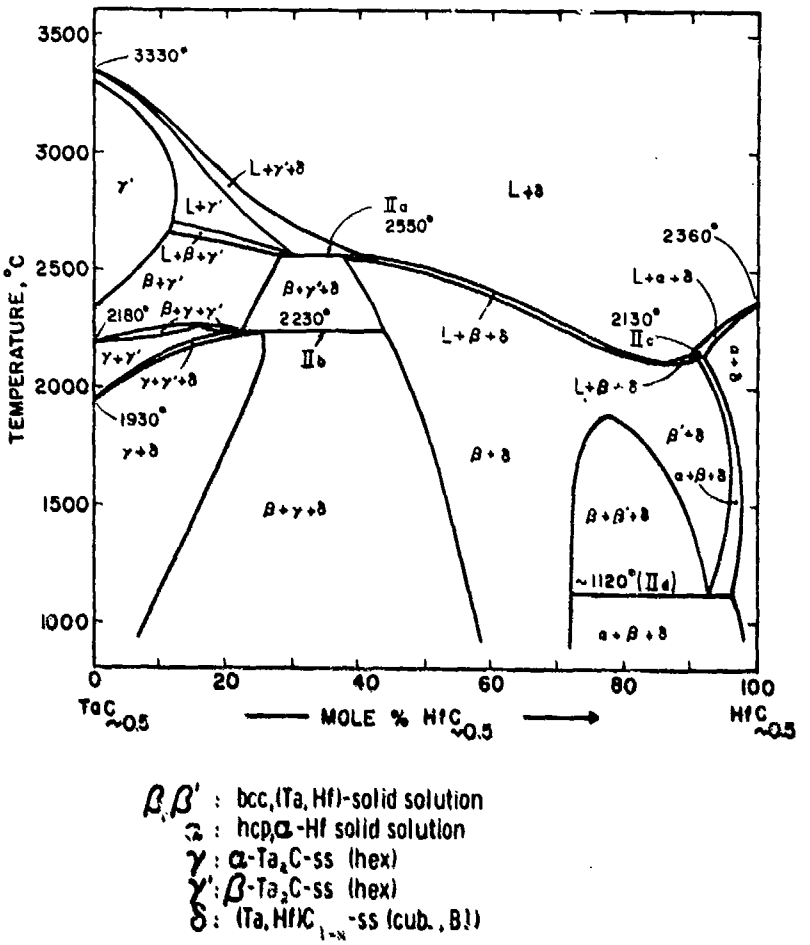

β, β' : bcc, (Ta, Hf)-solid solution
α : hcp, α-Hf solid solution
γ : α-Ta_2C-ss (hex)
γ' : β-Ta_2C-ss (hex)
δ : $(Ta, Hf)C_{1-x}$-ss (cub., B1)

Figure 5. Ta-Hf-C: Isopleth Across 33 Atomic % Carbon

(b) The minimum tie line at 2120° (dotted line "mi" in Figure 2) designates a minimum eutectic point (quasibinary eutectic) in the ternary system:

$$\text{Liquid} \xrightleftharpoons[T \leq 2120°]{T \geq 2120°} (Hf, Ta)\ (\beta) + (Hf, Ta)C_{1-x}\ (\delta)$$

Two three-phase equilibria result from this reaction towards higher temperatures.

(c) The formation of the miscibility gap in the binary (Hf, Ta) system is reflected in the existence of a critical tie line in the ternary system (dotted line "l" in Figure 2). One three-phase equilibrium results from this reaction towards lower temperatures.

The invariant and univariant reactions (p = const) occurring in the ternary alloy system are summarized in the Scheil-Schultz reaction scheme shown in Figure 4. The phase reactions in the metal-rich solution are shown in consolidated form in the isopleth across 33 atomic % carbon (Figure 5).

II. LITERATURE REVIEW

A. BOUNDARY SYSTEMS

In the binary hafnium-carbon[2, 7-11] system (Figure 6) one intermediate carbide phase with extreme high melting point[2, 6, 12] and a wide homogeneous range exists[11, 13].

Hafnium-monocarbide, with a face centered cubic (B1) unit cell, extends from approximately 34 (a = 4.608 Å) to 49.5 At% C (a = 4.640 Å) at ~2300°C[8, 2]. The lower carbon boundary at 1500°C[11] lies at 37.5 At% C. The face-centered cubic α-modification is stabilized to higher carbon concentrations by incorporation of carbon-atoms into interstitial lattice sites[10], and decomposes in a peritectic reaction at 2360° into the monocarbide phase and melt[2]. The carbon solubility in β-Hf is below one atomic percent[2].

A eutectic is formed between the α- and β-Hf-solution at 2180° and a carbon concentration of approximately 1.5 atomic percent[2].

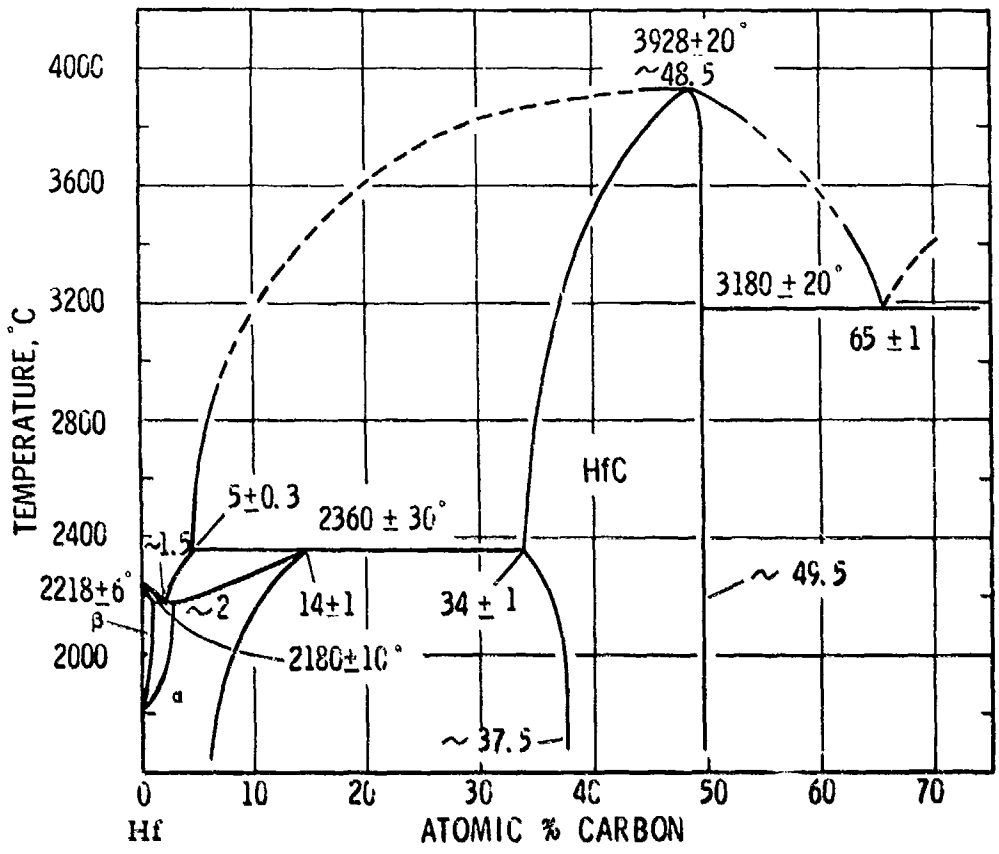

Figure 6. Constitution Diagram Hafnium-Carbon (E. Rudy, C.E. Brukl, and D.P. Harmon, 1965)

The eutectic point in the carbon-rich portion of the system is located at 3180° and 65 ± 1 At% C[2,8].

The tantalum-carbon system has been investigated by F.H. Ellinger[14]. The phase-diagram, based on a recent redetermination of the system by E. Rudy, C.E. Brukl, and D.P. Harmon[3] is shown in Figure 7. Partial investigations of the system were recently carried out by R.V. Sara and C.E. Lowell[8] and C.F. Zalabak[15].

Two refractory intermediate phases are formed:

Ta_2C[7] with a hexagonal close-packed arrangement of metal atoms (a = 3.102 Å ; c = 4.940 Å at 33 At% C) and a negligible range of

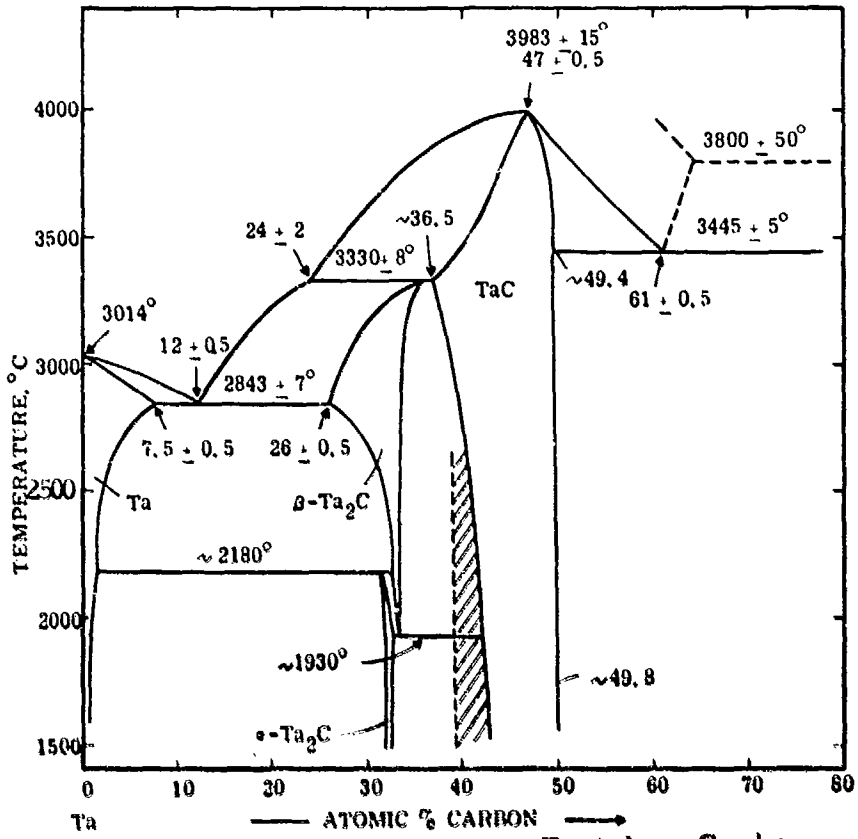

Figure 7. Constitution Diagram Tantalum-Carbon (E. Rudy, C.E. Brukl, and D.P. Harmon, 1965)

homogeneity at temperatures below 1700°C, is unstable above 2180°C and decomposes in a peritectoid reaction into β-Ta_2C and tantalum[3].

β-Ta_2C, probably with identical arrangement of metal atoms[16] but differing in the degree of disorder in the carbon sublattice from the α-modification[3] forms in a peritectic reaction at 3330° from the monocarbide and melt. At 2843°C, the temperature of the Ta-β-Ta_2C eutectic, the low carbon boundary is located at 26 At% C[8, 3]. The phase, which extends

to a maximum carbon concentration of ~35.5 At% at 3330°C, decomposes in a eutectoid reaction at 1930°C into the monocarbide and the α-Ta_2C-phase[3]. The appearance of the ζ-phase reported by R. Lesser and G. Brauer[17] was attributed as being the result of a non-equilibrium precipitation from the monocarbide[8, 3].

The extreme high melting monocarbide[6] forms an extended range of defect solid solutions[14, 16, 17, 19, 20]. The carbon-rich boundary is located closely to 50 At% C[7](Figure 8). Reported melting temperatures vary between 3800°C[21] and 3890°C[6]. More recent determinations at the Los Alamos Scientific Laboratory yielded 4000 - 4200°C[22], and 3983° at 47 At% were measured in this laboratory[3]. A transformation of the monocarbide at high temperatures reported by P.T.B. Shaffer[23] was not confirmed in our investigations[3].

Our determination of a solid solubility of 7.5 atomic percent carbon in tantalum at the Ta-Ta_2C eutectic temperature[3] is in essential agreement with the very recent investigations by E. Fromm and U. Roy[24].

A tentative phase diagram for the system tantalum-hafnium has been proposed by D.K. Deardorff[4] (Figure 9), showing the formation of a miscibility gap between tantalum and β-Hf-ss at temperatures below 1500°C. Somewhat higher critical solution temperatures (1600 - 1800°C) were reported by H. Kato and M.L. Copeland[5]. The hafnium-rich β-(Ta, Hf) solution decomposes at 1050°C into a tantalum-rich (~12 Wt% Hf) metal phase and α-Hf solid solution (7 Wt% Ta).[4]

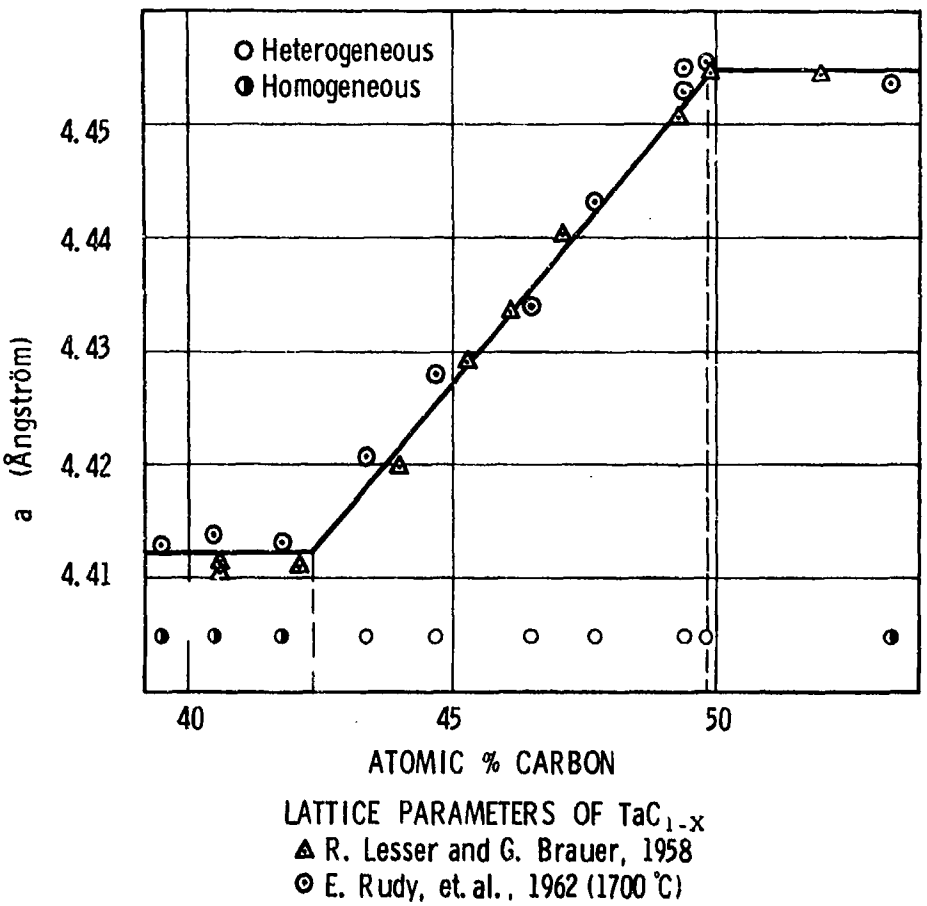

Figure 8. Lattice Parameters of TaC_{1-x}

B. TANTALUM-HAFNIUM-CARBON

The formation of a continuous series of solid solutions between the monocarbides has been ascertained by the work of C. Agte and H. Alterthum[6] as well as by H. Nowotny and co-workers[26,27]. The plot of the lattice parameters of the solution of the compounds at

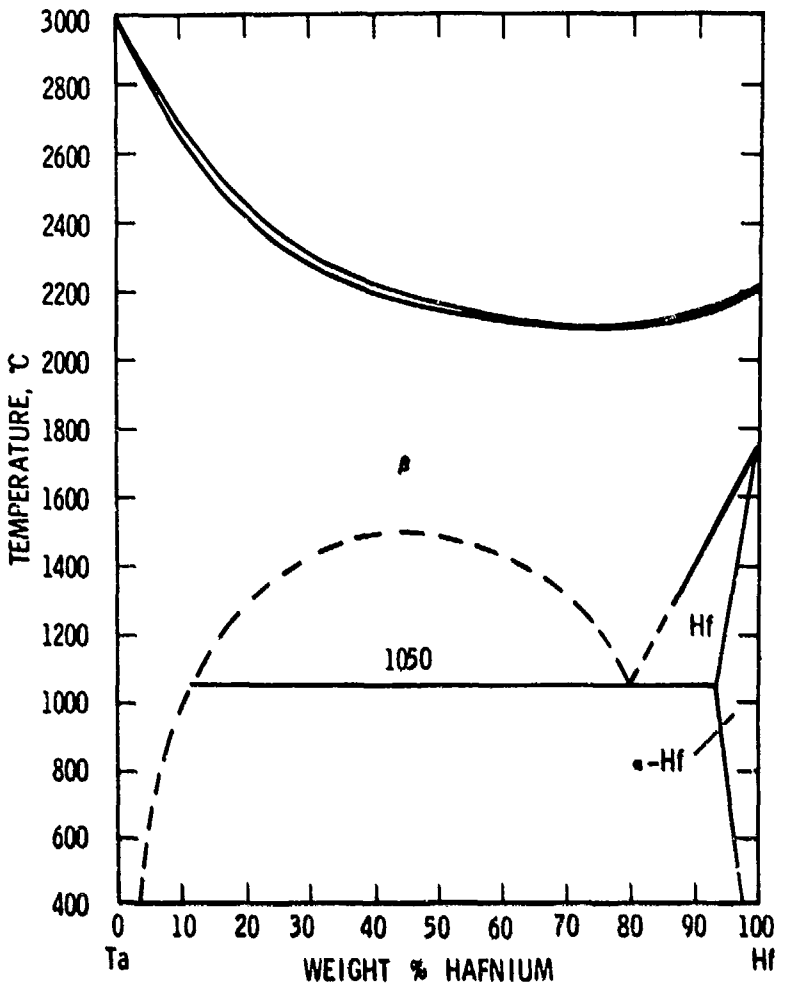

Figure 9. Tantalum-Hafnium Phase Diagram

(D.K. Deardorff, 1961, work quoted by J.J. English, 1961)

composition close to stoichiometry shows a slight contraction over the entire concentration range (Figure 10).

A temperature section of the ternary alloy system at 1850°C was determined by E. Rudy and H. Nowotny[28] (Figure 11). No

new ternary compounds were found in the system, and the hafnium exchange in the Ta_2C-phase did not exceed 12 At%. The phase-relationships occurring in this system were evaluated thermochemically with regard to compound stability and appearance of the ternary equilibria.

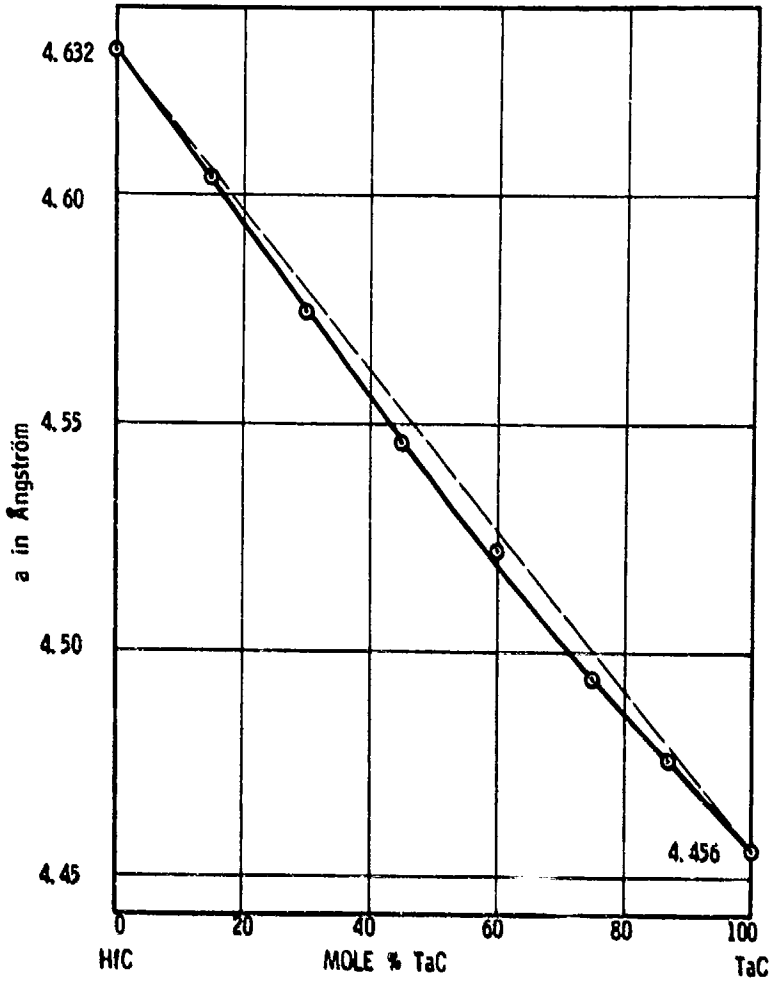

Figure 10. Lattice Parameters of the Solid Solution $(Ta, Hf)C_{1-x}$ (H. Nowotny, et.al., 1959)

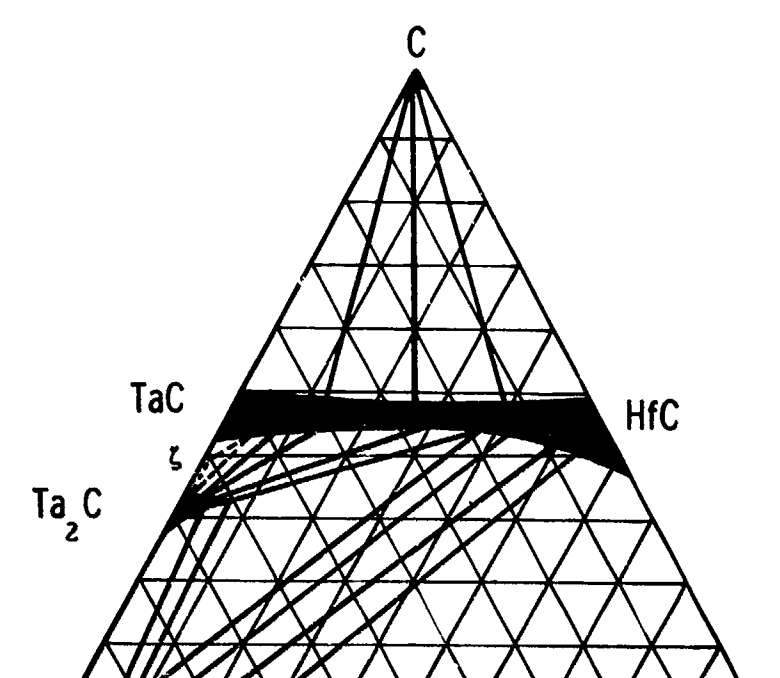

Figure 11. Section of the Phase Diagram Ta-Hf-C at 1850°C (E. Rudy and H. Nowotny, 1963)

III. EXPERIMENTAL PROGRAM

A. EXPERIMENTAL PROCEDURES

1. Starting Materials

The elemental powders as well as pre-prepared tantalum and hafnium monocarbide served as starting materials for the preparation of the alloys.

For selected alloy compositions, hafnium sponge was used for introducing hafnium into the alloys. The hafnium metal powder was purchased from Wah Chang Corp., Albany, Oregon and had the following impurities (contents in ppm): Al-20, C-210, Nb-680, Cr-< 20, Cu-40,

Fe-265, H-55, Mo-40, N-200, O-810, Si-< 40, Ta-< 200, W-235. It also contained 4.1 At% zirconium. The lattice parameter of this starting material determined on a powder pattern with Cu-K_α radiation was $a = 3.19_6$ Å, $c = 5.05_7$ Å. The hafnium sponge had the following analysis (in ppm): Al-94, Cu-< 40, Fe-185, Cl-100, Mg-450, N-30, O-680, Si-< 40, Ti-250, W-< 20. The zirconium content was 4 At%.

Hafnium monocarbide was prepared by direct combination of the elements under high vacuum (< 5.10^{-5} Torr) and temperatures ranging between 1000 and 2200°C. The resulting reaction product, which had a total carbon content of 49.3 At% was comminuted in hard metal lined ball mills and the cobalt traces, which were picked up during milling, were removed by acid-leaching.

Tantalum (Wah Chang Corp., Albany, Oregon) had the following impurities (contents in ppm): C-140, Nb-100, O-280, sum of other impurities - < 300. The lattice parameter obtained for this raw material (Cu-K_α) was $a = 3.303 \pm 0.003$ Å.

Tantalum monocarbide was purchased from Wah Chang Corporation, Albany, Oregon and was acid-leached and high vacuum degassed at 2200°C. The lattice parameter of the purified material was $a = 4.4560 \pm 0.0003$ Å. The total carbon content of the product was 6.15_5 Wt%, from which 0.04 Wt% were present in free form. Main contaminants (in ppm) were: Nb-150, Ti-400, Y-200, sum of other impurities-< 100.

The spectrographic grade graphite powder (Union Carbide Corporation, Carbon Products Division) had the following analysis:

Sum of metallic impurities (Al + Cu + Mg + Si + Fe) - < 9 ppm, ash - < 500 ppm, volatile matter - 100 ppm. No second phase impurities could be detected in strongly overexposed powder patterns, and lattice parameters of a = 2.463 Å, and c = 6.729 Å were obtained from a powder pattern with Cu-K_α radiation.

2. Alloy Preparation and Heat Treatment

Both hot- and cold-pressing of the well-mixed powder mixtures, with subsequent equilibration treatment under high vacuum, were used for the preparation of compact alloy samples. Pertinent equipment has been described in a previous report[25]. For the preparation of alloys in the very metal-rich region, cold-compacted specimens were melted in an electron beam furnace (Heraeus ES 2/4) prior to the homogenization treatment. For the investigation of the solid state temperature sections of the system, approximately 0.1 Wt% cobalt were added to alloys located within the homogeneous range of the monocarbide solution, to aid in the attainment of equilibrium.

Three principal equilibration temperatures, 1500, 2000, and 2200°C were selected for the investigation of the solid state sections. The annealing schedules of the alloys are described in Table 5. Except for those instances where rapid solid state reactions {$\alpha \rightarrow \beta$-Ta_2C, disproportionation of the (Ta, Hf) solid solution} interferred and prevented quenching of the high temperature equilibrium states, the majority of the alloys were homogeneous and the diffraction patterns sharp.

In addition to the equilibration treatment described above, the change of specific equilibria with temperature was studied on

quenched alloys. Rapid quenching was achieved by dropping the sample from the equilibration temperature into a tin bath, which was preheated to 300°C.

Table 5. Annealing Schedules for Tantalum-Hafnium-Carbon Alloys

Equilibration Temperature, °C	Annealing Time (hrs)	Vacuum
1500	69	2×10^{-6} Torr
2000	15 to 25	5×10^{-6} Torr
2200	15	5×10^{-6} Torr

3. Melting Points

Melting temperatures of the alloys were determined with the previously described Pirani-technique[25]. Excess metal containing alloys were melted under vacuum. To prevent carbon and hafnium losses from the alloys in the high melting monocarbide region, the furnace chamber was pressurized to 2 1/4 atmospheres with high purity helium after a short degassing treatment at 2200°C. The temperature measurements were carried out with a disappearing filament type micropyrometer, which was calibrated against a certified standard lamp from the National Bureau of Standards.

The temperature correction terms to be applied to the observed temperatures, including absorption losses in the quartz observation window as well as deviations due to non-black body conditions of the observation hole were calculated from the equation[25]

$$\Delta T \text{ corr} \simeq - T_m^2 \cdot \frac{C_2}{\lambda} \ln D \cdot A \cdot \epsilon$$

ΔTcorr	=	Correction to be added to the measured temperature
Tm	=	Measured Temperature
ϵ	=	Emissivity coefficient of the black body hole
C_2	=	$\frac{hc}{k}$ = const = 1.4384 [cm.deg.]
λ	=	Wave length of radiation used in the measurement ($0.65\ \mu$)
D	=	Relative reflection loss at the quartz window
A	=	Relative absorption loss in the quartz window

From experimental measurements, a total transmission of 0.92 for the quartz system was obtained[25]. The resulting temperature correction curves are shown in Figure 12. From the bore-hole geometry (1 mm dia x 4 mm deep) an average emissivity coefficient of ϵ = 0.98 was used[25] to account for non-black body conditions (curve 4 in Figure 12).

A total of 91 ternary alloy (Figure 13) compositions were investigated and subjected to X-ray diffraction and chemical analysis after the runs.

Two independent series of runs were performed for the highest melting composition series across 47 to 49 atomic % carbon. Alloys within the homogeneous range of the B1-phase and excess carbon containing alloys were analysed for free and combined carbon.

In no instance did the analysed carbon contents after the runs deviate more than one atomic percent from the weighed in composition. The same also applies to the metal ratio where in four

specimens from the monocarbide region, no deviations from the nominal compositions could be detected.

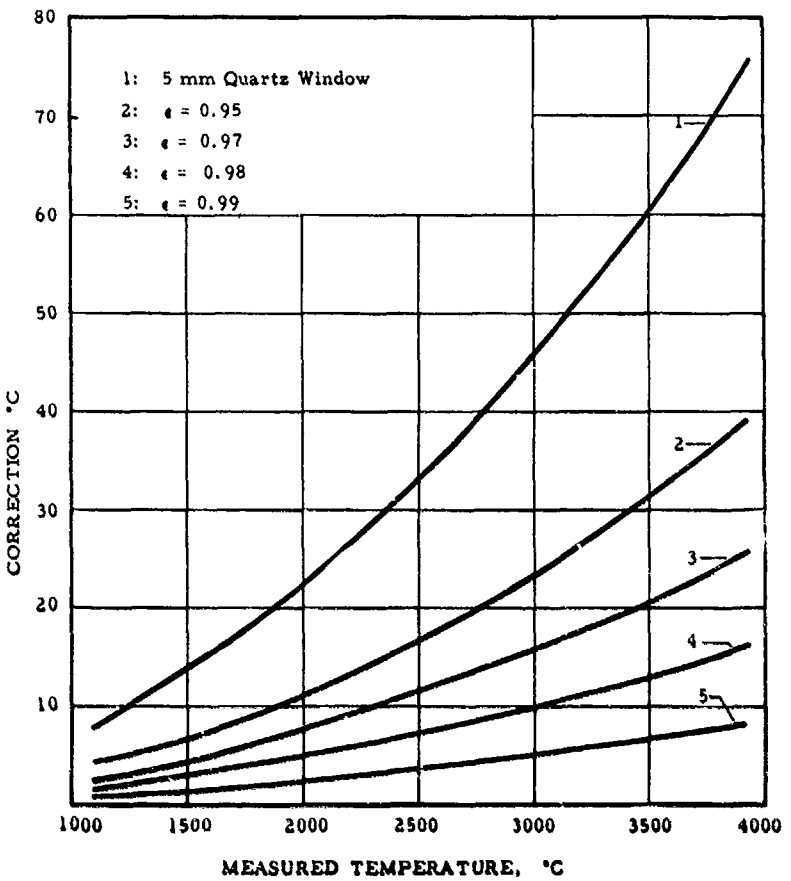

Figure 12. Temperature Correction Chart

These low losses are probably to be attributed to the use of porous (20 - 40%) samples in the melting point determinations. The steep temperature gradient between the interior and the surface of the sample causes the melt first to form in the center portion of the specimen (Figure 14a and b). The experiment is usually completed before

the boundaries of the melt cavity reaches the sample surface, i.e. the temperature of the sample surface stays below that of melting throughout the experiment and consequently material losses due to vaporization from the surface are diminished.

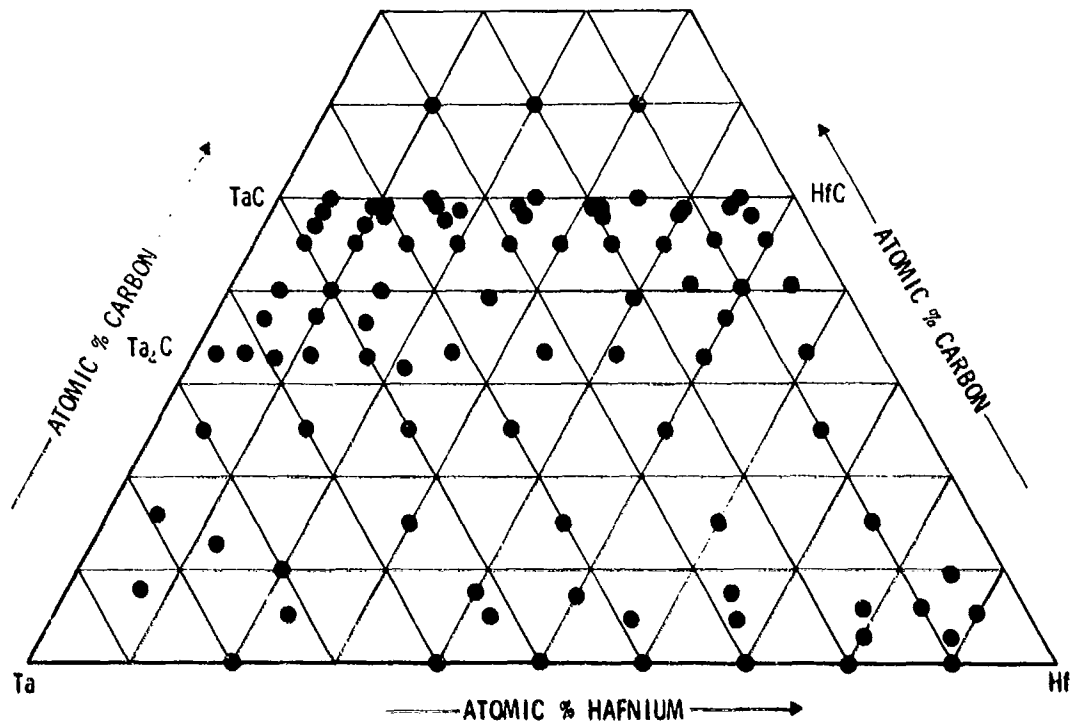

Figure 13. Ta-Hf-C: Composition of Melting Point Specimens

4. Differential Thermal Analysis[25, 29]

Differential thermal analysis provided an extremely useful and important tool for the elucidation of the phase-reactions occurring in the vicinity of the Ta_2C-phase: The α-β-Ta_2C-phase reaction proceeds with extreme speed and hence would be extremely difficult to follow by metallographic techniques on quenched alloy materials. DTA also proved to be a valuable tool in determining the temperatures

of the four-phase reaction planes in the ternary system and the reaction isotherms in the binary Ta-Hf system. For the determination of solidus temperatures, it provided a valuable supplemental technique to the Pirani method, where incipient melting close to homogeneity ranges of phases was difficult to observe.

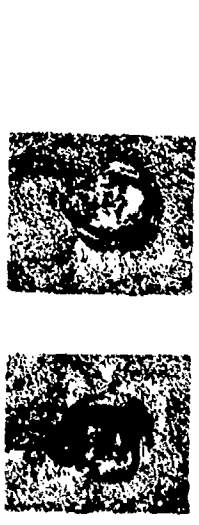

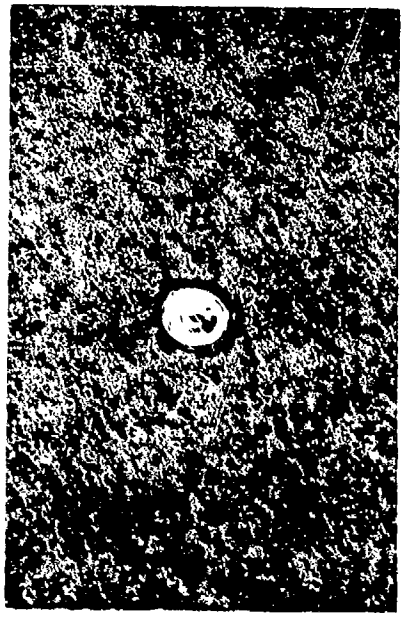

(a) (b)

Figure 14a and b.

Appearance of a Pirani Melting Point Specimen After Melting.

Alloy: Ta-Hf-C (33/18.5/48.5 At%), 3920°C Melting Temperature

(a) Section of the Specimen After the Experiment. Note Melt Cavity in the Interior

(b) Same Sample, Showing Black Body Hole Filled with Liquid.

The DTA-investigations in the binary alloy system Ta-Hf were carried out with electron-beam molten alloy material which was machined to the required dimensions (14 mm dia x 16 mm high, with a concentric black body hole of 4 mm dia x 10 mm deep at one end). Ternary alloys were prepared by hot-pressing the well-blended powder mixtures in graphite dies.

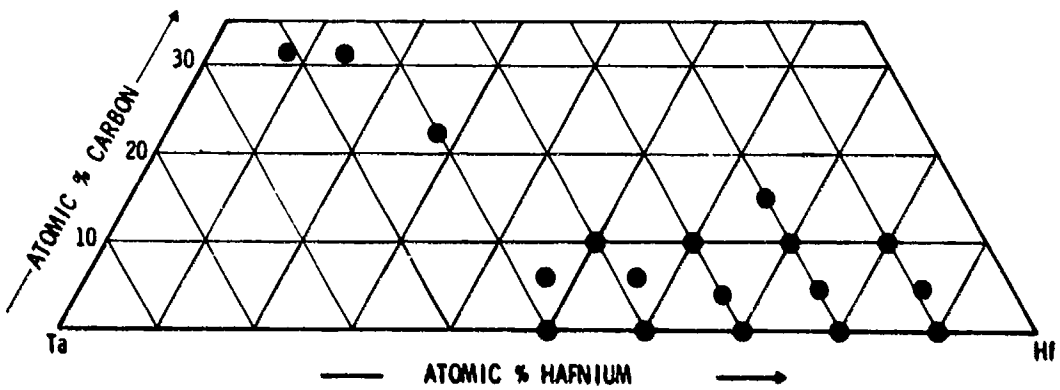

Figure 15. Ta-Hf-C: Position of the DTA-Samples

A total of 18 ternary sample compositions were prepared and investigated (Figure 15). Graphite containers were used in all experiments. Measurements were performed under a high purity helium atmosphere as well as under vacuum, yielding identical results.

5. Metallography

Approximately 45 alloys of defined heat-treatment and composition were metallographically analyzed. The samples were mounted in an electrically conductive mixture of diallylphtalate-lucite-copper

powder. Coarse grinding was performed on silicon carbide paper with grit sizes varying between 120 and 600. The samples were finally polished on microcloth, using a suspension of 0.05 micron alumina in Murakamis solution. Etchants and etching procedures varied with the carbon concentrations of the alloys. Good results for alloys with total carbon concentrations below 25 atomic percent were obtained by electropolishing and subsequent electroetching in a 10% oxalic acid solution. Alloys from the concentration range 30 to 50 atomic percent carbon were dip-etched in an aqueous solution of aqua regia and hydrofluoric acid (60% HCl-20% HNO_3 - 20% HF). The concentrated solution was applied to single phase monocarbide alloys.

6. X-Ray Analysis

Powder diffraction patterns with Cu-K_α-radiation were prepared of all alloys after the equilibration treatments.

The crystal structures of all phases in the ternary alloy stem are simple, and furthermore were known from previous work. Indexing of the patterns and evaluation of the lattice parameters therefore offered no problem and need therefore not be described in detail.

7. Chemical Analysis*

The carbon determinations were carried out using the standard combustion technique. A wet-chemical method was used for the determination of the metal-constituents. Oxygen analysis on the starting materials was carried out with the gas-fusion technique in a

*The chemical analysis quality work was performed under the supervision of Mr. W.E. Trahan, Quality Control Laboratory of Aerojet-General Corporation.

platinum bath (2100 - 2300°C for Hf). Low metallic impurity contents were determined in a semiquantitative way spectrographically.

In general, slightly higher oxygen contents (10 - 15%) than those reported by the supplier were found in the starting materials; however, because of the relatively low level of the total impurity contents, this difference is insignificant. The main objective of the check analysis on the starting materials was to ascertain that selected impurities, (iron metals, silicon, etc) which would drastically influence the melting temperatures and consequently affect the resulting layout of the high temperature phase relationships, were below a critical level.

B. RESULTS

1. Tantalum-Hafnium

This alloy system was only superficially examined in the course of the investigations of the ternary phase diagram. The main objective was to ascertain basic features of the system reported previously[4, 5].

Alloys in the concentration range from 20 to 60 At% hafnium, melt very heterogeneously (Figure 1), indicating a comparatively wide separation between the solidus- and liquidus line in this concentration region. The thermal arrest due to the eutectoid reaction appeared relatively sharp at ~1100°C on the heating as well as the cooling cycle of the DTA-experiments in alloys with hafnium contents varying between 70 and 80 At% Hf. At 90 At% Hf only a very faint signal was obtained, indicating that the boundary of the α-Hf-solid solution almost had been reached.

In addition to the thermal arrests stemming from the eutectoid reaction at 1100°C, a second, strongly rate dependent and gradually initiating series of heat effects were observed to occur between

1500 and 2000°C, and were correlated to the formation of the miscibility gap in the body centered cubic Ta-Hf solution.

Metallographic studies were carried out on (Ta-Hf) samples available from another project. They consisted of electron-beam melted samples, which had received annealing treatments at temperatures varying between 800 and 1500°C (Figures 16 to 24).

Figure 16. Ta-Hf (9 At% Hf), 1500°C X70
Single Phase β

The metallographic examinations as well as the results from the differential-thermoanalytical investigations indicate the miscibility gap to extend to somewhat higher temperatures than estimated by D.K. Deardorff[4]. This finding is in accordance with the recent investigations at the National Bureau of Standards[5], showing the

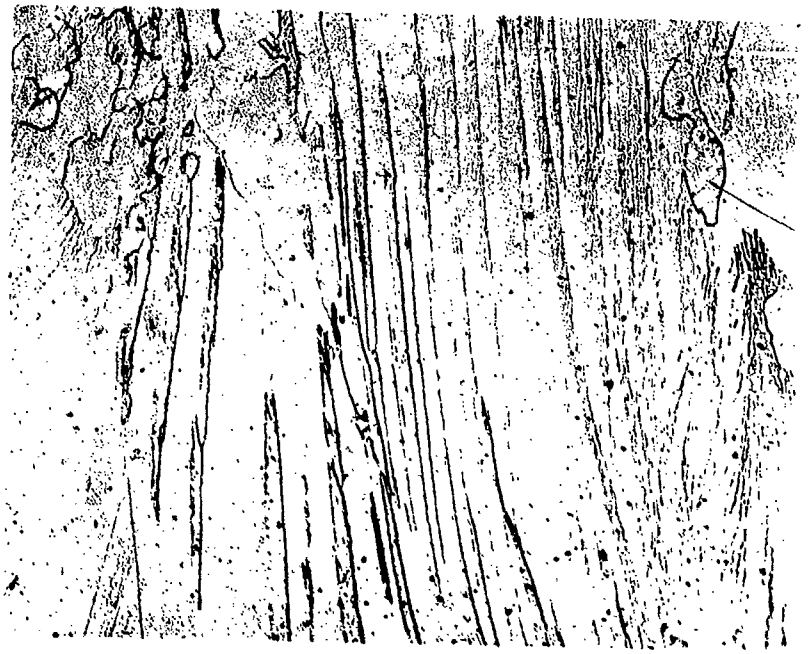

Figure 17. Ta-Hf (9 At% Hf), Annealed at 1500°C, X70
Reannealed at 815°C
$\beta + \alpha$

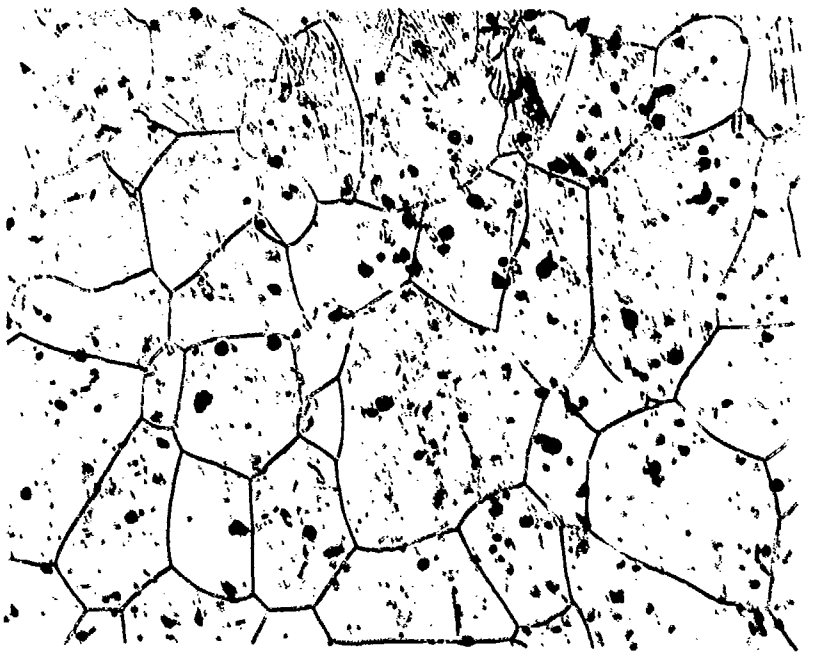

Figure 18. Ta-Hf (19 At% Hf), 1500°C. X70
Single Phase β with Beginning
Precipitation of β'. Pores (black)

Figure 19. Ta-Hf (19 At% Hf), 1500°C, Reannealed at 815°C. X70

$\alpha + \beta$

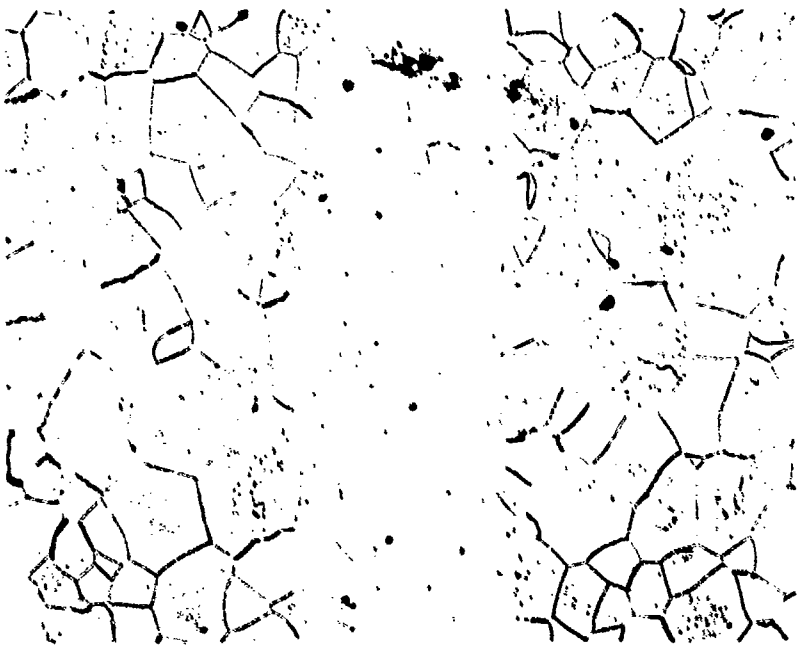

Figure 20. Ta-Hf (30 At% Hf), 1500°C . X75

β + Traces of β' at the Grain Boundaries

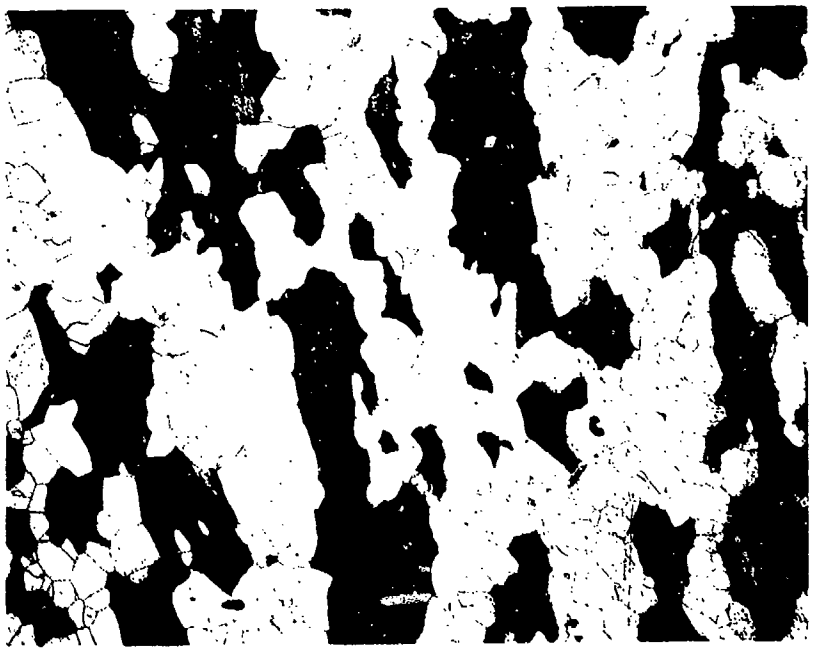

Figure 21. Ta-Hf (30 At% Hf), 1500°C, Reannealed at 1300°C. X70

$\beta + \beta'$ (dark), with Initiation of the Eutectoid Reaction in the β'-Phase

Figure 22. Ta-Hf (40 At% Hf), 1500°C. X75

β with Precipitations (light phase), and β' (dark), Showing Initiation of Eutectoid Reaction

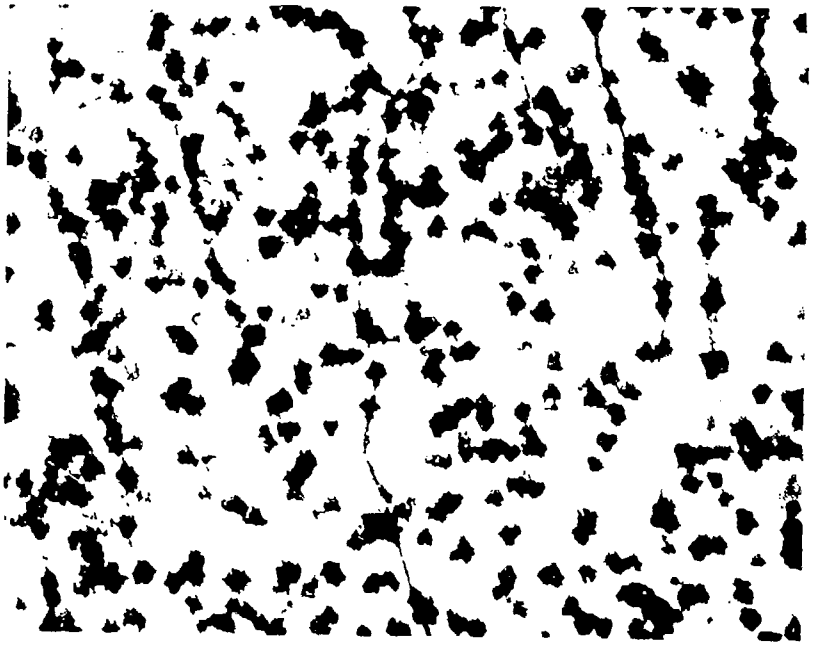

Figure 23. Ta-Hf (40 At% Hf), 1500°C. X1000

Nucleation of the Eutectoid Reaction in Originally Homogeneous β'-Grains

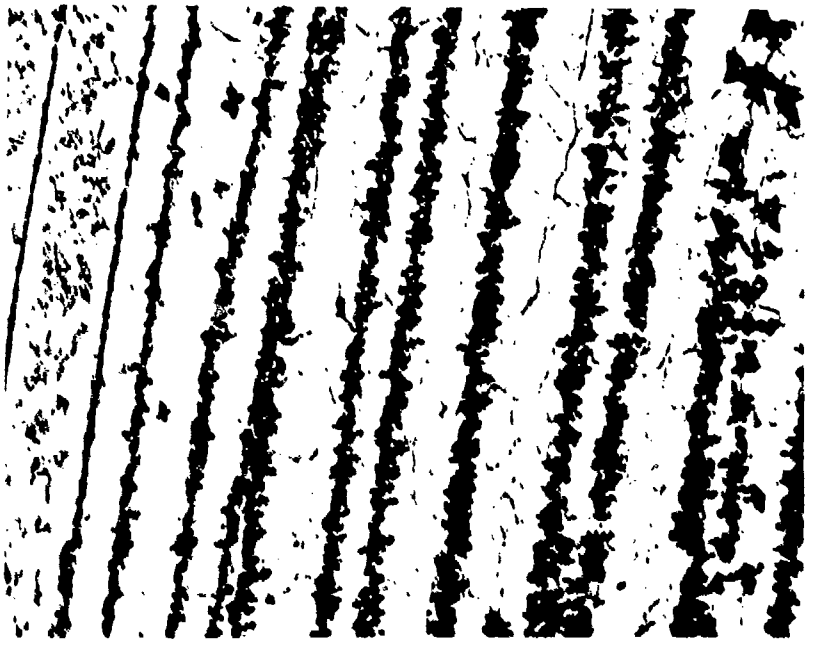

Figure 24. Ta-Hf (40 At% Hf), 1500°C. X1000

Rows of Nucleation Centers for the Eutectoid Reaction in the β'-Phase

miscibility gap to close somewhere between 1600 and 1800°C. Based on the results from the latter authors as well as the present investigation, a critical solution point at ~ 50 atomic % hafnium and a temperature of approximately 1900°C was assumed. A more detailed investigation, however, will be necessary in order to clarify system details within the solidus range.

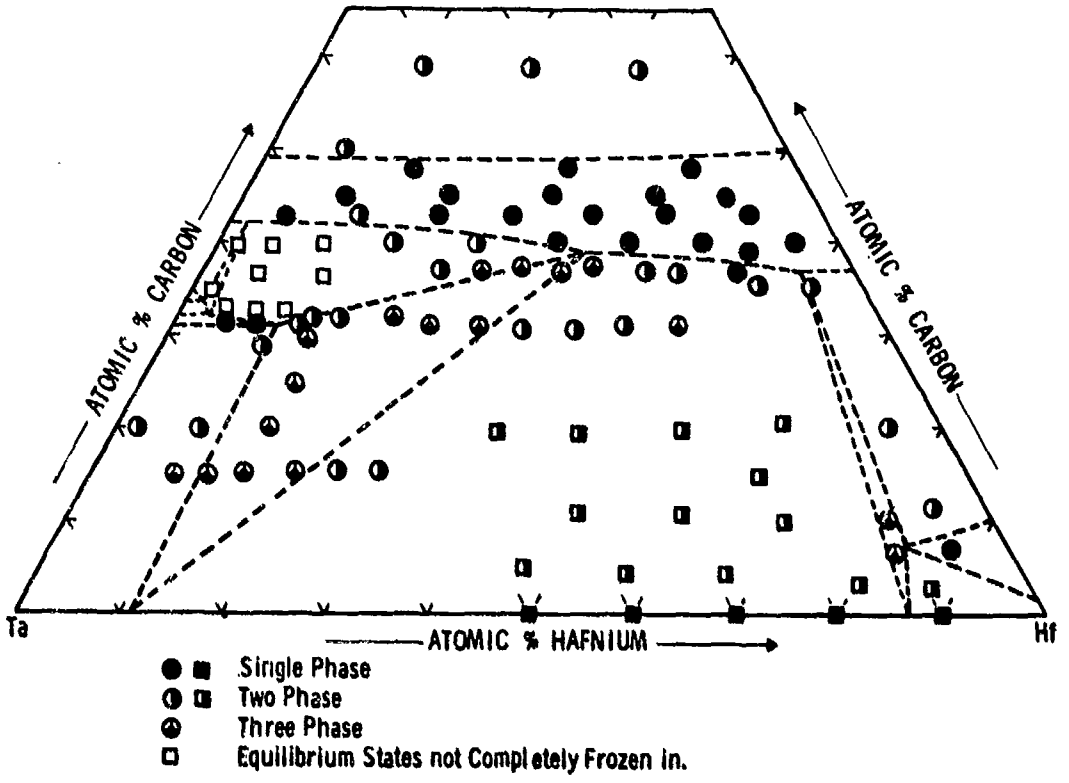

Figure 25. Ta-Hf-C: Sample Position and Qualitative Phase Analysis of the Alloys Equilibrated at 2000°C. - - - Phase Relations at 2000°C.

2. Tantalum-Hafnium-Carbon

A total of 114 alloy compositions in the ternary phase field were prepared for the investigation of the solid state phase relationships. Principal equilibration temperature within the solidus region was 2000°C (Figure 25). At this temperature, tantalum

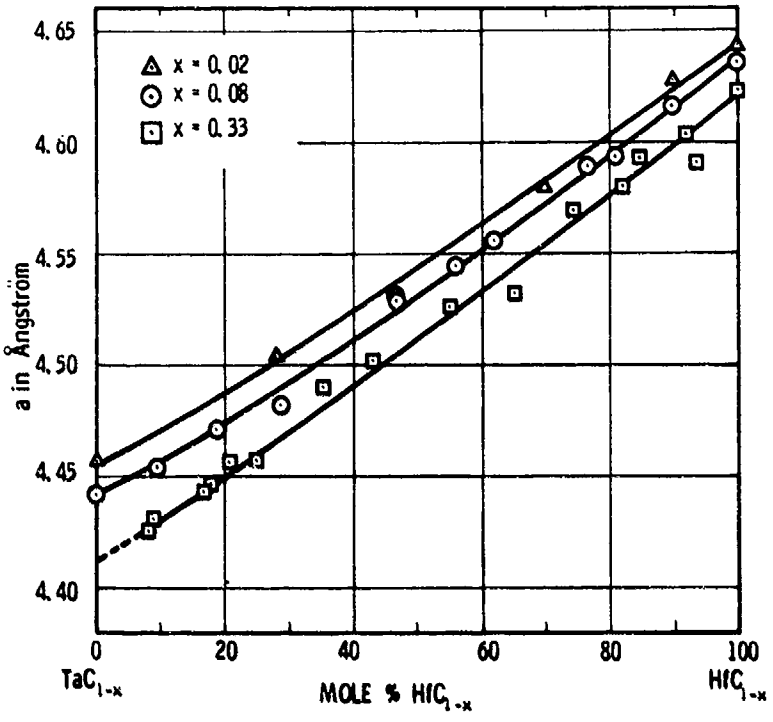

Figure 26. Lattice Parameters of the $(Ta, Hf)C_{1-x}$ Solid Solution as a Function of the Carbon Defect.

and hafnium form a continuous series of solid solutions. Disproportionation of the metal alloys occurs relatively rapid and the cooling rates obtainable in the high vacuum furnace were not sufficient to prevent partial dissolution of the metal phase in the ternary alloys.

Tantalum monocarbide and hafnium monocarbide form a continuous series of solid solutions. The plot of the lattice parameters shows a slight contraction (Figures 26 and 27).

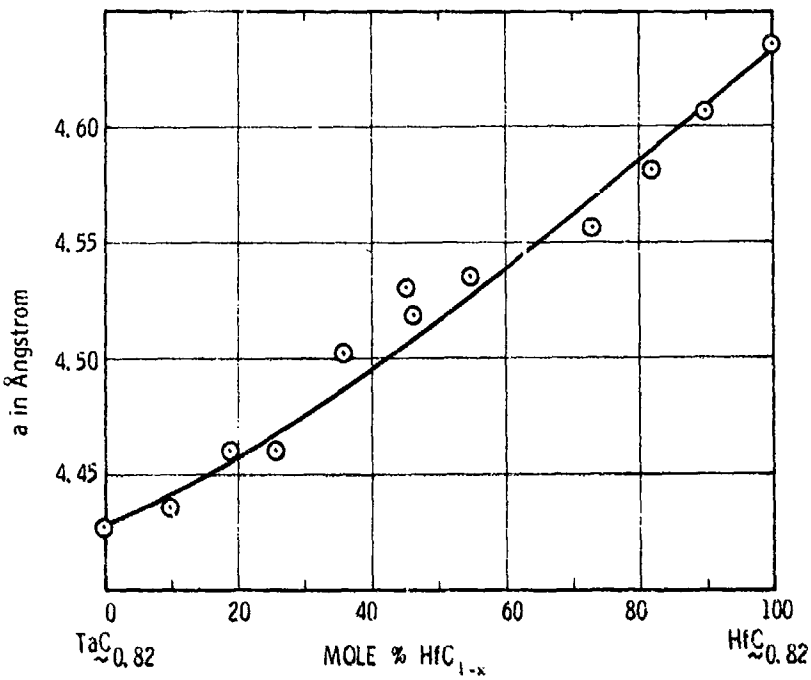

Figure 27. Lattice Parameters of the Solid Solution $(Ta, Hf)C_{1-x}$ at a Carbon Defect of 5 Atomic Percent.

At the chosen equilibrium temperature, α-Ta_2C takes under lattice expansion approximately 18 mole % 'Hf_2C' into solid solution (a = 3.102 Å, c = 4.940 Å for the binary Ta_2C; a = 3.124, c = 4.986 Å for the terminal solid solution) (Figure 28).

The α-Ta_2C (γ) phase is terminated in the ternary phase field by a three-phase equilibrium

$$\alpha\text{-}Ta_2C\text{-}(Ta,Hf)C_{1-x}\ (\beta)\ -\ (Ta,Hf)\ (\delta)$$

Another three-phase equilibrium in the metal-rich portion of the system involves the carbon-stabilized α-Hf solid solution (α), the monocarbide phase (δ) and the metal solid solution (β). Both three-phase equilibria are separated by a wide two-phase range, with the monocarbide and the metal solution as coexisting phases.

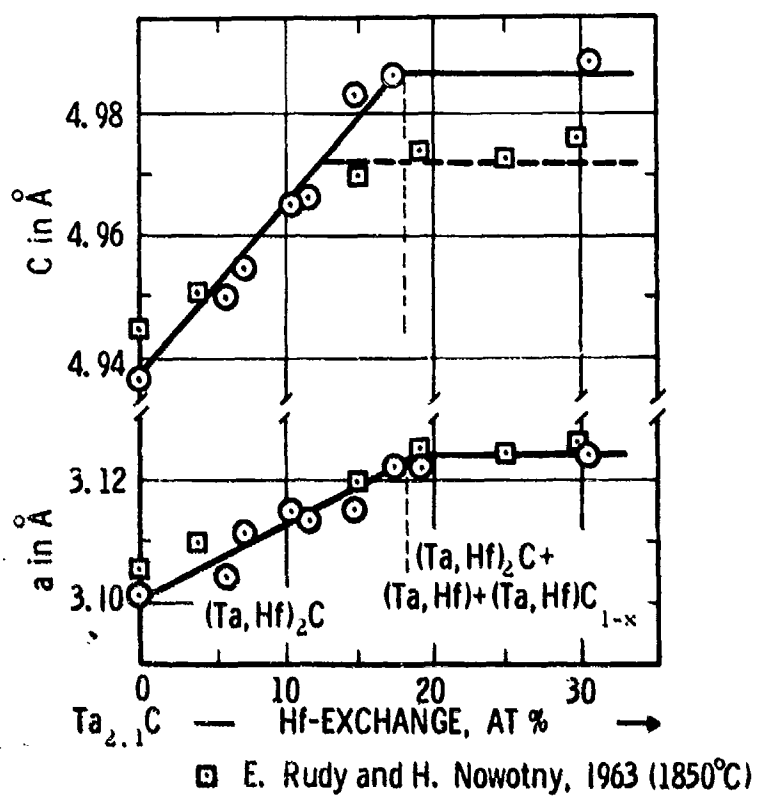

Figure 28. Variation of the Lattice Parameters of the Ta_2C-Phase with the Hafnium Content. (Alloys Equilibrated at 2000°C).

Towards lower temperatures, no new equilibria are introduced on the Ta-side of the system, i.e. the three-phase equilibrium α-Ta_2C-Ta, Hf-$(Ta, Hf)C_{1-x}$ persists, although the hafnium-exchange in the Ta_2C decreases with decreasing temperatures (approximately 10 At% at 1500°C, and 3 mole % at 1000°C), and the limiting tie line of the three-phase equilibrium moves closer to the tantalum-corner of the system.

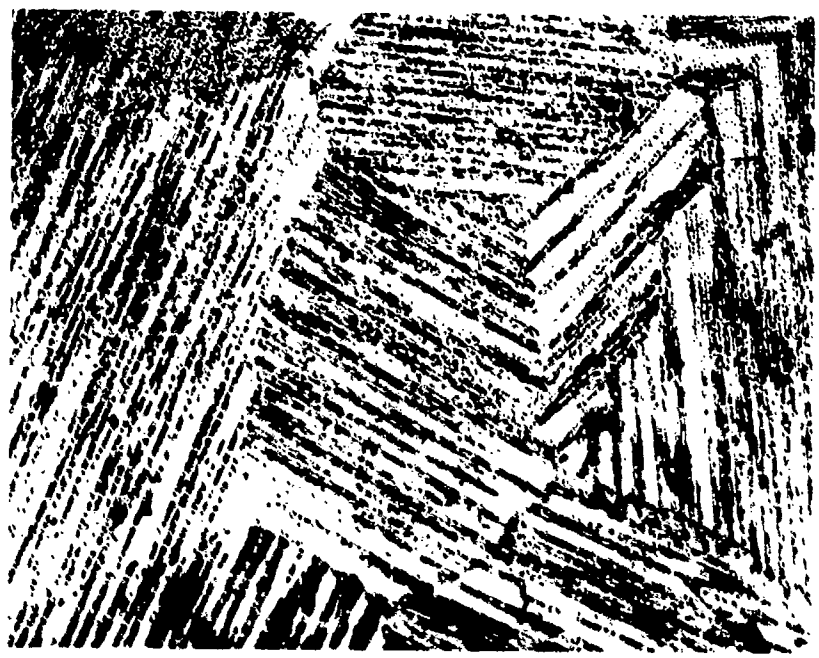

Figure 29. Ta-Hf-C (10/80/10), Cooled ~1°C per Second from 2150°C. X500

α-(Ta, Hf)-Solid Solution with Monocarbide Precipitations

Carburization of tantalum-hafnium alloys occurs strongly preferential with regard to hafnium, as evidenced by the data

presented in Table 6. The relative enrichment of hafnium in the carbide phase follows as a consequence of the higher free energy of formation of the hafnium carbides as compared with tantalum carbide phases.

Table 6. Lattice Parameters and Concentrations of Coexisting Phases in the Two-Phase Equilibrium (Ta,Hf)-(Ta,Hf)C_{1-x} (Alloys Equilibrated at 2000°C)

Concentration At%			Present Phases (X-Ray)	Lattice Parameters, Å		Approximate Hf-Exchange, At%	
Ta	Hf	C		Metal Phase	Monocarbide Phase	Metal Phase	Monocarbide Phase
70	15	15	β + γ + δ	3.318	4.532	11	60
60	15	25	β + γ + δ	3.315	4.531	10	60
65	20	15	β + δ	3.320	4.539	12	65
61	24	15	β + δ	3.324	4.547	13	68
57	28	15	β + δ	3.326	4.560	14	74
35	34	31	β + δ	3.319	4.555	12	71
39	30	31	β + δ	3.327	4.565	15	76
43	20	37	β + δ	n.d.	4.564	n.d.	76

Legent to Table 6: n.d.... not determined

β ..... body-centered cubic (Ta,Hf) solid solution

γ ..... hexagonal close-packed $(Ta,Hf)_2C$ solid solution

δ..... face-centered cubic (B1) $(Ta,Hf)C_{1-x}$ solid solution

As a result of the miscibility gap formed in the binary Ta-Hf-system, a three-phase equilibrium: Ta-rich-ss (β) —— Hf-rich-ss (β') —— monocarbide-ss is formed at temperatures below ~1900°C.

The maximum tantalum exchange in the α-Hf phase is approximately 10 At% at temperature close to melting (Figure 29) and gradually decreases, as the temperature is lowered, (Figures 30 to 34).

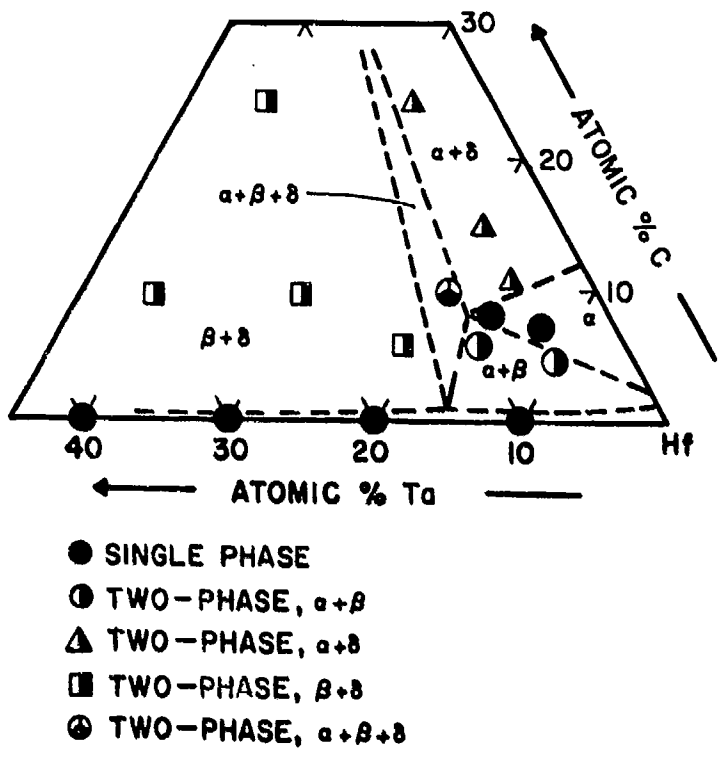

Figure 30. Ta-Hf-C: Metallographic Examination of Hf-Rich Alloys Quenched from Temperatures Ranging Between 2050°C and 2100°C.

No α-phase is observed in the alloys with tantalum contents of more than 20 atomic percent (Figure 35) and at temperatures above the four-phase reaction plane II_d, i.e. the three-phase equilibrium

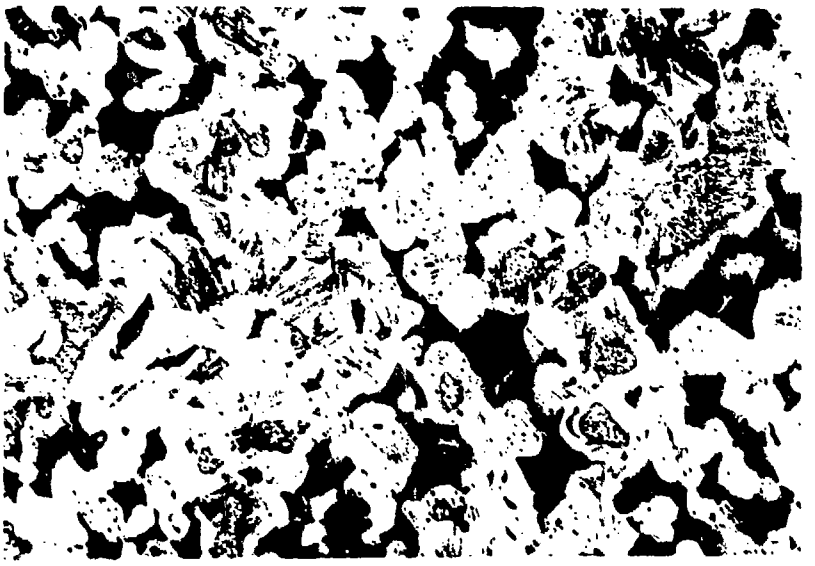

Figure 31. Ta-Hf-C (10/80/10), Rapidly Cooled from 1900°C. X125

α(Major Constituent) with Precipitations, β' (dark, partially decomposed), and Small Amounts of Monocarbide Phase.

Figure 32. Ta-Hf-C (10/80/10), Rapidly Cooled from 1900°C, and Annealed for 32 hrs at 1100°C. X300

α + β (Stained Dark by Electroetch)

Note the Carbide Phase Agglomerates Within the α-Grains and at the Grain Boundaries

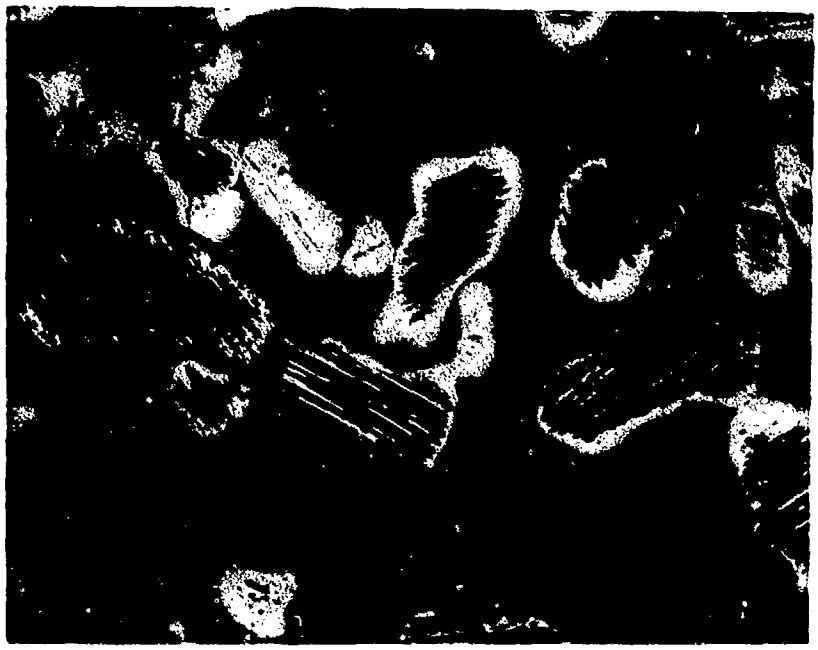

Figure 33. Ta-Hf-C (84/10/6), Rapidly Cooled from 2050°C. X250
α with Precipitations, and Partially
Decomposed β

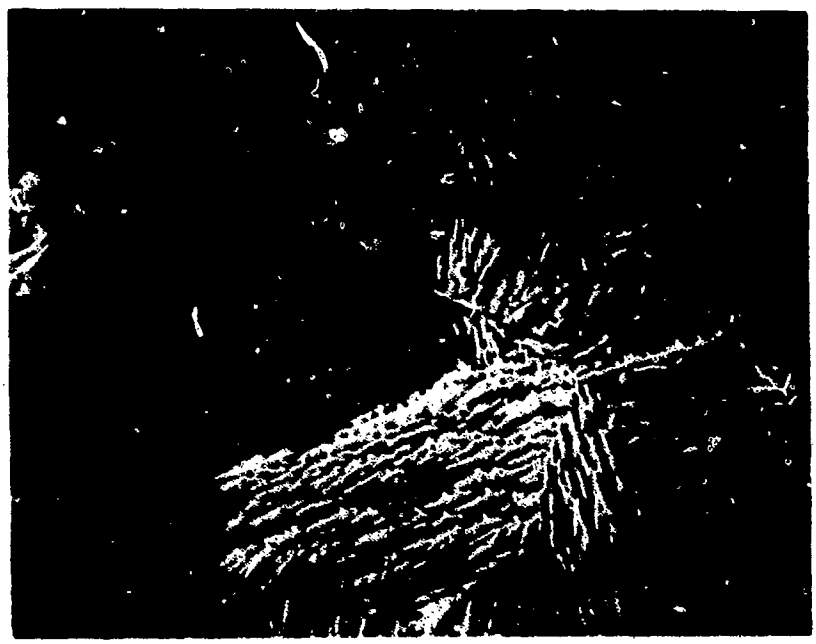

Figure 34. Ta-Hf-C (5/93/2), Cooled with Approximately X250
10°C Sec^{-1} from 2000°C.
β (Decomposed), with Traces of α

$$\alpha + \beta\ (\beta') + (\delta)$$

is confined to the compositional limits

$$Ta_{0.2}\,Hf_{0.8} - Hf - Ta_{0.2}\,Hf_{0.8}\,C_{1-x}$$

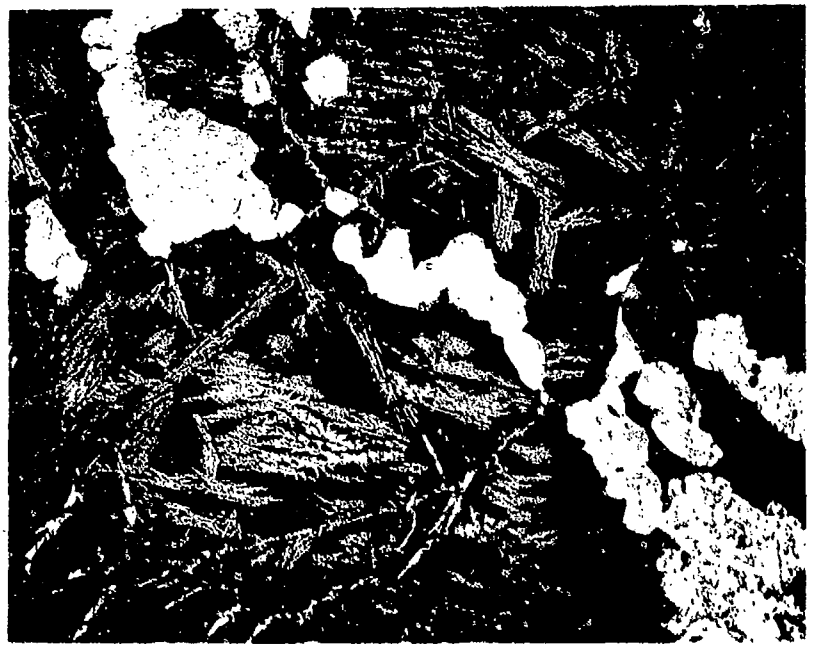

Figure 35. Ta-Hf-C (15/79/6), Rapidly Cooled From 2050°C. X500 β (Decomposed), and Monocarbide Solution (δ)

The β-solid solution, which can be retained by rapid quenching of the alloys (Figure 36) disproportionates into two distinct metal phases upon annealing at temperatures below the critical solution temperature (Figure 37).

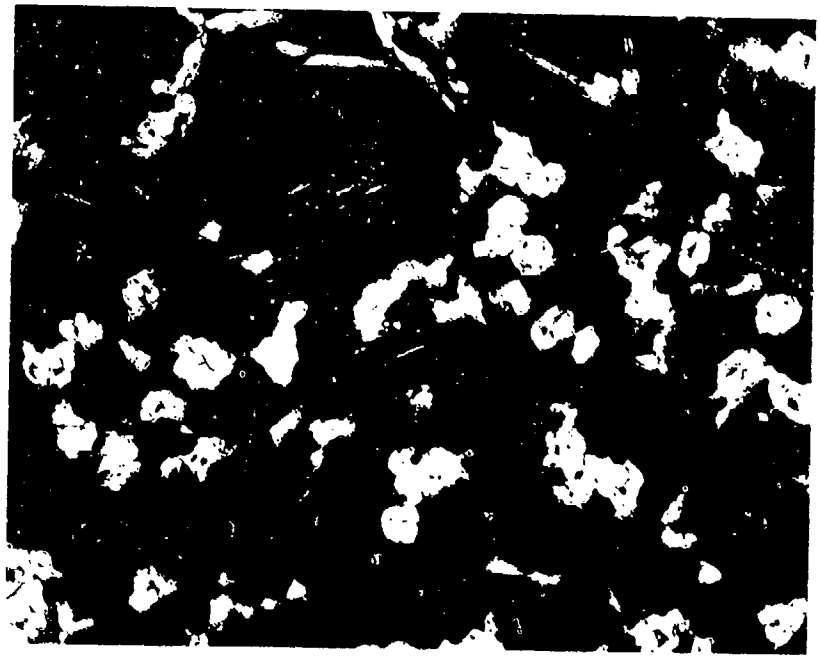

Figure 36. Ta-Hf-C (40/50/10), Quenched from 2100°C X500
Monocarbide (Light Grains), and β.
(Metal Phase Stained Dark by Electroetch)

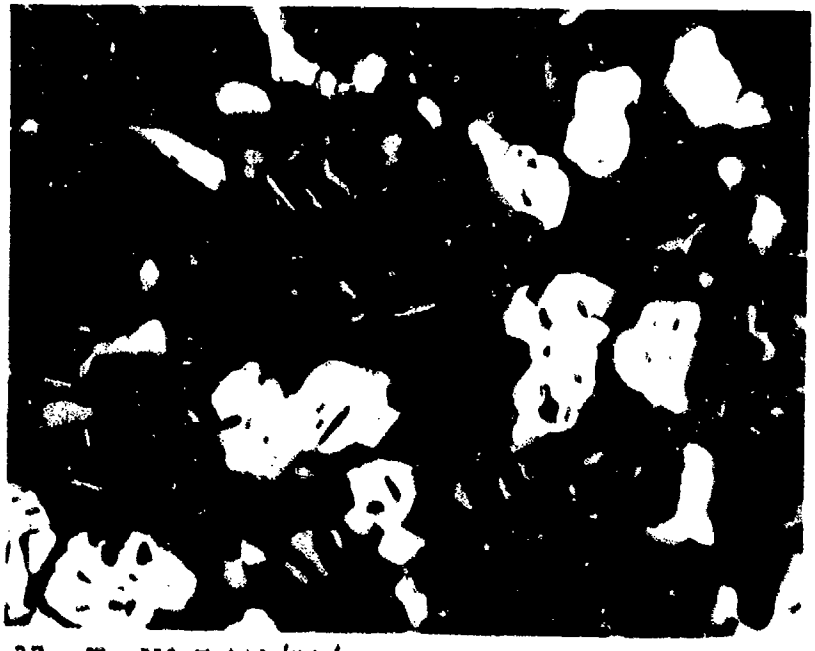

Figure 37. Ta-Hf-C (40/50/10), Quenched from 2100°C, X1000
Annealed for 30 hrs at 1380°C.
Monocarbide (Light) in a Matrix of β' (Dark)
and β (Grey) -Solid Solution.

The eutectoid reaction isotherm in the binary Ta-Hf system is observed at 1100°C. The four-phase reaction in the ternary,

$$\beta' + \delta \leftrightharpoons \alpha + \beta \quad (II_d \text{ in Figure 2})$$

which emerges from this reaction, is observed at somewhat higher temperatures (Figure 38).

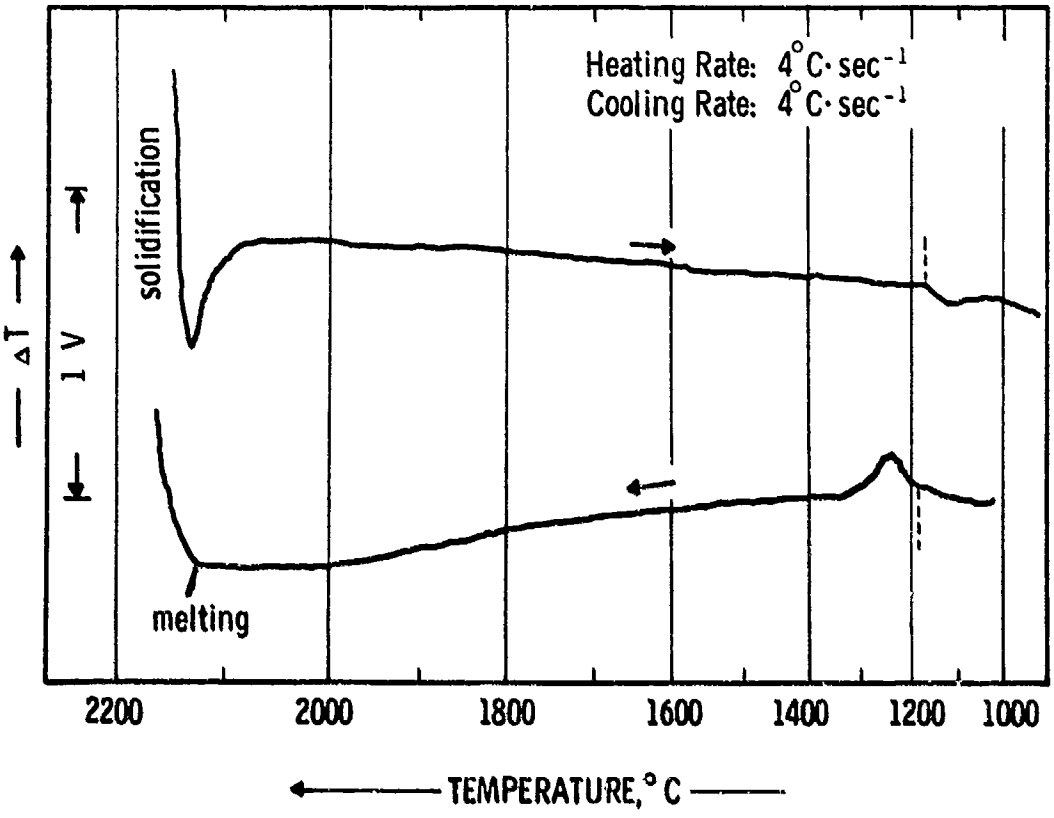

Figure 38. DTA-Thermogram of a Ta-Hf-C (30/60/10 At%) Alloy

The thermal arrest due to this four-phase reaction disappears, as the hafnium content of the alloys increases, (Figure 39).

Evidently, the disproportionation of the α-solution in the sample with 10 At% tantalum, 10 At% carbon, balance hafnium, is too slow in order to reveal the appearance of the four-phase reaction at the chosen cooling speed of the experiment.

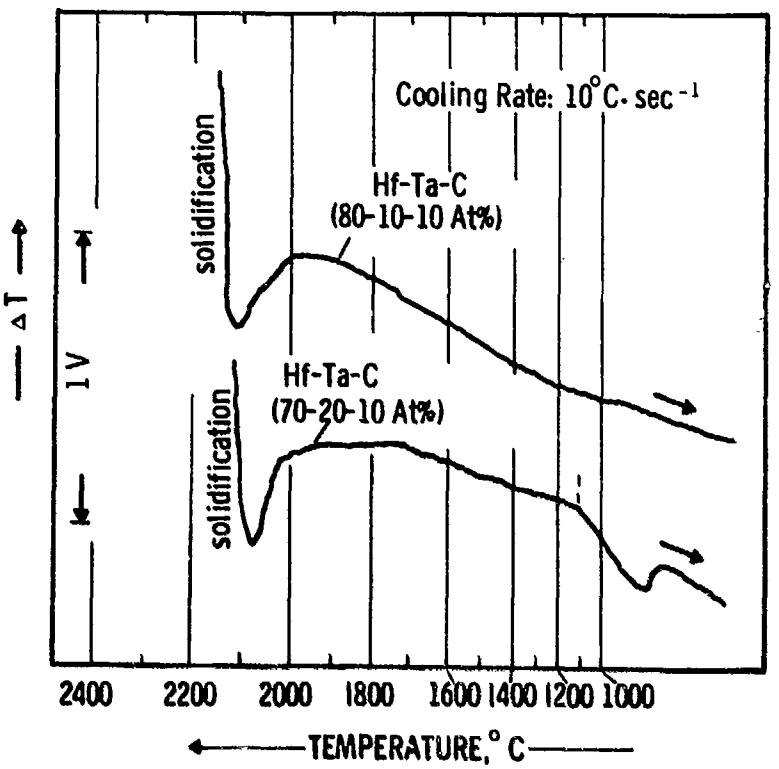

Figure 39. DTA-Thermograms (Cooling) of Hf-Ta-C Alloys in the Hafnium-Corner of the System.

The lowest liquidus temperatures in the ternary system were measured at a Hf:Ta ratio around 4 and carbon concentrations below 10 atomic percent (Figures 38, 39, and 40). Differences between the solidus temperatures of the metal solution and the melting temperatures of the eutectic trough are small (10 - 20° for the lowest melting composition), indicating that over a large concentration range the eutectic trough is located very close to the Hf-Ta edge of the system.

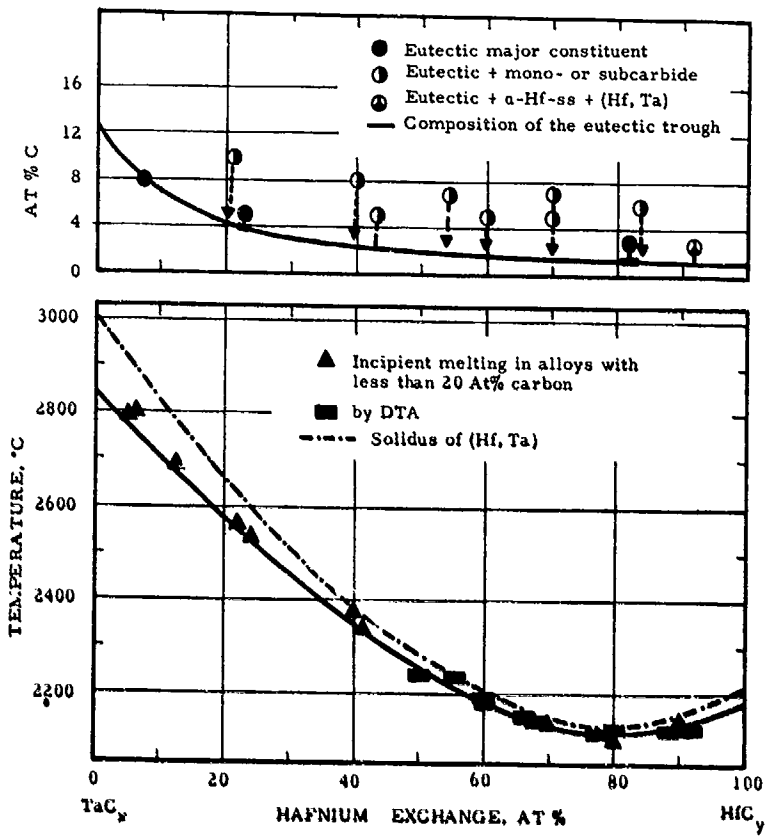

Figure 40. Composition (Top) and Temperatures of the Eutectic Trough in the Metal-Rich Portion of the Tantalum-Hafnium-Carbon System.

This was confirmed by metallographic examination of the alloys after melting and subsequent quenching, which, with the exception of alloys in the very tantalum-rich region (Figure 41),

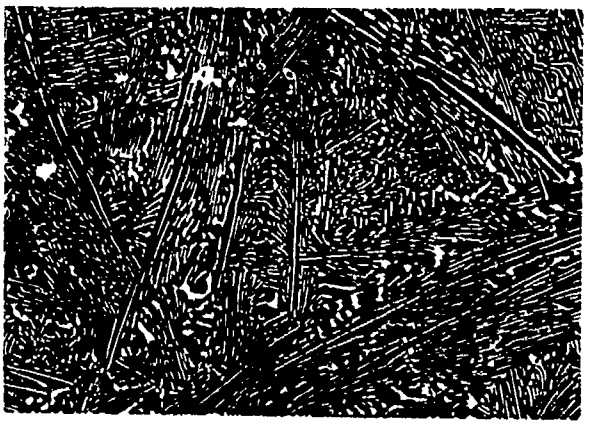

Figure 41. Ta-Hf-C (85/7/8), Quenched from ~2800°C. X400
(Ta, Hf) - $(Ta, Hf)_2C$ Eutectic

showed the monocarbide to be the primary crystallizing phase in the alloy series with 5 atomic percent carbon (Figures 40, 42).

What probably corresponds most closely to a eutectic structure obtained in samples of the more hafnium-rich and low carbon portion of the system is shown in Figures 42 and 43. The structures are not very characteristic. This may be attributed to the low carbon concentration of the eutectic, as well as to interference from carbide precipitation from the body centered cubic solution at subsolidus temperatures.

Figure 42. Ta-Hf-C (29/66/5 At%), Quenched from 2150°C X500

Primary Monocarbide (δ) and Eutectic
(Metal Phase Stained Dark by Electroetch)

Figure 43. Ta-Hf-C (17/80/30 At%), Quenched from 2130°C X500

β - δ Eutectic

The continuation of the α-β-Ta_2C reaction into the ternary phase field was studied differential-thermographically on two alloys with nominal carbon concentrations of 31 atomic percent. Starting

Figure 44. Ta-Hf-C (9/88/3), Quenched from 2170°C X750
α + β Eutectic

from the binary Ta-C system, in the average a slight shift of the observed reaction onset to higher temperatures upon hafnium substitution is observed (Figure 45).

Since the temperature of the α-β-phase reaction is raised by hafnium additions, two types of four-phase reactions, leading to the ternary decomposition of the α-Ta_2C-phase are to be considered:

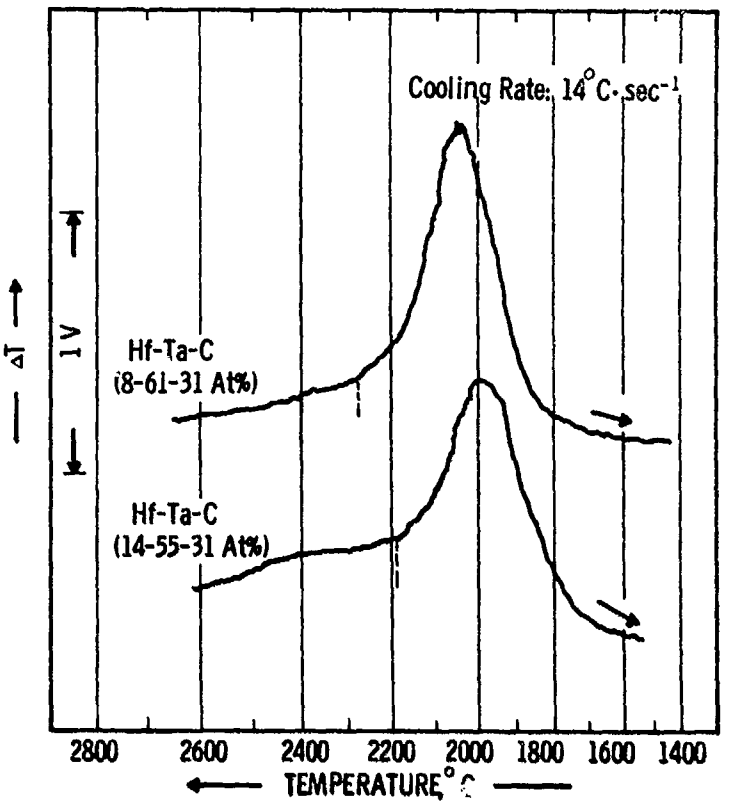

Figure 45. Ta-Hf-C: DTA-Thermograms (Cooling) of Alloys in the Stability Range of the $(Ta, Hf)_2C$ Solid Solution.

a. Decomposition of the α-phase in a ternary peritectoid (Class III four-phase reaction) according to

$$\gamma \leftrightharpoons \beta + \gamma' + \delta \qquad \text{(Figure 46)},$$

with the temperature stability maximum of the α-phase coinciding with the four-phase temperature plane.

b. Termination of the α-Ta_2C solid solution by a Class II four-phase reaction towards the ternary (hafnium-richer) field, according to

$$\gamma + \delta \longleftrightarrow \gamma' + \beta,$$

followed by a quasibinary peritectoid reaction isotherm at some intermediate composition and at a temperature which is higher than that of the four-phase reaction.

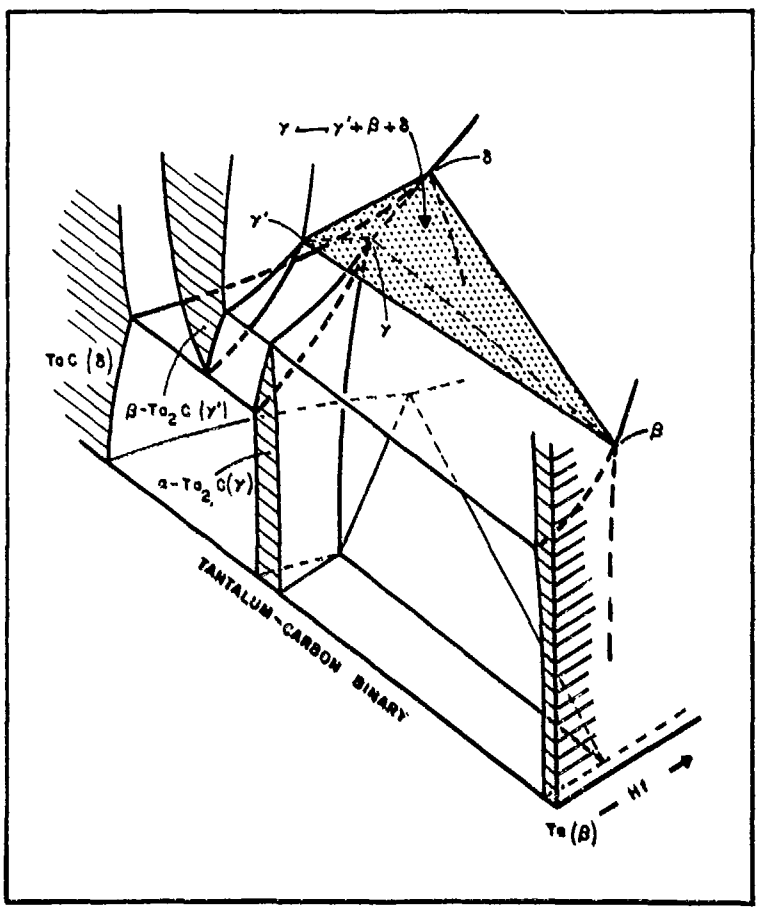

Figure 46. Possible Decomposition of the α-Ta_2C Solution in a Class III Four-Phase Reaction (Schematic).

Due to the small temperature changes involved, no firm decision could be reached. Since the differential-thermoanalytical

studies (Figure 45) favor the second version (b), a class II four-phase reaction plane in conjunction with a maximum tie line was given preference.

Two-phase melting, with a wide separation between incipient melting and the temperatures where the black-body holes collapsed, was observed in all alloys with carbon concentrations varying between 10 and 40 atomic percent.

The maximum solidus temperatures of the $(Ta, Hf)_2C$ solid solution obtained from incipient melting with the Pirani-technique as well as by differential thermal analysis, are shown in Figure 47.

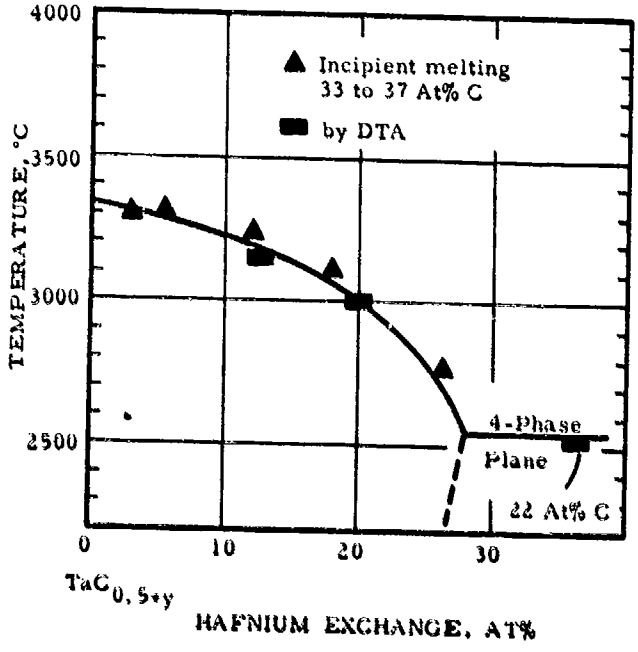

Figure 47. Approximate Solidus Curve for the $(Ta, Hf)_2C$ Solid Solution.

From the metallographic examination of samples, which were quenched from the temperature range 2300 - 2600°C, in conjunction with post X-ray examinations of the alloys, a maximum hafnium exchange of 28 atomic percent was deduced. The maximum lattice parameters for the Me_2C-phase were obtained from a three-phase sample Me-Me_2C-MeC, (a = 3.131 Å, c = 4.994 Å), which was quenched from 2500°C.

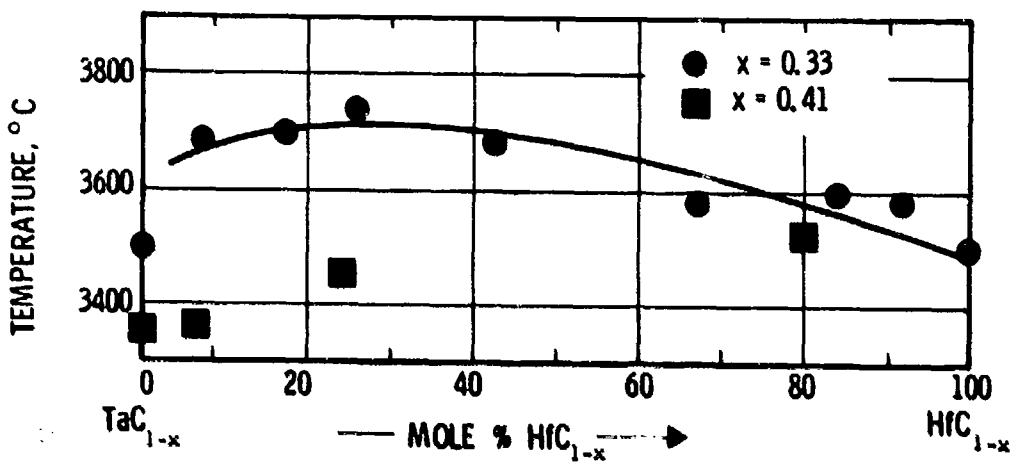

Figure 48. Solidus Temperatures of the Hafnium and Tantalum Monocarbide Solid Solution at Carbon Defects of 10 and 13 Atomic Percent.

The melting temperatures of the monocarbide solution were studied with approximately 40 alloys, which were analyzed after the runs. Alloys of the series with carbon concentrations of up to 45 atomic percent melted extremely heterogeneously, indicating a wide temperature range of coexistence of Liquidus + Solidus. Alloys from the concentration range 45 to 49 atomic percent melted fairly sharp.

Comparison of the solidus curves of the monocarbide solution at fixed carbon content (Figures 48 to 50) do indicate a solidus maximum such as proposed by C. Agte and H. Alterthum[6]. The carbon concentrations for the maximum solidus, however, vary with the hafnium exchange (Figure 3).

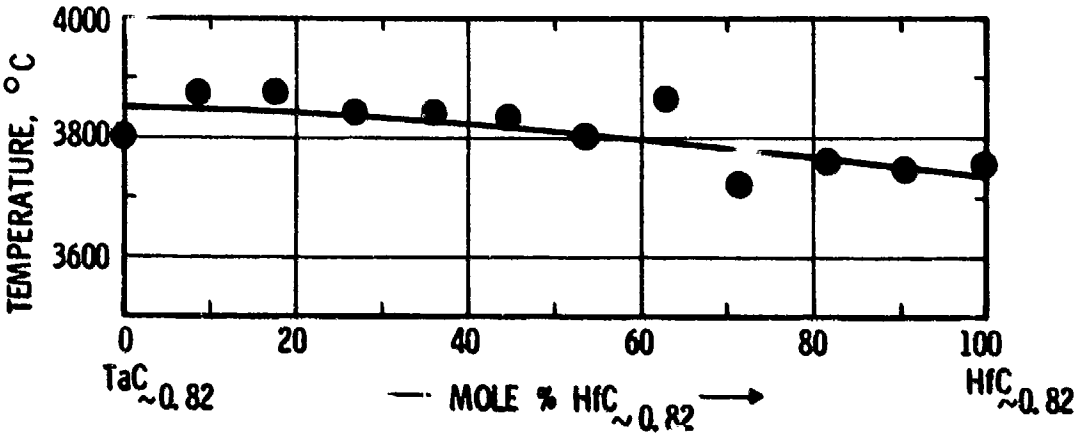

Figure 49. Solidus Temperatures of the $(Ta, Hf)C_{1-x}$ Solid Solution at a Carbon Defect of 5 Atomic Percent.

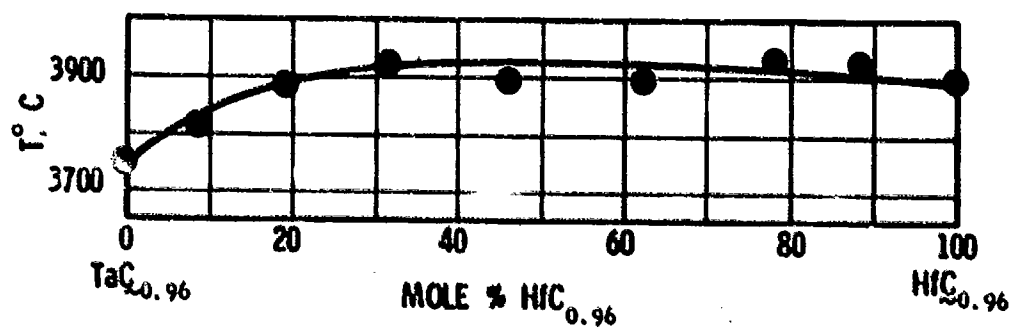

Figure 50. Solidus Temperatures of the $(Ta, Hf)C_{1-x}$ Solid Solution at a Carbon Defect of Approximately 1 Atomic Percent.

It is interesting to note, that due to the large drop of the solidus temperatures of TaC_{1-x} when either stoichiometry is approached or the solution becomes more deficient in carbon, as well as the experimental observation, that the concentration line for maximum melting shifts to higher carbon concentrations upon solid solution formation with hafnium, solidus maxima at x_c = const are simulated. The investigations of C. Agte and H. Alterthum were restricted to the measurement of one alloy series at a carbon concentration close to stoichiometry. The fact, however, that they did observe this phenomena in their limited number of experiments, is a proof of the high quality of their results, obtained over 30 years ago.

The metal and carbon-rich boundary of the monocarbide solution at high temperatures (2100 - 3200°C) was studied metallographically on quenched alloys with analyzed carbon content (Figures 51 through 56).

At 2550°C, the temperature of the four-phase-reaction isotherm, the tantalum-rich monocarbide solution in equilibrium with the solid metal phase extends to a maximum carbon defect of approximately 12 atomic percent; the width of the defect solution increases with increasing hafnium content, until at 2360°C, the peritectic reaction isotherm, the low carbon boundary reaches 34 atomic percent.

The carbon-rich boundary of the monocarbide solid solution is located at slightly substoichiometric compositions over the entire range of metal concentrations; Average carbon deficiencies varying between 0.4 and 0.7 atomic percent (2000 - 2300°C) were obtained

Figure 51. Ta-Hf-C (58/5/37 At%), Quenched from 3200°C. X750
$(Ta, Hf)C_{1-x}$ Solid Solution with Oriented
Precipitations of [ζ and $(Ta, Hf)_2C$]

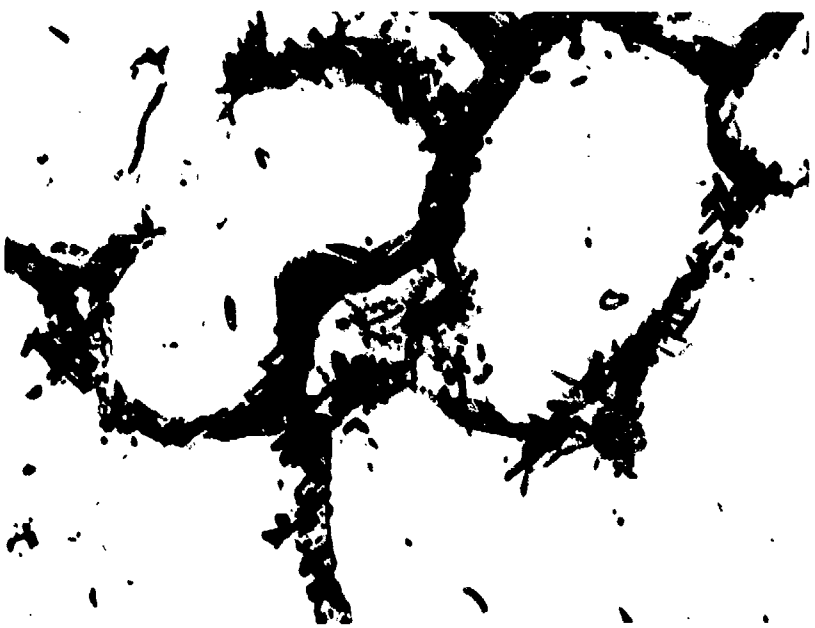

Figure 52. Ta-Hf-C (35/26/38 At%), Partially Molten at 3600°C, Equilibrated at 2600°C, and Quenched X1000
Monocarbide Solution (Cored) with Formation of New Phases { $(Ta, Hf)_2C$ and (Ta, Hf) } at the Grain Boundaries Upon Cooling.

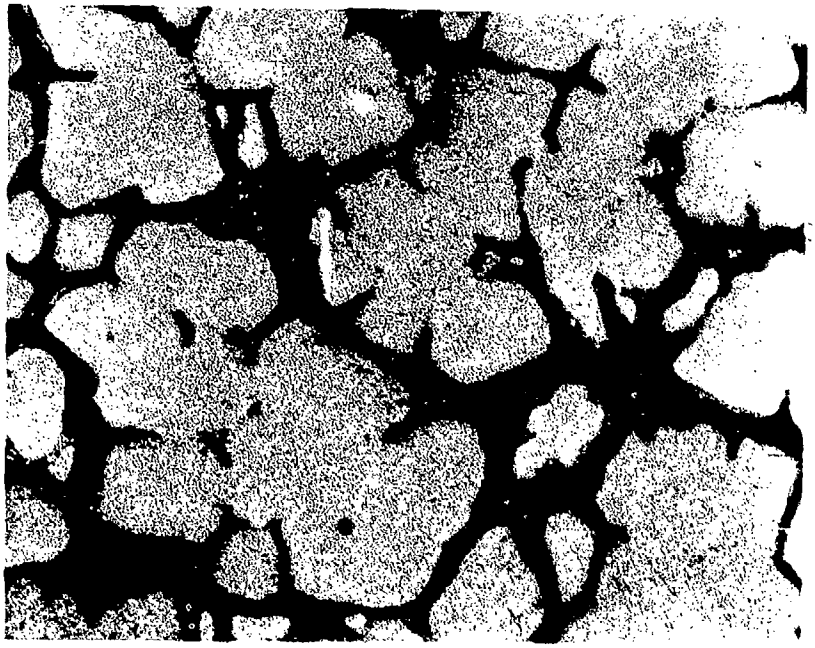

Figure 53. Ta-Hf-C (42/25/33 At%), Quenched from 2400°C. X400
Monocarbide (Light) and Metal Solution (Dark)

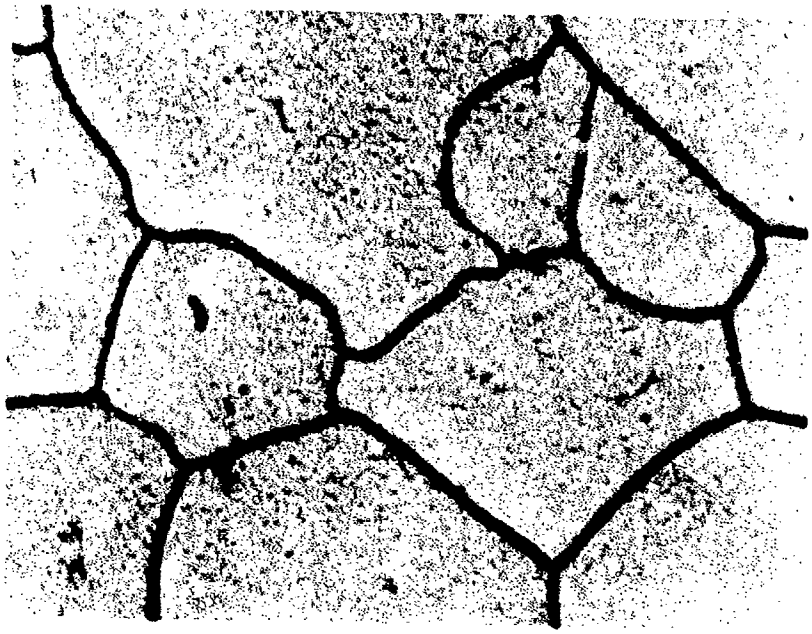

Figure 54. Ta-Hf-C (35/26/39 At%), Quenched from 2500°C. X1000
Single Phase Monocarbide Solution

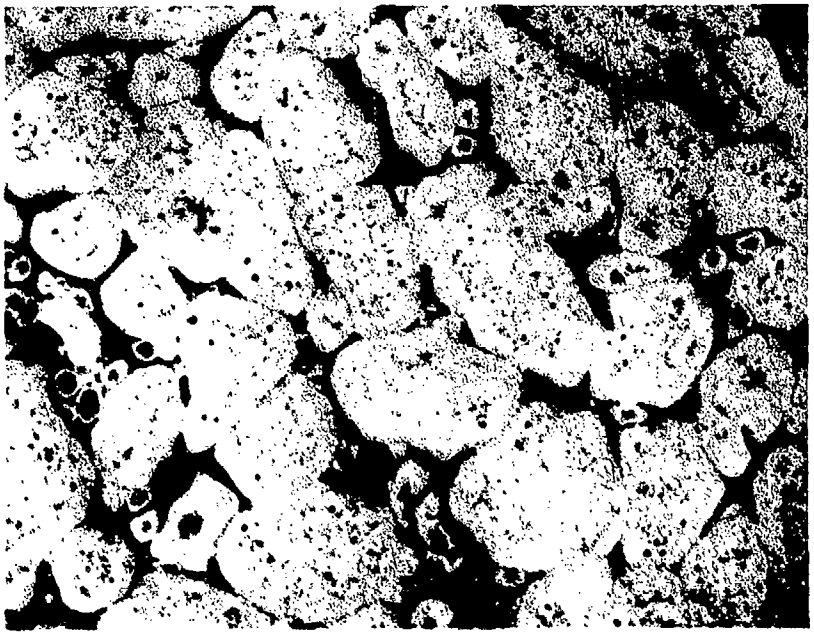

Figure 55. Ta-Hf-C (59/7/32 At%), Quenched from 2400°C. X400
Monocarbide (Light) with Metal Phase
at the Grain Boundaries

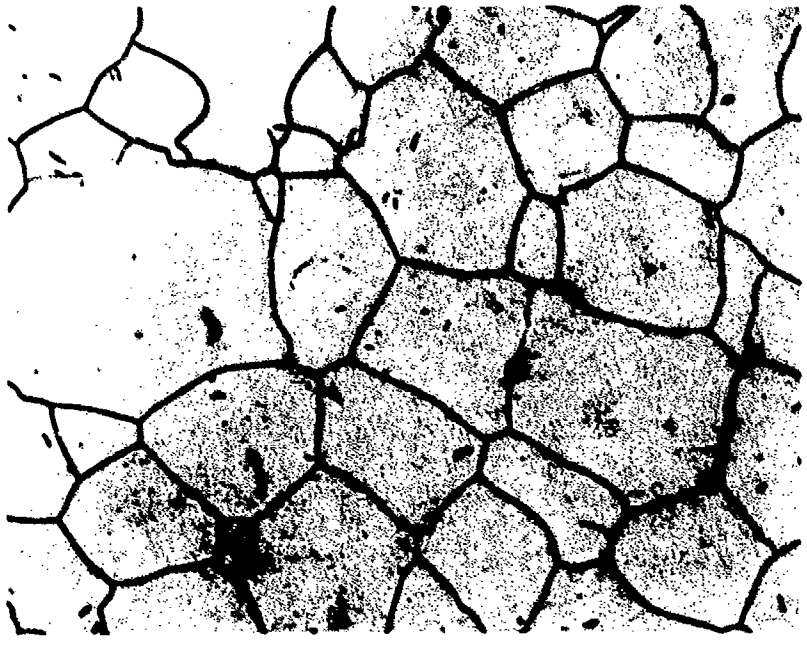

Figure 56. Ta-Hf-C (13/50/37 At%), Quenched from 2400°C. X400
Single Phase Monocarbide Solution

from analysis of free and combined carbon in excess carbon containing alloys. Although only a few analysis data were available fro. .loys which were equilibrated at slightly subsolidus temperatures (3000 - 3200°C), the results did indicate only an insignificant change of these values towards higher temperatures.

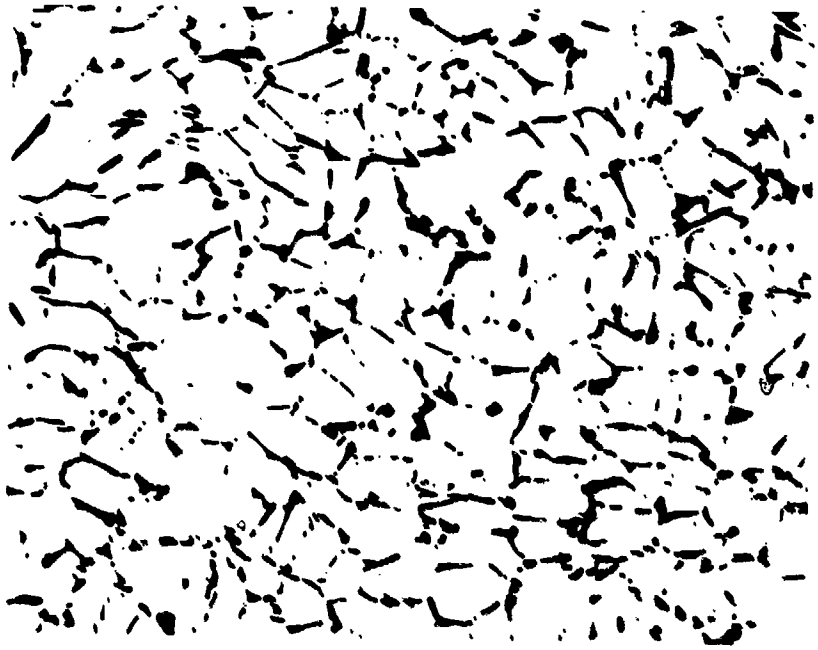

Figure 57. Ta-Hf-C (32/15/54 At%), Equilibrated at 3400°C, and Quenched. X500

Monocarbide Solution with Graphite (Carbide-Depleted Eutectic) at the Grain Boundaries.

Temperatures for the eutectic trough in the two-phase area: monocarbide solution - graphite were obtained from three samples with nominal carbon concentrations of 60 atomic percent (Figure 13). A practically linear variation between 3445°C, the TaC-C eutectic, and 3180°C, the eutectic reaction isotherm in the hafnium-carbon binary system, was obtained.

The experimental evidence is summarized in the constitution diagram shown in Figure 2, covering the temperature range above 1000°C. In view of the extreme slow reaction rates to be expected

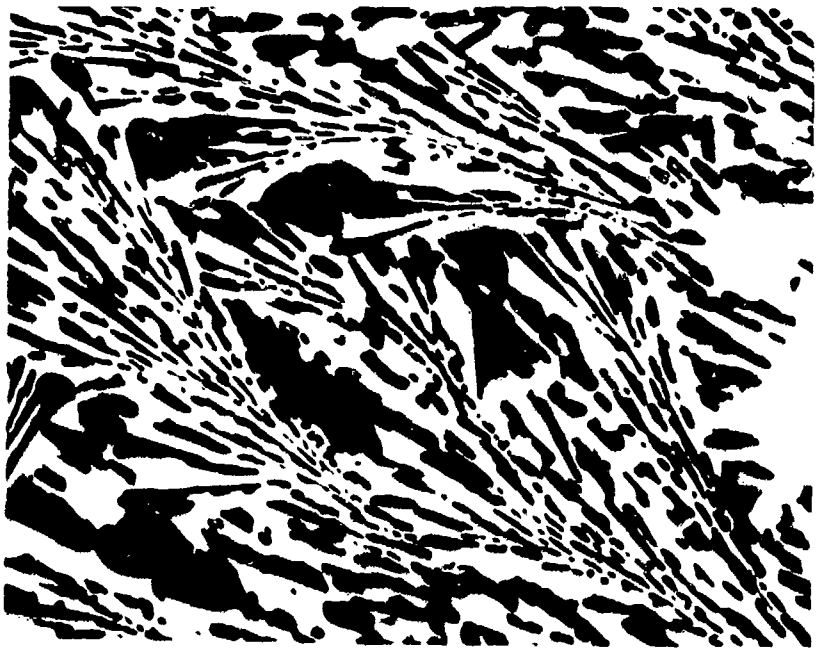

Figure 58. Ta-Hf-C (20/20/60) At% Nominal Composition X1000
64 At% Carbon After Equilibration with
Graphite at 3330°C
Monocarbide - Graphite Eutectic

for temperatures below 1000°C, no attempt was made to extend the experimental investigations below this temperature.

To facilitate reading of the phase diagram, a series of temperature sections were prepared and are presented in Figures 59 through 80. Somewhat closer spaced temperature intervals were employed in the vicinity of the four-phase temperature planes in order to depict more clearly the phase changes taking place at these reaction isotherms. Only one isopleth, which was felt to be most comprehensive in the presentation

of the complex equilibria in the metal-rich portion of the system, was prepared (Figure 5). For specific needs, isopleths across any given composition ratios can be developed from the temperature sections.

Finally, the phase diagram data are supplemented by the sketch of the liquidus projections shown in Figure 81.

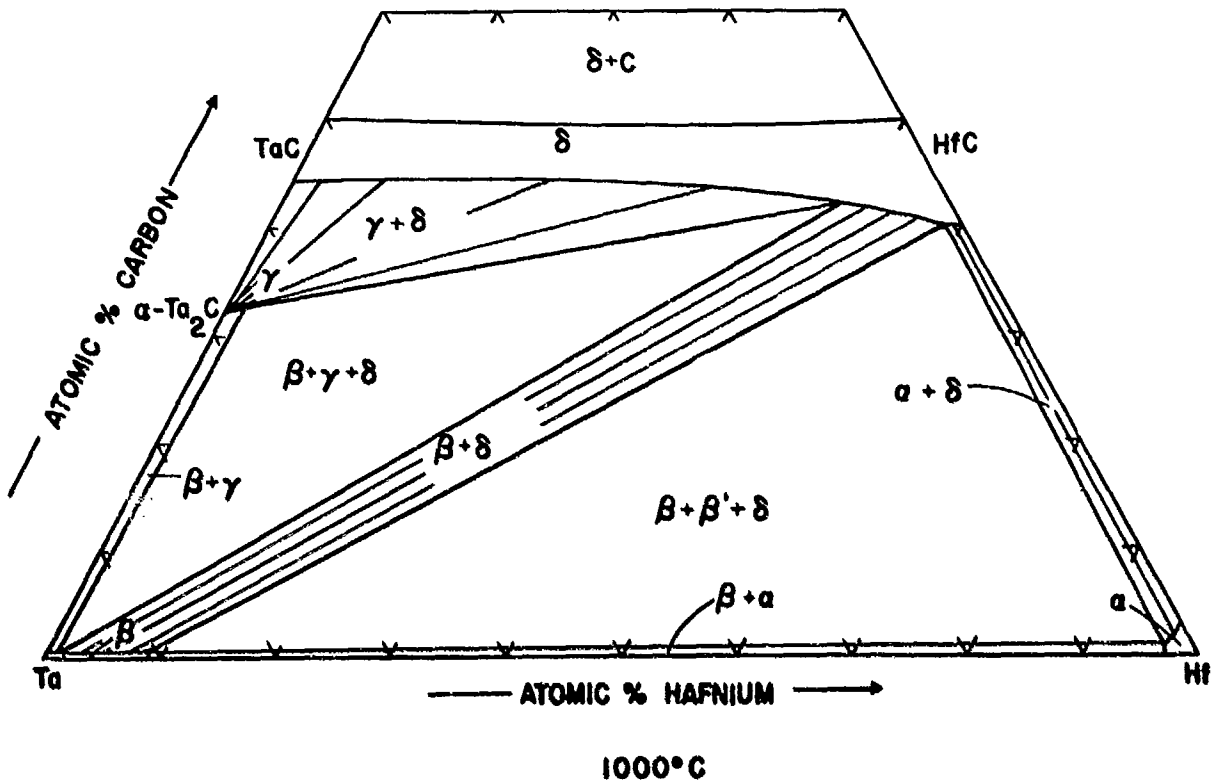

Figure 59.

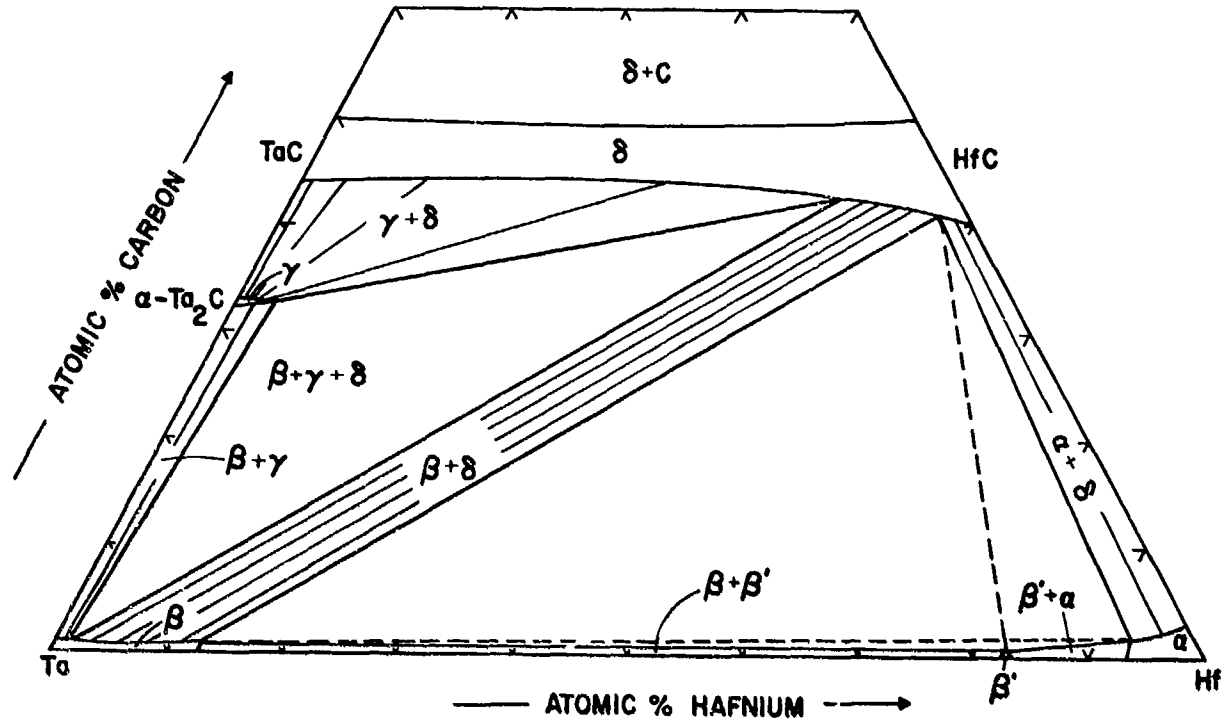

Figure 60

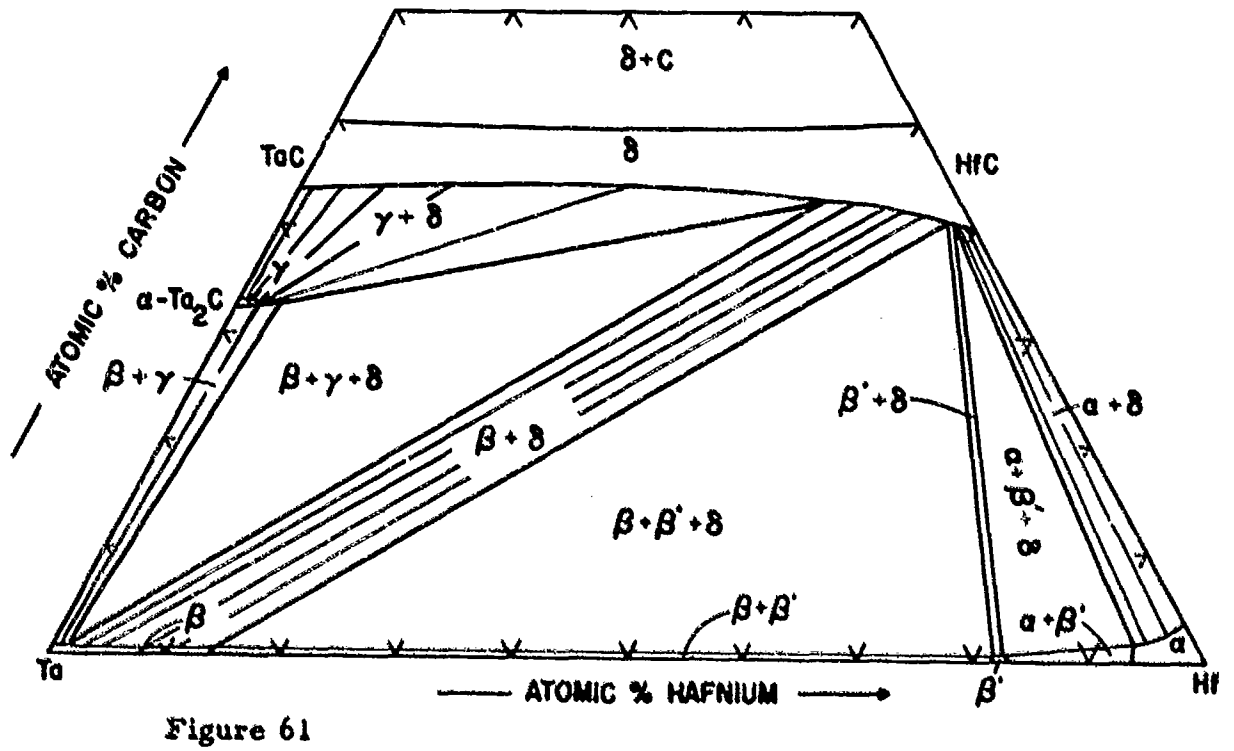

Figure 61

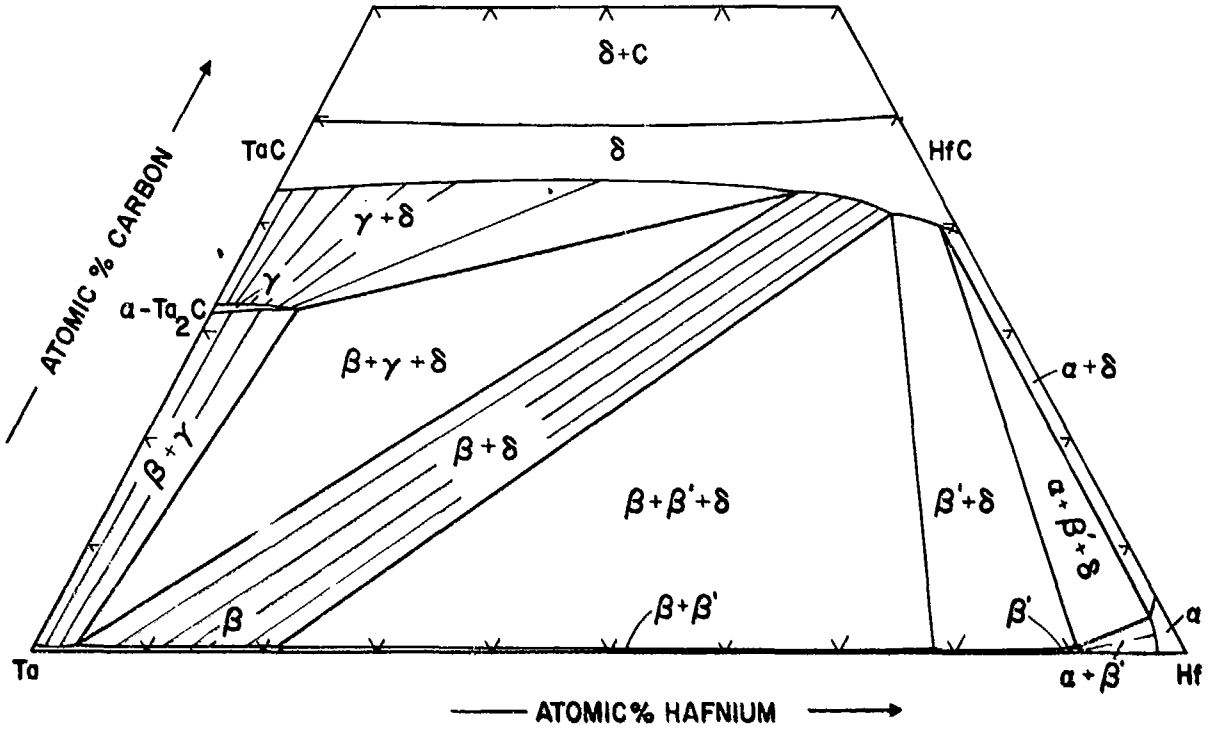

Figure 62

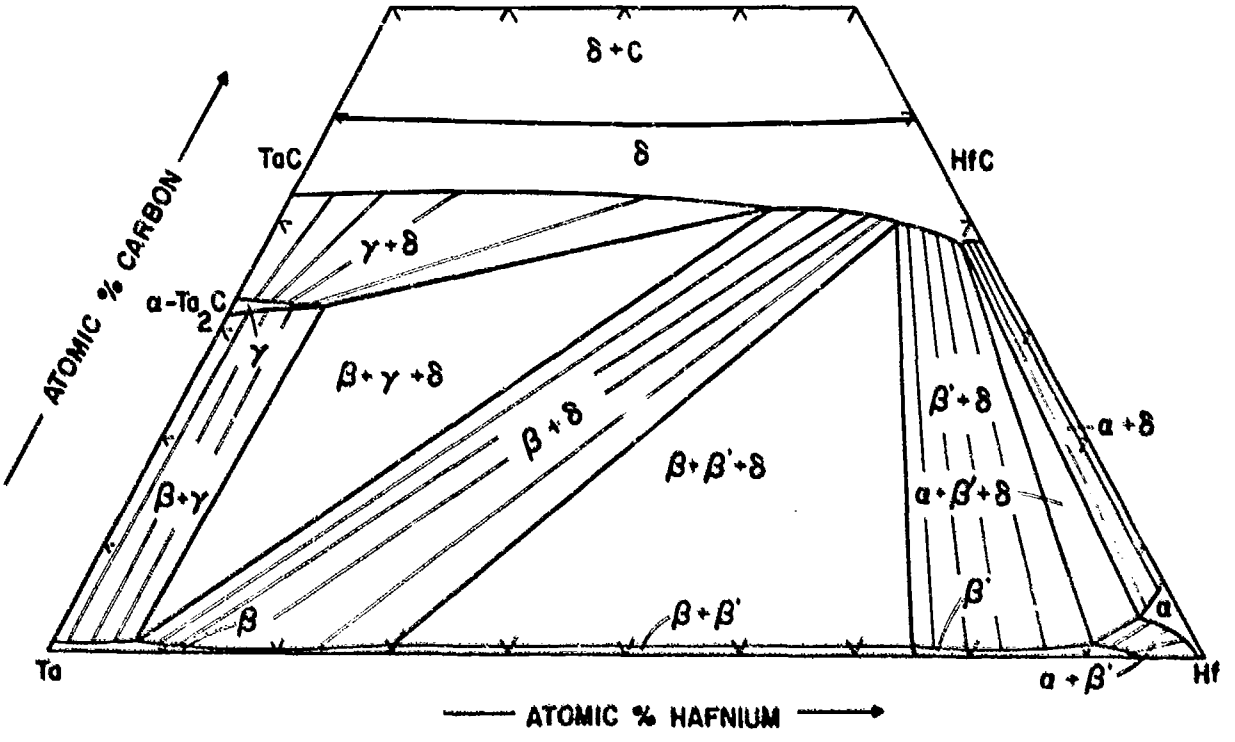

Figure 63

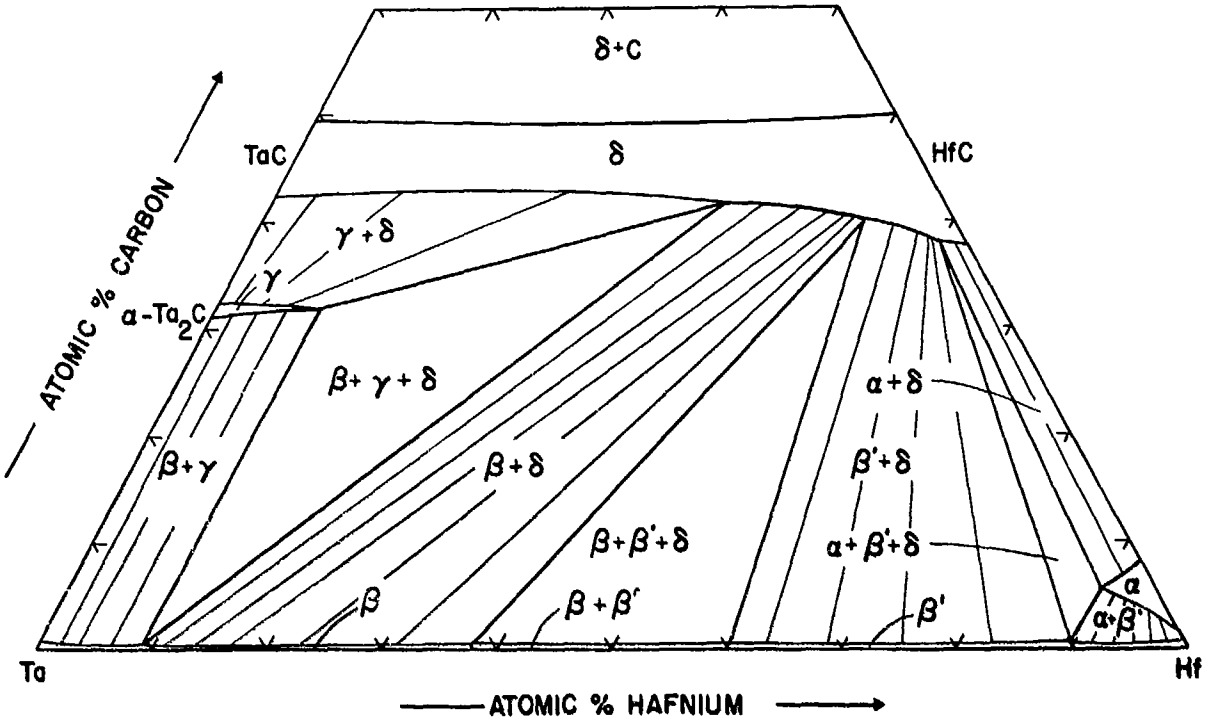

Figure 64

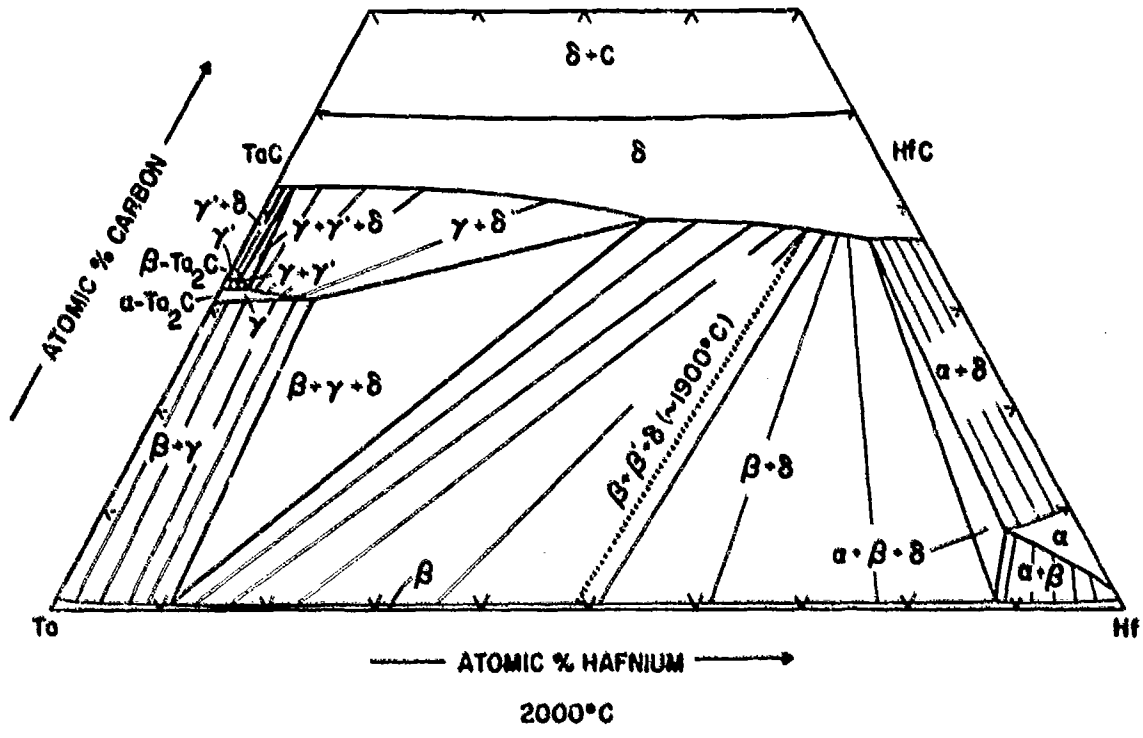

Figure 65

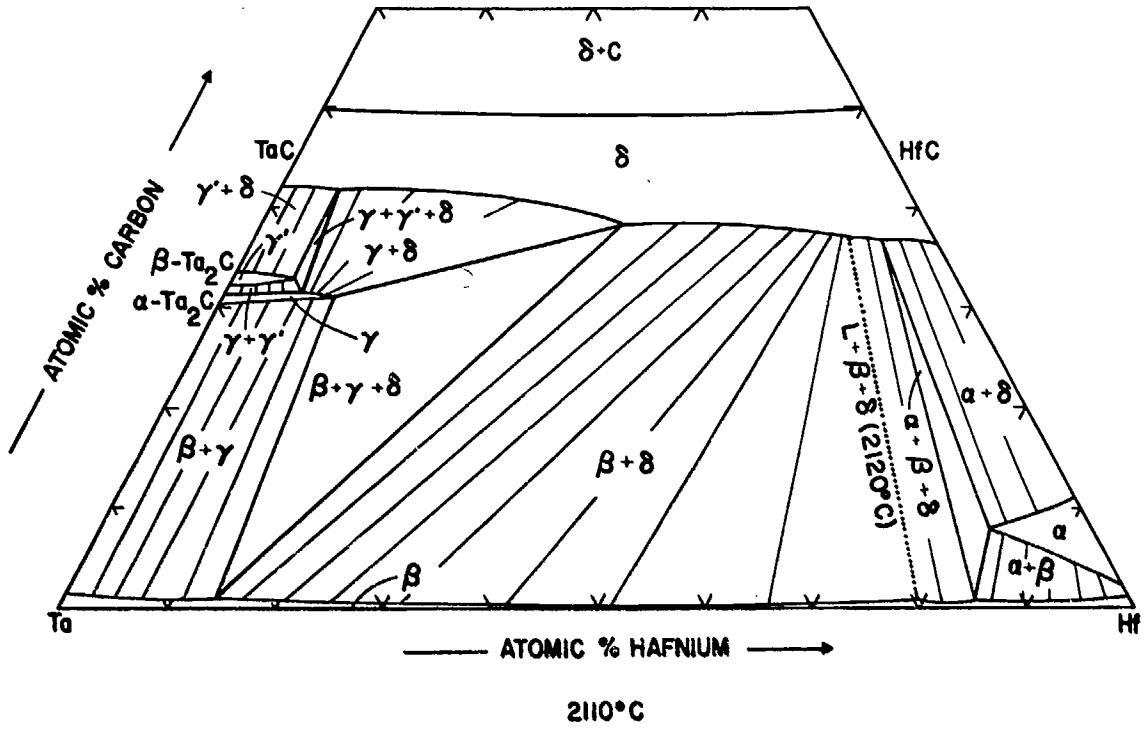

Figure 66

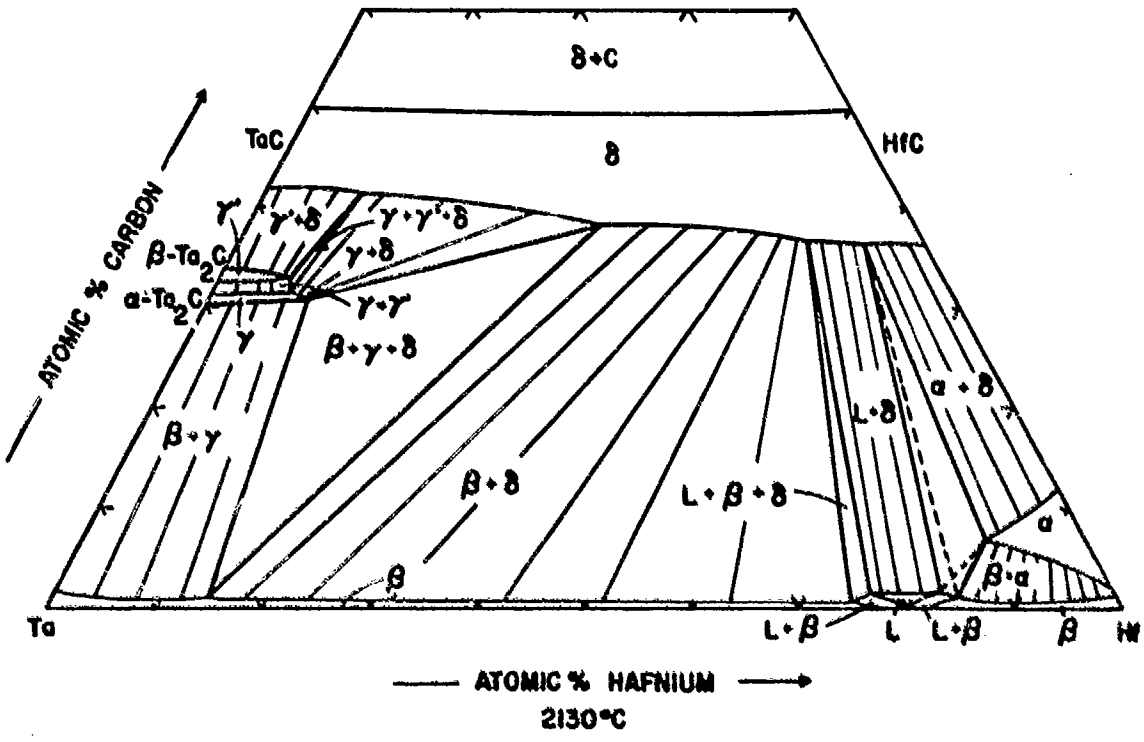

Figure 67

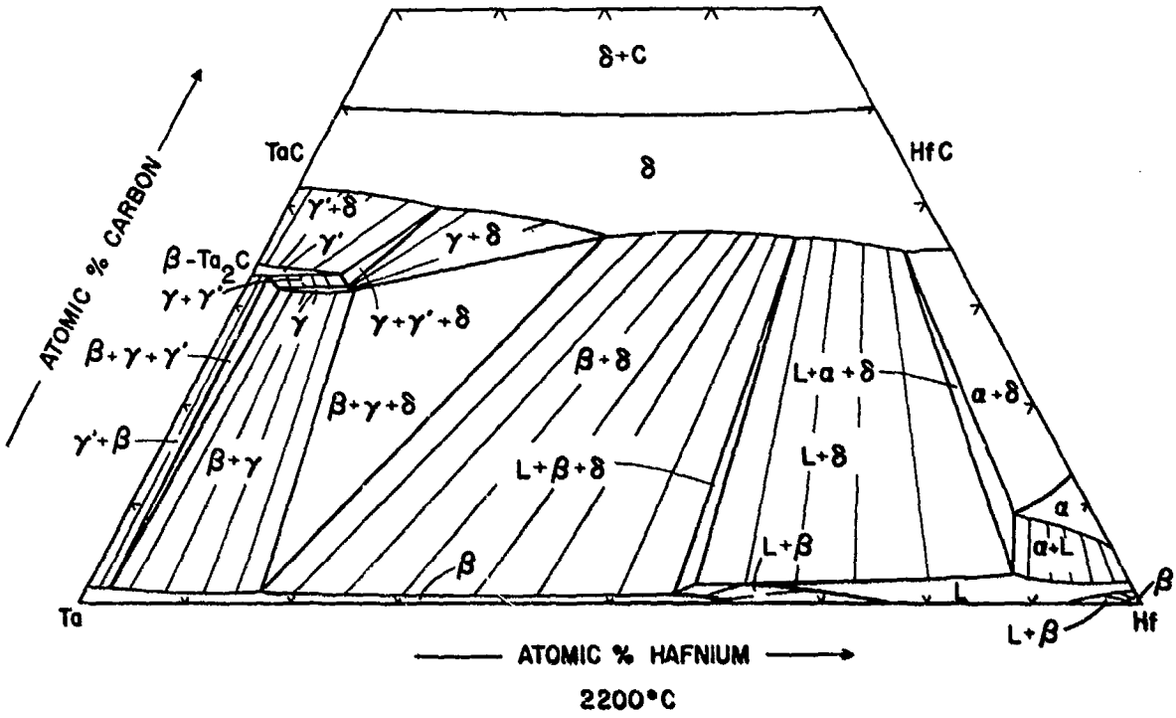

Figure 68

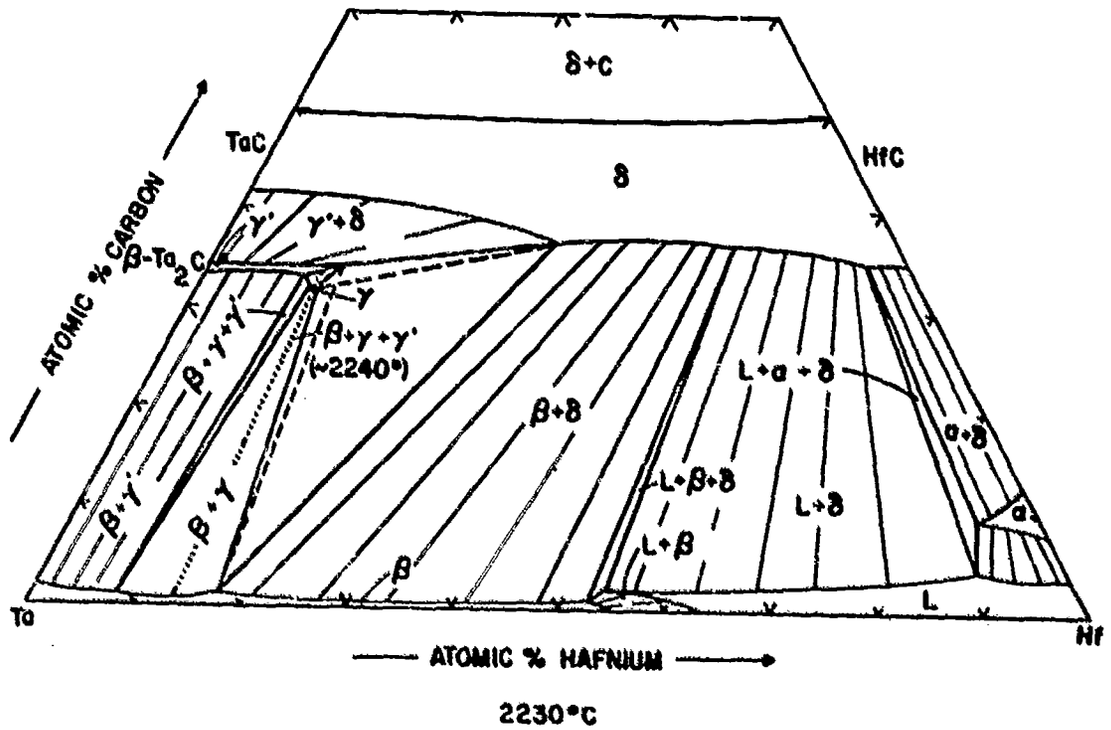

Figure 69

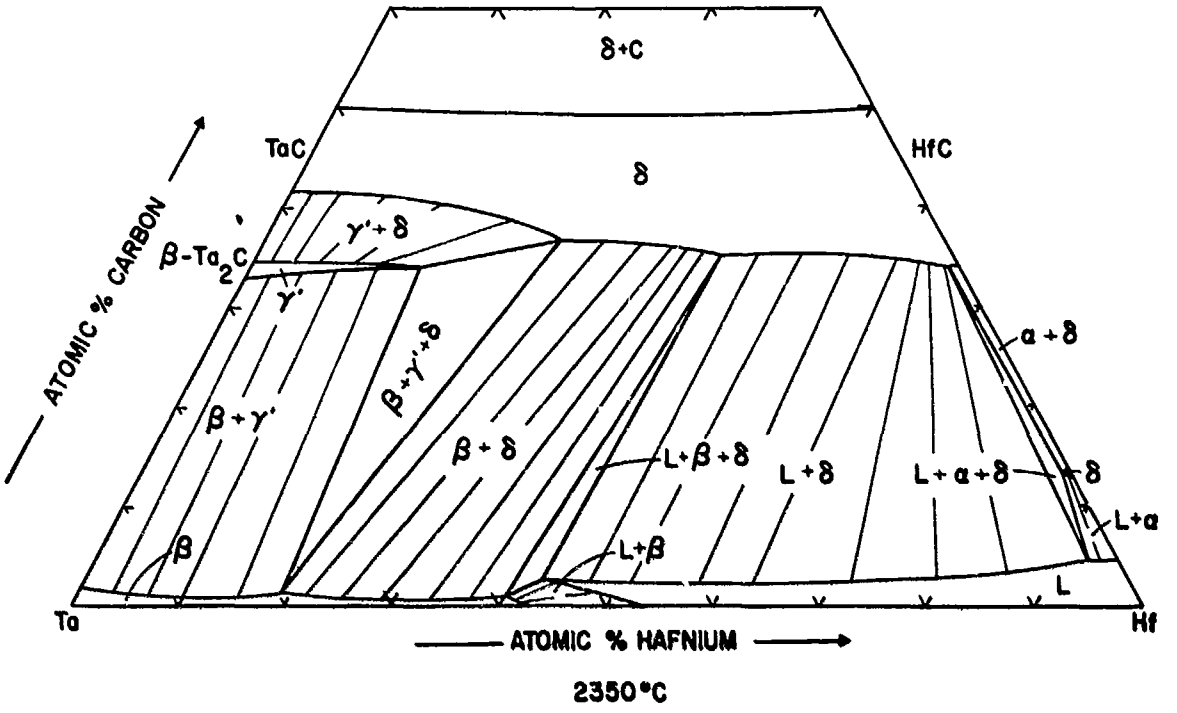

Figure 70

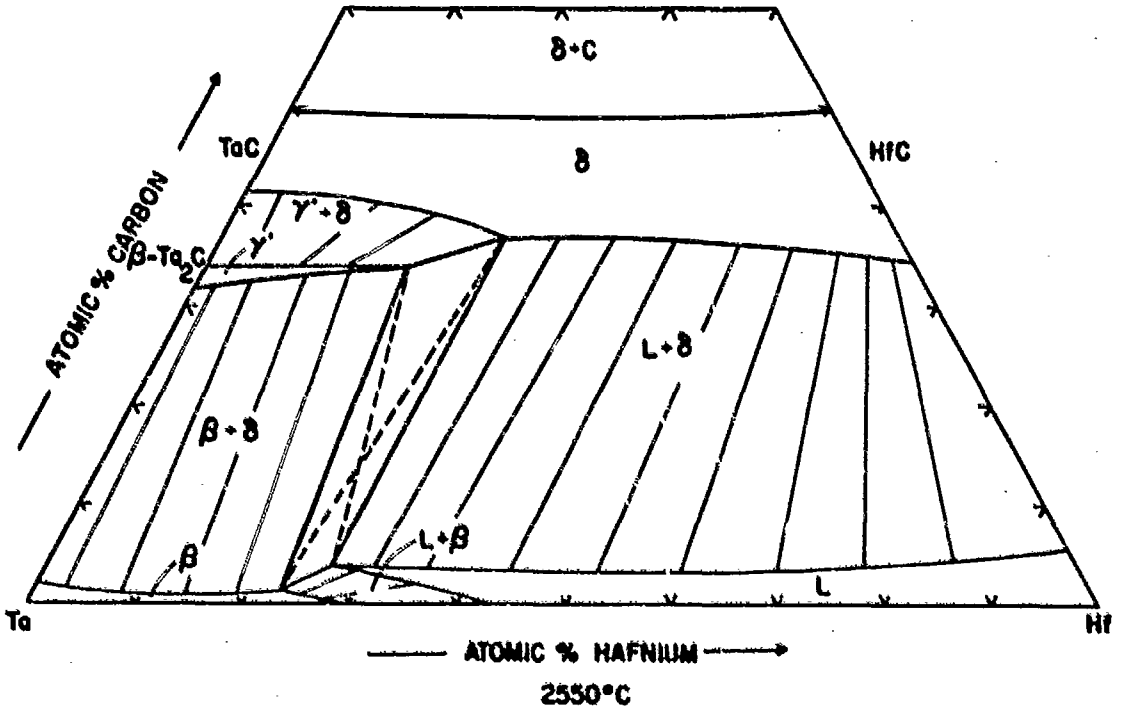

Figure 71

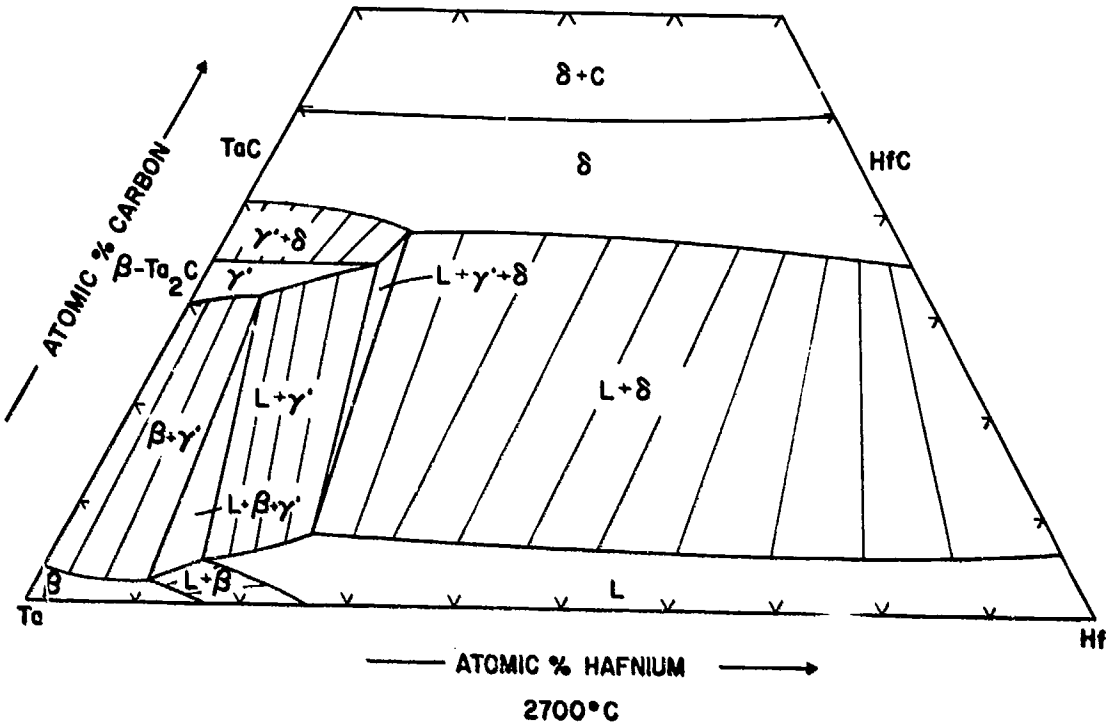

Figure 72

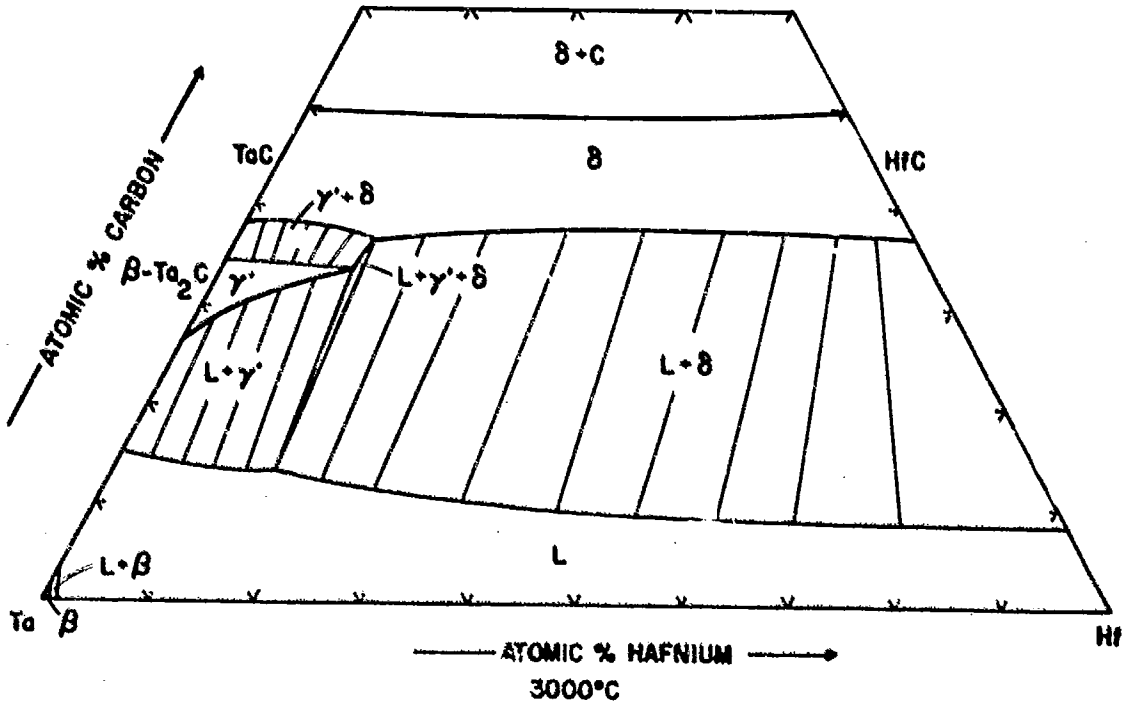

Figure 73

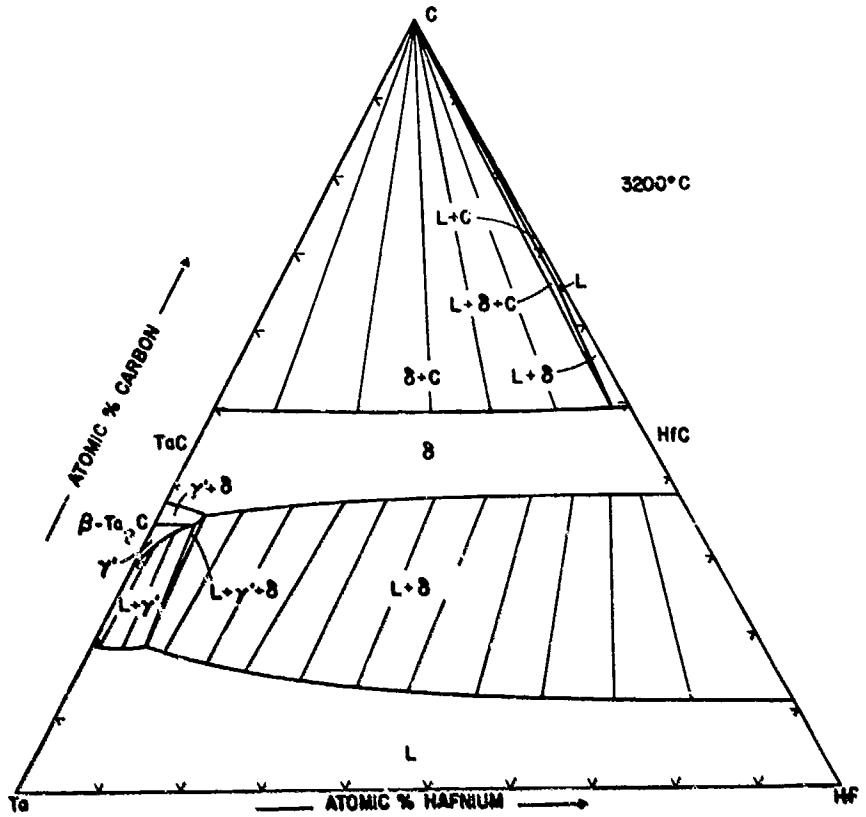

Figure 74

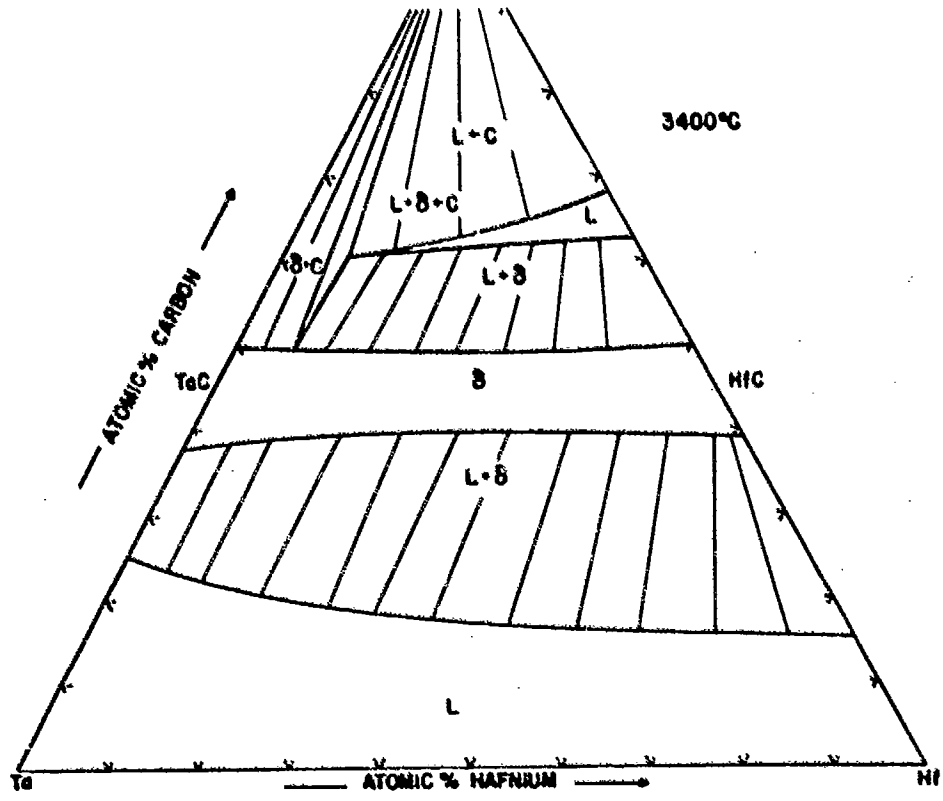

Figure 75

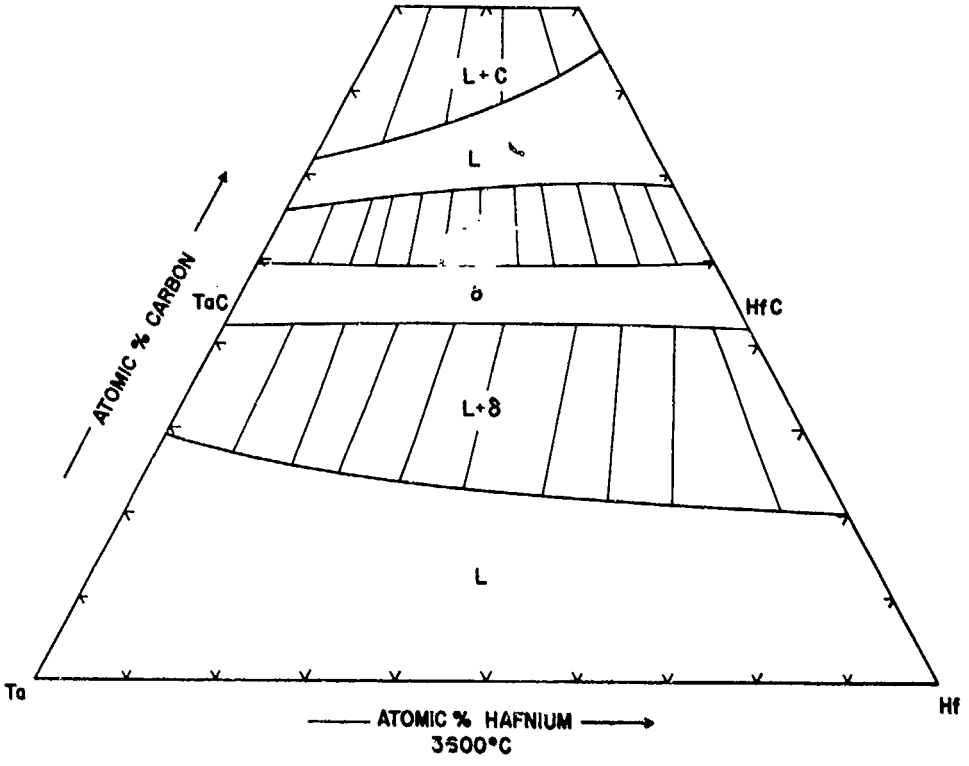

Figure 76

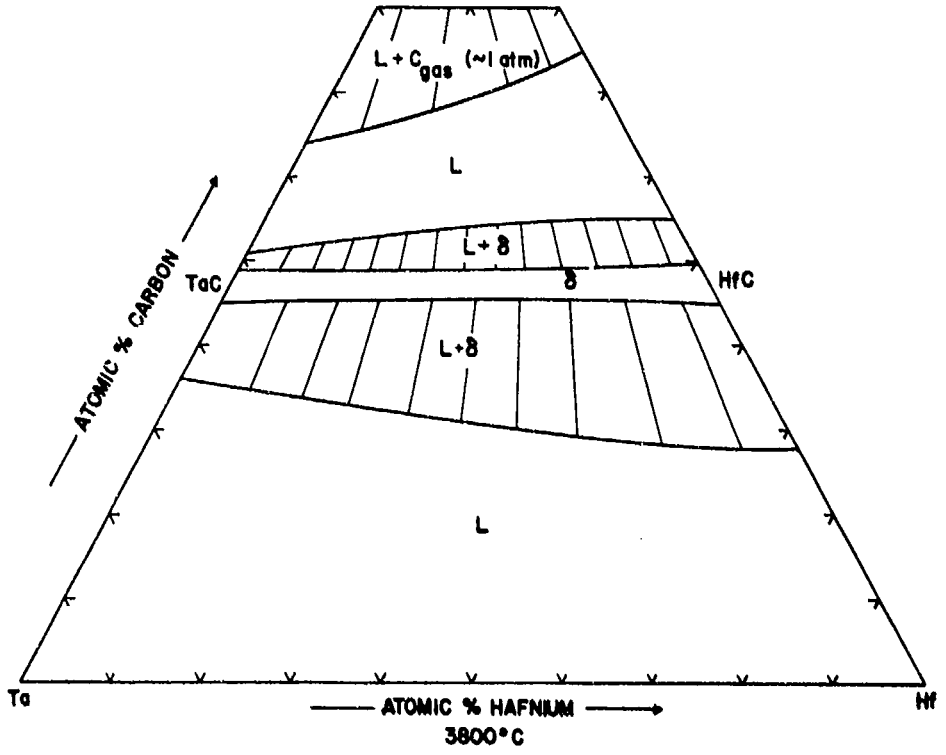

Figure 77

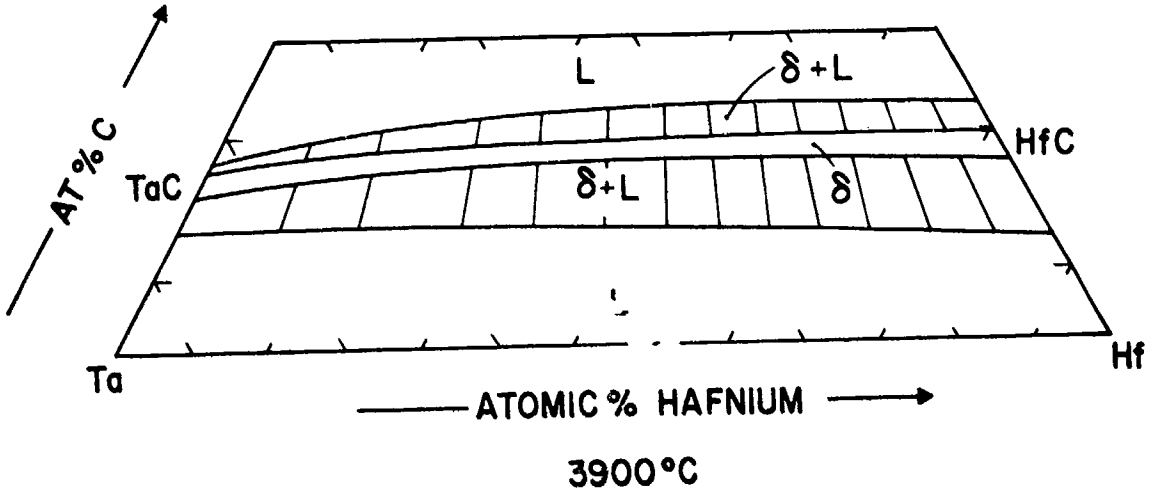

Figure 78

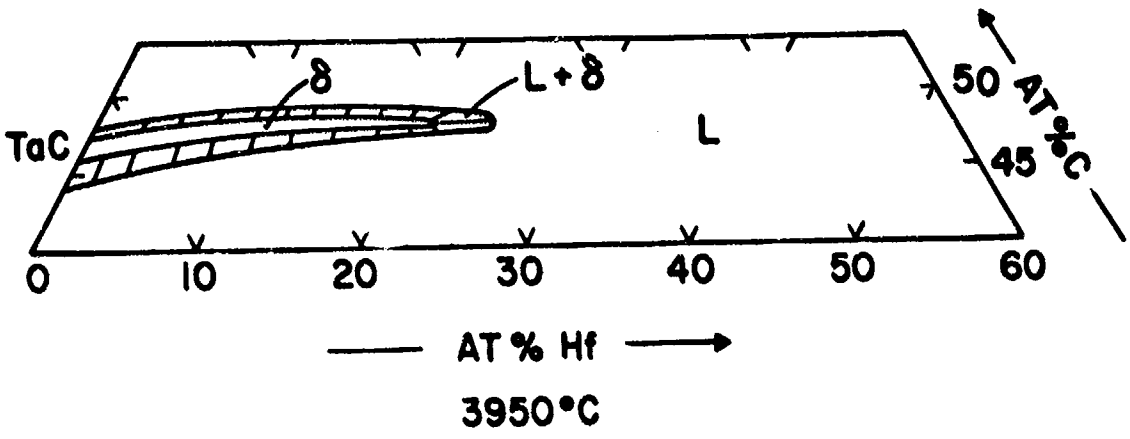

Figure 79

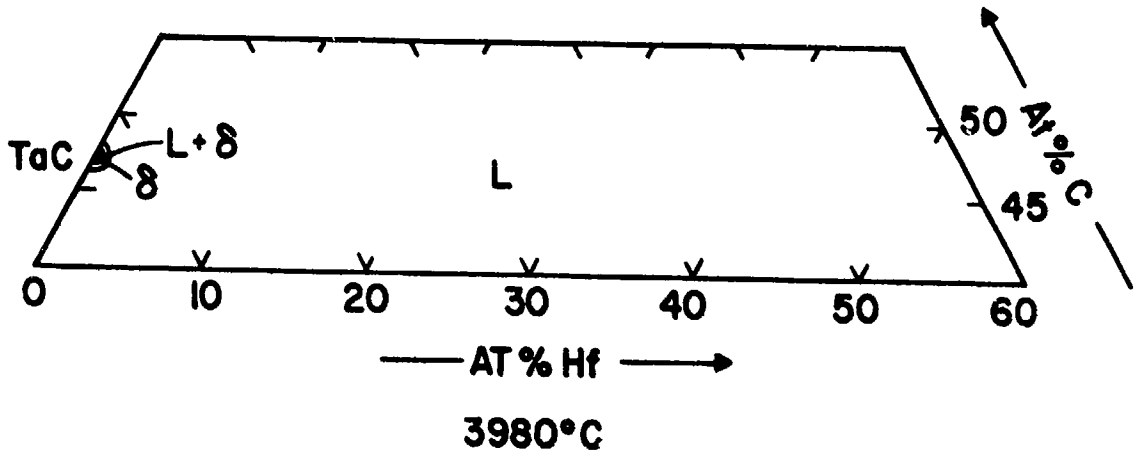

Figure 80

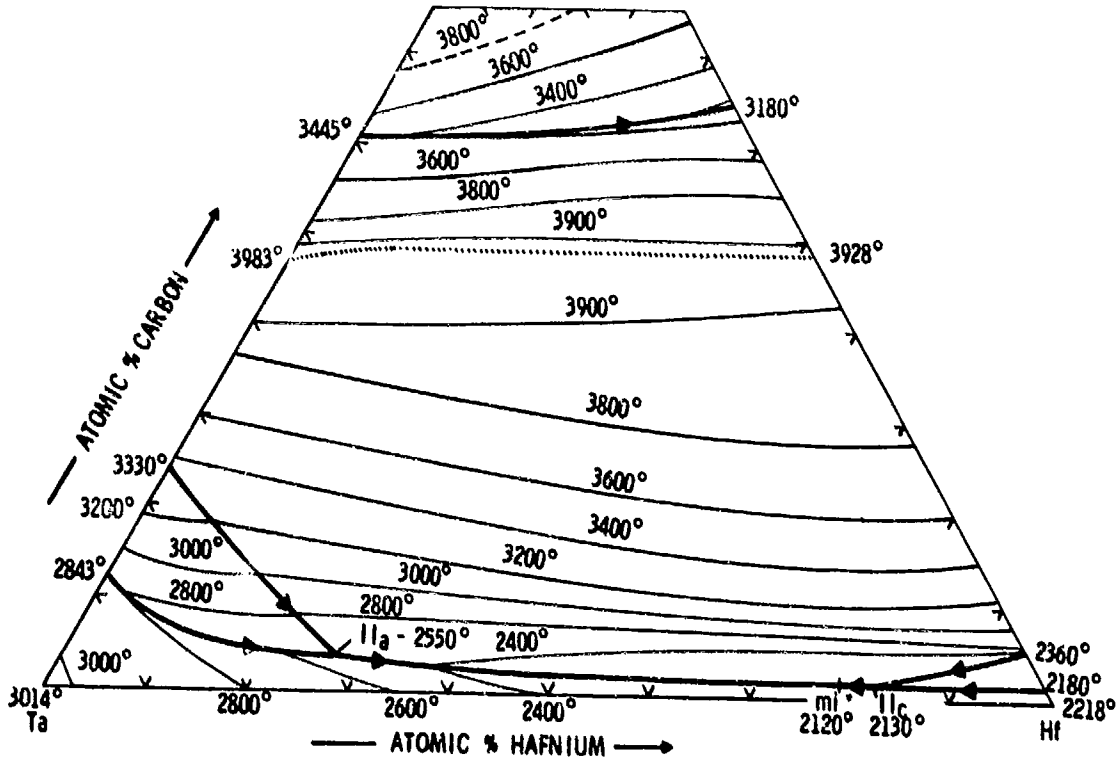

.... MAXIMUM SOLIDUS TEMPERATURES OF $(Ta,Hf)C_{1-x}$

Figure 81. Liquidus Projections in the System Tantalum-Hafnium-Carbon

(Liquidus Data Estimated from the Melting Behavior of the Alloys)

IV. DISCUSSION

A. PHASES AND PHASE EQUILIBRIA

With the exception of the equilibria in the hafnium-corner of the system, where the corresponding binary data have been established only recently[2], the solid state sections at the corresponding temperatures determined in this investigation are in good agreement with the previous findings by E. Rudy and H. Nowotny[28].

The tie line distribution in the two-phase field (Ta, Hf)-(Ta, Hf)C_{1-x} is a direct consequence of the higher stability (free energy of formation) of the hafnium monocarbide phase as compared to tantalum monocarbide. A thermodynamic evaluation of the distribution equilibrium[28] yielded a value of

$$\Delta G_f\,(HfC_{\sim 0.82}) - \Delta G_f\,(TaC_{\sim 0.82}) \simeq -8500 \text{ cal per gram atom}$$

which is in reasonable agreement with data obtained by calorimetric methods[30]. Surprisingly high appears the free energy difference between a Ta_2C-type 'Hf_2C' phase and the homootectic defect - monocarbide[28], since the close structural relationships would suggest small energetical differences between both modifications only. The solid solution model for the Me_2C-phase employed in the previous calculations is certainly an over-simplifications, since not only the metal exchange, but also the change of order in the carbon sublattice upon metal-substitution will affect the course of the free energy of the solid solution and hence the data obtained from such back calculations. Nevertheless, the same trend is indicated by the

phase relationships in the binary hafnium-carbon system (Figure 6), where the carbon-stabilized α-modification of hafnium is terminated at relatively low temperatures and carbon concentrations (14 At% C at 2360°C, the peritectic reaction isotherm) by an equilibrium monocarbide-metal-rich melt. An explanation for this behavior may possible be sought in differences in the electronic structure of the compounds, a factor which often is grossly underestimated[31]. A systematic application of the concepts followed by L. Brewer[32] may shed some light into the complex nature of phase relations and allow, at least on a semiquantitative basis, a correlation between phase stability and electronic structure.

Other problems of extreme theoretical, as well as practical, interest concern phase-separation phenomena, and the question of internal partition equilibria in crystal phases, for which a semiquantitative mathematical treatment on the example of α- and β-Mo_2C has been given in an earlier report[25]; the ultimate problem, however, is far more extended, and efforts are being made[33] to generalize the thermodynamic treatment with regard to phase composition, equivalency of crystal site, and order of equilibrium. A detailed thermodynamic treatment of this as well as other ternary systems investigated under this program will be given in a separate report.

B. APPLICABILITY - COMPOSITE STRUCTURES

For the possible high temperature application of Ta-Hf-C alloys probably the most interesting feature in the system is the existence of a wide two-phase equilibrium metal-monocarbide, which offers possibilities for reinforcing refractory carbides with ductile metal phases.

The concept of compatible metal-carbide composite systems has been pursued through a number of years in the Metallwerk Plansee Research Laboratories, and has resulted in the development of interesting composite systems for high temperature applications,[28, 34-37], such as in rocket propulsion.

Alloy combinations of such types, with proper adjustment of the microstructures, also could be of considerable interest for the development of cutting tools with improved temperature capabilities (cutting speeds), since the comparatively low-melting cobalt could be replaced by high strength and ductile refractory alloys.

Although the specific demands may vary within wide limits, the inherent brittleness of the carbides and, as a consequence, their fracture sensitivity, is in each instance the main obstacle to overcome. This problem becomes especially severe in the application of carbides in rocket nozzles, where single phased material fails within the first firing seconds as a result of thermally induced stresses. Carbide-graphite composites behave similarly, although an extremely fine and even distribution of the component phases (Figure 82) somewhat improves their characteristics[38].

Carbide-metal composites offer greater possibilities, although other problems, such as low interphase melting, have to be overcome by suitable choice of the alloy components (Figure 83) as well as preparation techniques.

Infiltration of porous carbide structures with high conductivity, low melting metals, such as silver or copper, essentially eliminates the problem of thermal stress-induced fracture[38], but the problem

of accelerated erosion of the porous carbide after complete vaporization of the low-melting metal phase has not yet been solved to full satisfaction[38]. Typical results from subscale solid propellant motor firings (Figures 84 and 85) showed good performance (erosion rates < 1 mil per second at a flame temperature of ~6500°F and the first 30 firing seconds), while transpiration of the low melting phase was still operative; however,

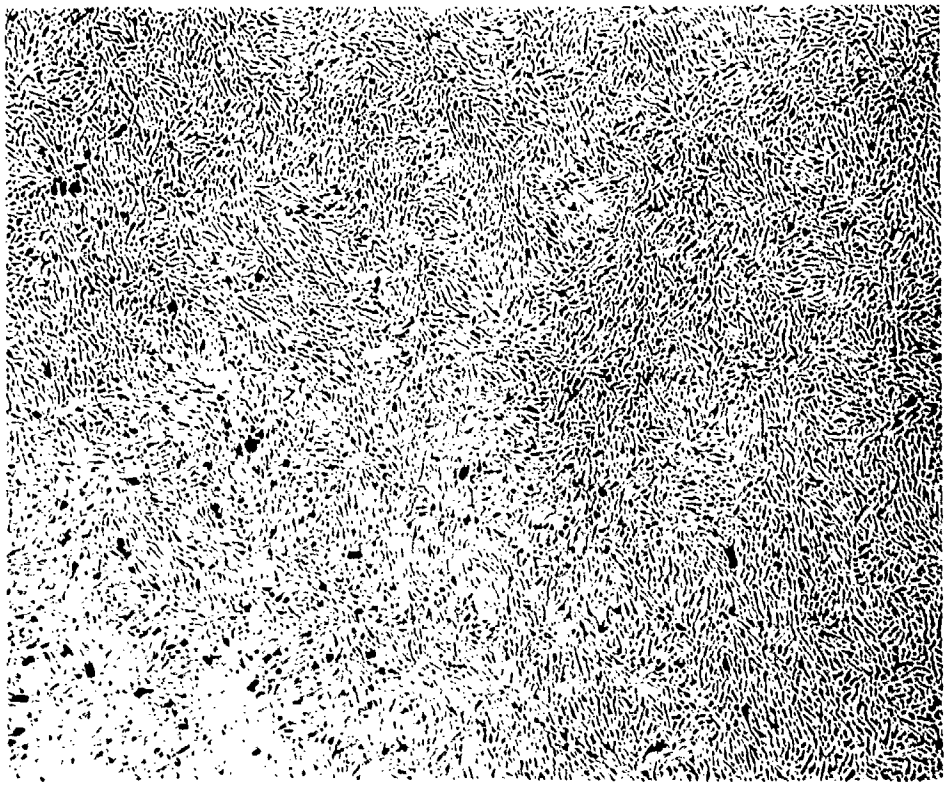

Figure 82. Tantalum-Carbide-Graphite Composite Structure X500

higher erosion rates (2-3 mils per second) and gradual deterioration of the inserts were encountered after the silver or copper had been lost.

Apart from these effects careful control of the microstructure is a necessity for adequate performance (Figures 86 through 89); as an example, weak linkage between carbide grains (low

strength carbide skeleton), and, likewise, use of 'heavy metal'-type composites results in practically immediate failure (washout).

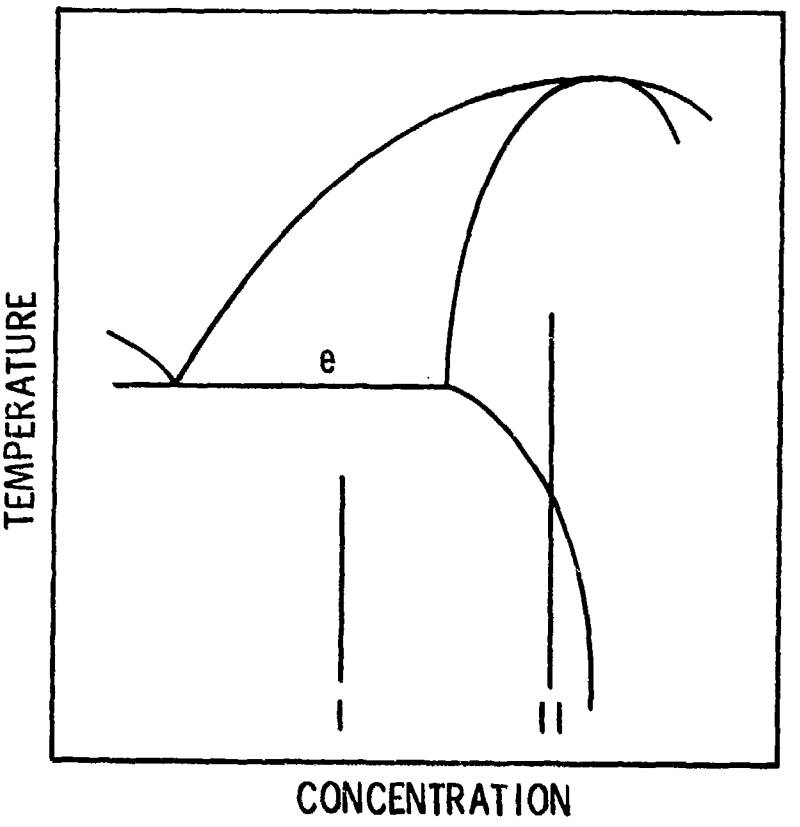

Figure 83. Reinforcing Principles (Schematic)

I. Cementation

II. Disappearing Binder Phase

(e.... Eutectic Melting)

Figure 84. Silver- and Copper-Infiltrated Tantalum Carbide Test Nozzle Inserts (Scale in Centimeters)

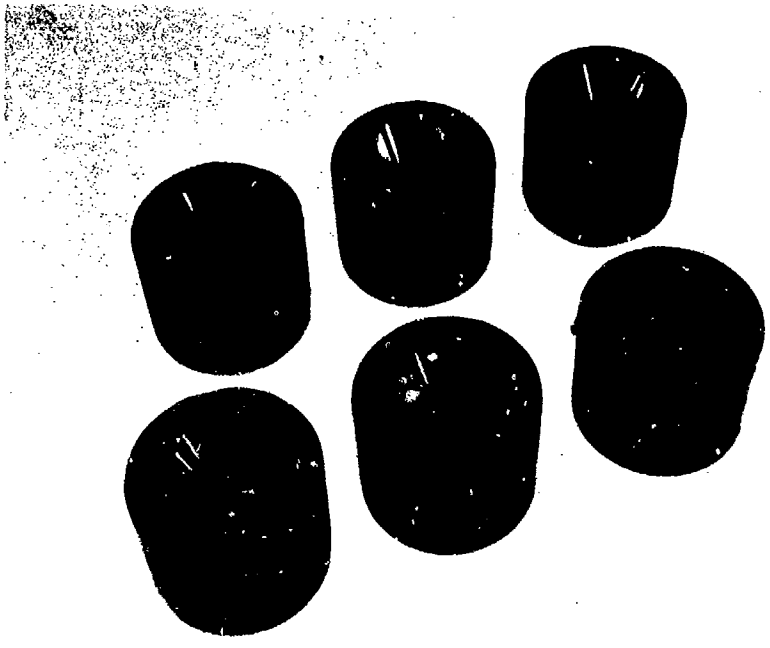

Figure 85. Silver- and Copper-Infiltrated Tantalum Carbide Nozzle Inserts, Assembled in Holders

Figure 86. Silver-Infiltrated Tantalum Carbide. X1000

Note Heavy Crosslinkage of Carbide Grains (Light Phase)

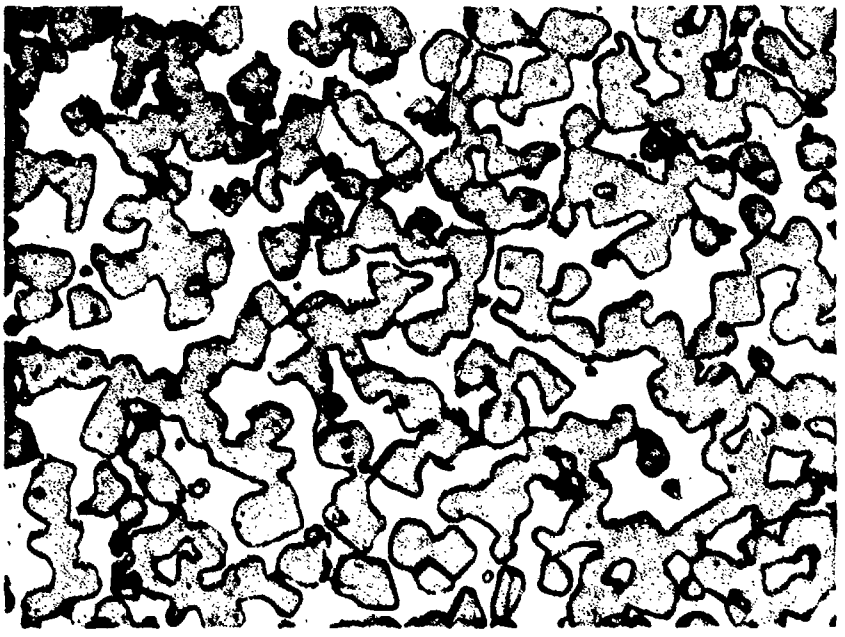

Figure 87. Silver-Infiltrated Tantalum Carbide X500

Weak Interlinkage of the Carbide Grains (Dark Phase)

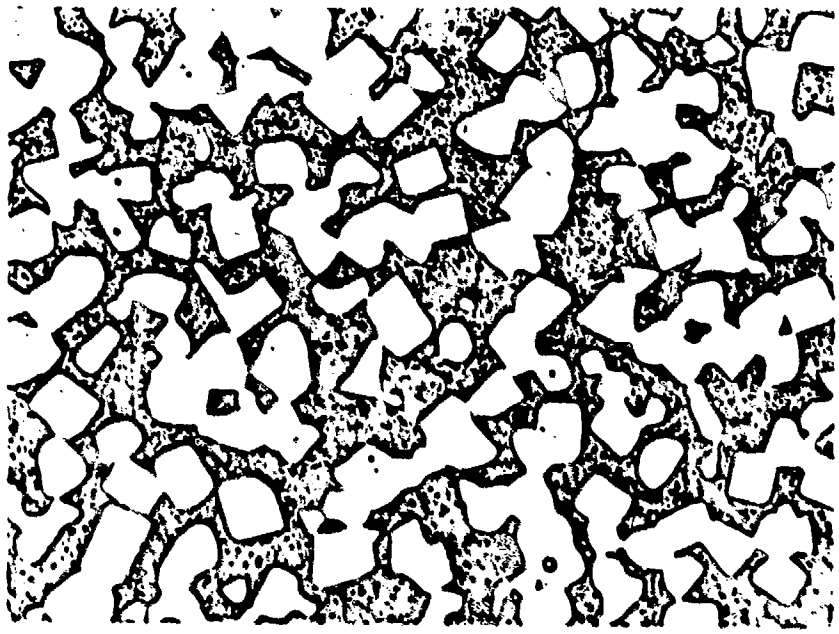

Figure 88. Silver-Infiltrated Tantalum-Carbide, 'Heavy-Metal' Structure. X750

Continuous Silver Phase (Dark), Isolated TaC Grains (Light)

Analysis of the failure criteria and comparison with previous results[39] indicates, that low porosity, i.e. refractory metal-reinforced structures, or a combination of both concepts, reinforcement and infiltration, may offer certain advantages. In view of the phase-relationships found in the tantalum-hafnium-carbon system, ternary alloys on this basis seem to offer a logical choice for feasibility studies on metal-carbide composite structure systems for high temperature applications.

REFERENCES

1 F.N. Rhines: Phase Diagrams in Metallurgy (McGraw-Hill, 1956).

2 E. Rudy, C.E. Brukl, and D.P. Harmon: AFML-TR-65-2, Part I, Vol. IV (May 1965).

3 E. Rudy, C.E. Brukl, and D.P. Harmon: AFML-TR-65-2, Part I, Vol. V (May 1965).

4 D.K. Deardorff, 1961: (Work quoted by J.J. English, DMIC-report 152, 1961).

5 H. Kato and M.I. Copeland: USBM-U-863, Prog. Rept. Sept. 1961.

6 C. Agte and H. Alterthum: Z.techn. Physik 11 (1930), 182.

7 For an exhaustive compilation of earlier work, reference may be made to the book by R. Kieffer and F. Benesovsky, Hartstoffe and Hartmetalle (Springer Wien, 1963).

8 R.V. Sara and C.E. Lowell: WADD-TDR-60-143, Part V (Oct 1964)

9 M. I. Copeland: U.S. Bureau of Mines Prog. Rept. USBM-U-952 (June 1962).

10 R.G. Avarbe, A.L. Avgustinnik, Yu.N.Vilk, Yu.D. Konrashov, S.S. Nikolskii, Yu.A. Omelchenko, and S.S. Ordanyan: J. Appl. Chem. USSR 35 (1962), 1899.

11 F. Benesovsky and E. Rudy: Planseeber. Pulvermet. 8 (1960), 66

12 R.P. Adams and R.A. Beall: U.S. Bureau of Mines, Report of Investigation 6304 (1963) 8 (1960), 66.

13 G.V. Samsonov, and J.S. Umanski: Hard Compounds of Refractory Metals (Moscow 1957), 118.

14 F.H. Ellinger: Trans. Am. Soc. Met. 31 (1943), 89.

15 C. F. Zalabak: NASA-TN-D-761 (1961).

16 W.G. Burgers and J.C.M. Basart: Z.anorg.Allg.Chemie 216 (1934), 209.

17 R. Lesser and G. Brauer: Z. Metallkde 49 (1958), 622

18 H.B. Probst, NASA Lewis Research Center, Private Communication March 1965.

References (continued)

19 A.L. Bowman: J. Phys. Chem. 65 (1961), 1596.

20 E. Rudy, El. Rudy, and F. Benesovsky: Mh.Chem. 93 (1962), 1176.

21 E. Friedrich and G. Sittig: Z. anorg. Allg. Chem. 144 (1925), 169.

22 M.G. Bowman: Paper presented at the V. Plansee Seminar in June 1964 in Reutte, Tirol, Austria (Plansee Proc. 1964, in print).

23 P.T.B. Shaffer: J.Am. Ceram.Soc. 46 (1963), 177.

24 E. Fromm and U. Roy: J. Less Common Metals, 8 (1965), 73.

25 E. Rudy, St. Windisch, and Y. A. Chang: AFML-TR-65-2, Part I, Vol I. (January 1965).

26 H. Nowotny, R. Kieffer, F. Benesovsky, C.E. Brukl, and E. Rudy: Mh. Chem. 90 (1959), 669.

27 E. Rudy, H. Nowotny, F. Benesovsky, R. Kieffer, and A. Neckel: Mh. Chem. 91 (1960), 176.

28 E. Rudy and H. Nowotny: Mh. Chem. 94 (1963), 507.

29 H.D. Heetderks, E. Rudy, and T. Eckert: AFML-TR-65-2 (Apr 1965). Planseeber. Pulvermet (in print).

30 Compare the very recent compilation of thermodynamic data on carbides by Y. A. Chang: AFML-TR-65-2, Part IV, Vol. I, (May 1965).

31 L. Brewer: Private communication, Dec. 1964.

32 L. Brewer: UCRL-10701, Rev. 2 (1964).

33 E. Rudy, work in progress.

34 E. Rudy, F. Benesovsky, and K. Sedlatschek: Mh.Chem. 92 (1961) 841

35 E. Rudy, F. Benesovsky, and El.Rudy: Mh.Chem. 93 (1962), 693

36 E. Rudy, El. Rudy, and F. Benesovsky: Planseeber.Pulvermet. 10 (1962), 42

37 E. Rudy, Austrian Patent Appl. A-9113/62

38 E. Rudy and St. Windisch: Aerojet-General Corporation, IR&D Project, 1964 and 1965.

References (continued)

39 A.V. Levy, Aerojet-General Corporation: Personal communication, 1964 and 1965.

THIS REPORT HAS BEEN DELIMITED
AND CLEARED FOR PUBLIC RELEASE
UNDER DOD DIRECTIVE 5200.20 AND
NO RESTRICTIONS ARE IMPOSED UPON
ITS USE AND DISCLOSURE.

DISTRIBUTION STATEMENT A

APPROVED FOR PUBLIC RELEASE;
DISTRIBUTION UNLIMITED.

DOCUMENT CONTROL DATA - R&D

(Security classification of title, body of abstract and indexing annotation must be entered when the overall report is classified)

1. ORIGINATING ACTIVITY *(Corporate author)* Aerojet-General Corporation Materials Research Laboratory Sacramento, California	2a. REPORT SECURITY CLASSIFICATION Unclassified 2b GROUP N.A.

3. REPORT TITLE Ternary Phase Equilibria in Transition Metal-Boron-Carbon-Silicon Systems

Part II. Ternary Systems, Volume I. Ta-Hf-C System

4. DESCRIPTIVE NOTES *(Type of report and inclusive dates)*

5. AUTHOR(S) *(Last name, first name, initial)*

E. Rudy

6. REPORT DATE	7a. TOTAL NO. OF PAGES	7b. NO. OF REFS
September 1965	84	39

8a CONTRACT OR GRANT NO. AF 33(615)-1249 b. PROJECT NO. 7350 c. Task No. 735001 d	9a. ORIGINATOR'S REPORT NUMBER(S) AFML-TR-65-2 Part II, Vol. I. 9b. OTHER REPORT NO(S) *(Any other numbers that may be assigned this report)* N.A.

10 AVAILABILITY/LIMITATION NOTICES This document is subject to special export controls and each transmittal to foreign governments or foreign nations may be made only with prior approval of the Metals and Ceramics Division (MAM), Air Force Materials Laboratory, Wright-Patterson AFB, Ohio.

11. SUPPLEMENTARY NOTES	12. SPONSORING MILITARY ACTIVITY AFML (MAMC) Wright-Patterson AFB, Ohio 45433

13 ABSTRACT

The ternary alloy system tantalum-hafnium-carbon was investigated by means of X-ray, DTA, melting point, and metallographic techniques on chemically analyzed alloys, and a complete phase diagram for temperature above 1000°C was established.

The system is characterized by a very high melting solid solution of the refractory monocarbides in both binary systems, and a limited exchange of hafnium in the low- and high-temperature modification of Ta_2C. Four Class II four-phase reaction planes as well as three limiting tie lines occur in the concentration area metal-monocarbide solution.

The results of this investigation are discussed and compared with previous, partial investigations of this system. Fields of application are outlined.

DD FORM 1 JAN 64 1473

Unclassified

Security Classification

Unclassified

Security Classification

14. KEY WORDS	LINK A		LINK B		LINK C	
	ROLE	WT	ROLE	WT	ROLE	WT
Ternary Phase Equilibria Carbide Systems						

INSTRUCTIONS

1. ORIGINATING ACTIVITY: Enter the name and address of the contractor, subcontractor, grantee, Department of Defense activity or other organization *(corporate author)* issuing the report.

2a. REPORT SECURITY CLASSIFICATION: Enter the overall security classification of the report. Indicate whether "Restricted Data" is included. Marking is to be in accordance with appropriate security regulations.

2b. GROUP: Automatic downgrading is specified in DoD Directive 5200.10 and Armed Forces Industrial Manual. Enter the group number. Also, when applicable, show that optional markings have been used for Group 3 and Group 4 as authorized.

3. REPORT TITLE: Enter the complete report title in all capital letters. Titles in all cases should be unclassified. If a meaningful title cannot be selected without classification, show title classification in all capitals in parenthesis immediately following the title.

4. DESCRIPTIVE NOTES: If appropriate, enter the type of report, e.g., interim, progress, summary, annual, or final. Give the inclusive dates when a specific reporting period is covered.

5. AUTHOR(S): Enter the name(s) of author(s) as shown on or in the report. Enter last name, first name, middle initial. If military, show rank and branch of service. The name of the principal author is an absolute minimum requirement.

6. REPORT DATE: Enter the date of the report as day, month, year; or month, year. If more than one date appears on the report, use date of publication.

7a. TOTAL NUMBER OF PAGES: The total page count should follow normal pagination procedures, i.e., enter the number of pages containing information.

7b. NUMBER OF REFERENCES: Enter the total number of references cited in the report.

8a. CONTRACT OR GRANT NUMBER: If appropriate, enter the applicable number of the contract or grant under which the report was written.

8b, 8c, & 8d. PROJECT NUMBER: Enter the appropriate military department identification, such as project number, subproject number, system numbers, task number, etc.

9a. ORIGINATOR'S REPORT NUMBER(S): Enter the official report number by which the document will be identified and controlled by the originating activity. This number must be unique to this report.

9b. OTHER REPORT NUMBER(S): If the report has been assigned any other report numbers *(either by the originator or by the sponsor)*, also enter this number(s).

10. AVAILABILITY/LIMITATION NOTICES: Enter any limitations on further dissemination of the report, other than those imposed by security classification, using standard statements such as:

(1) "Qualified requesters may obtain copies of this report from DDC."

(2) "Foreign announcement and dissemination of this report by DDC is not authorized."

(3) "U. S. Government agencies may obtain copies of this report directly from DDC. Other qualified DDC users shall request through

_____."

(4) "U. S. military agencies may obtain copies of this report directly from DDC. Other qualified users shall request through

_____."

(5) "All distribution of this report is controlled. Qualified DDC users shall request through

_____."

If the report has been furnished to the Office of Technical Services, Department of Commerce, for sale to the public, indicate this fact and enter the price, if known.

11. SUPPLEMENTARY NOTES: Use for additional explanatory notes.

12. SPONSORING MILITARY ACTIVITY: Enter the name of the departmental project office or laboratory sponsoring *(paying for)* the research and development. Include address.

13. ABSTRACT: Enter an abstract giving a brief and factual summary of the document indicative of the report, even though it may also appear elsewhere in the body of the technical report. If additional space is required, a continuation sheet shall be attached.

It is highly desirable that the abstract of classified reports be unclassified. Each paragraph of the abstract shall end with an indication of the military security classification of the information in the paragraph, represented as *(TS), (S), (C), or (U)*

There is no limitation on the length of the abstract. However, the suggested length is from 150 to 225 words.

14. KEY WORDS: Key words are technically meaningful terms or short phrases that characterize a report and may be used as index entries for cataloging the report. Key words must be selected so that no security classification is required. Identifiers, such as equipment model designation, trade name, military project code name, geographic location, may be used as key words but will be followed by an indication of technical context. The assignment of links, rules, and weights is optional.

Unclassified

Security Classification